NATURAL ROCK DRAINAGE ASSOCIATED WITH UNMINED PORPHYRY COPPER DEPOSITS IN THE RIO GRANDE DE ARECIBO WATERSHED, PUERTO RICO

by

Meralis Plaza Toledo

A thesis submitted in partial fulfillment of the requirements for the degree of

MASTER OF SCIENCES
in
GEOLOGY

UNIVERSITY OF PUERTO RICO
MAYAGÜEZ CAMPUS

2005

Approved by:

Robert R. Seal II, PhD Member, Graduate Committee	Date
Fernando Gilbes, PhD Member, Graduate Committee	Date
Johannes H. Schellekens, PhD President, Graduate Committee	Date
Jorge Rivera Santos, PhD Representative, Graduate Studies	Date
Johannes H. Schellekens, PhD Director, Department of Geology	Date

ABSTRACT

The Río Grande de Arecibo is located at the north-central part of the island of Puerto Rico; its watershed is unique because it contains most of the discovered porphyry copper deposits of Puerto Rico. Several of them were extensively explored but none were mined. The premining geochemical signature for areas around mineral deposits is essential for realistic reclamation goals at proposed mines and at abandoned mines (Runnels et al. 1998). This study represents a geochemical background characterization that can be used as a remote analogue for porphyry copper deposits in tropical climates. The characterization will be performed on the basis of the water and stream sediment geochemistry of the Río Viví in Utuado, which passes through the deposits, and Río Pellejas in Adjuntas which drains the deposits. In addition to these analyses, processed images from IKONOS were used to better characterize vegetation on the vicinity of the deposits.

RESUMEN

Río Grande de Arecibo está localizado en la parte norte-central de la Isla de Puerto Rico; su cuenca es única dado que esta contiene la mayoría de los depósitos pórfidos de cobre encontrados en Puerto Rico. Varios de estos fueron explorados pero no minados. El estado en el que se encuentra un depósito antes de ser minado, conocido como trasfondo geoquímico en áreas prístinas, son esenciales al momento de establecer reclamaciones en áreas después de minadas o en áreas a minar (Runnels et al. 1998). Este estudio representa una caracterización geoquímica que podría ser utilizada como un análogo remoto de otros pórfidos de cobre en climas tropicales. Esto se realizó a base de análisis geoquímicos de agua y sedimentos en el Río Viví en Utuado, el cual pasa por lo depósitos y Río Pellejas, en Adjuntas, el cual drena los depósitos. En adición a estos análisis, se utilizaron también imágenes procesadas de IKONOS para caracterizar la vegetación cercana a los depósitos.

.

A mi Reinita, quien siempre estará en mi corazón…

ACKNOWLEDGEMENTS

During the years that I spent doing my graduate studies in the University of Puerto Rico many people collaborated in many ways in this research; without them, this work would not have been possible.

I would like first to begin with the person that supported me in the idea of working with the porphyry copper deposits of Puerto Rico, my advisor Johannes Schellekens. I would also want to express a sincere acknowledgement to Robert Seal because his support and encouragement with this research during the past two years. I also want to thank Fernando Gilbes. I'm completely grateful for their help, availability and patience. THANKS!

Special thanks to Jane Hammarstrom, Nadine Piatak and Noelia Báez for their help in the field work and for Jane and Nadine's guidance in all the procedures related to sample characterization at the USGS labs in Reston, VA. Thanks to Zaida Aquino from the USGS Caribbean Water Science Center, who provided precipitation and discharge data from the study area. The encouragement and support of the Eastern Regional Geologist Office and the Mineral Resources Program, especially Ivette Torres, Dave Russ, James McNeal and Scott Tilley are greatly appreciated.

Finally, I would like to thanks my love ones, Memi, Omaris, Elvin, my lovely Reinita, Luis E., Samuel, Angel and all my friends who were always there when I need them.

Table of contents

List of Figures

List of Tables

Chapter 1

Introduction

Mineral deposits are anomalies that express themselves geochemically in the environment even prior to mining. In fact, their premining expression is the basis for the field of exploration geochemistry. The premining geochemical signature for areas around mineral deposits, known as a geochemical background in pristine areas, or a geochemical baseline in areas that have experienced anthropogenic activity, is essential for realistic reclamation goals after mining at proposed mines and at abandoned mines (Runnels et al., 1998). At proposed mines, permitting agencies require that pre-mining conditions be carefully documented to serve as targets for reclamation. At abandoned mines, premining conditions are more problematic because permitting agencies have not historically required premining conditions to be documented. Generic water-quality guidelines for the protection of human or ecosystem health are inadequate for the purposes of reclamation goals because most historically mined deposits were typically discovered because they croped out at the surface, where they were exposed to weathering and naturally elevated the concentrations of acidity and metals in the surrounding environment relative to nearby unmineralized terrains.

Research has attempted to estimate pre-mining geochemical backgrounds by a variety of methods. Several strategies have been developed, that include the use of historical and anecdotal data, comparisons with remote and proximal analogues, geochronological analysis of stream- and overbank-sediment

geochemistry, the use of stable isotopes to identify natural and human induced weathering pathways, geochemical modeling, statistical analysis and mass-balance studies of the weathering process (Alpers and Nordstrom, 2000).

This study represents a geochemical background characterization that can be used as a remote analogue for porphyry copper deposits in tropical climates. Remote analogues can be from anywhere in the world and use on water-quality and sediment-chemistry data from unmined mineralized areas that are distant from the area where natural background information is needed, but preferably from a similar climatic setting (Alpers et al., 1999). In contrast, an example of a proximal analogue would be an unmined deposit in an adjacent watershed from the mined deposit in question. Numerous factors control the weathering behavior of mineral deposits. One of the most important with respect to geochemical backgrounds is climate. Geochemical signatures surrounding unmined or mined mineral deposits in a humid tropical setting such as in Puerto Rico are likely to be different from those surrounding one in an arid setting such as Arizona or Nevada.

Porphyry copper deposits historically have been and continue to be the dominant sources of copper and important sources of gold globally (Titley and Beane, 1981; Sillitoe, 1993; Edelstein, 2002). They provide more than 50 % of the world's copper from over 100 producing mines; the world's largest deposits have reserves of 1.5 to 3 billion tons containing 0.8 to 2% copper. Porphyry copper deposits are large ore bodies characterized by disseminated to veinlet-controlled mineralization deposited throughout large volumes of altered,

intermediate-composition intrusive rocks (Plumlee et al., 1999). This type of deposit typically contains copper, molybdenum and gold. Its host rock is generally pyrite-rich porphyry such as granodiorite and tonalite. Notable examples are found in all climatic settings including tropical climates, for example the Cerro Colorado porphyry copper deposit in Panamá, with reserves estimated in 3 billion tons with 0.8% copper, and the Biga deposit in the Philippines, with 700 million tons with 0.5% copper. The deposits in Puerto Rico are small, but important, unmined examples of porphyry copper deposits.

The oxidative weathering of pyrite is the main catalyst for changes in the environment surrounding both unmined and mined mineral deposits. Pyrite (FeS_2), the main sulfide mineral found in porphyry copper deposits, oxidizes in the presence of water and oxygen through a series of generalized steps beginning with the reaction:

$$FeS_2 + \tfrac{7}{2}O_2 + H_2O \rightarrow Fe^{2+} + 2SO_4^{2-} + 2H^+$$

This reaction releases H^+ and if the sulfuric acid is not neutralized, the acidity of the water will increase. Oxidation of ferrous iron produces ferric iron through the reaction:

$$Fe^{2+} + \tfrac{1}{4}O_2 + H^+ \leftrightarrow Fe^{3+} + \tfrac{1}{2}H_2O$$

Ferric iron is much less soluble than ferrous iron and will precipitate at a pH greater than 2.5 through the reaction:

$$Fe^{3+} + 3H_2O \leftrightarrow Fe(OH)_{3(solid)} + 3H^+$$

Which further reduces pH. These reactions form the basis of natural acid-rock drainage. The formation of rock drainage can be accelerated by mining and incorrect land use by increasing the quantity of sulfides exposed. Acid-mine drainage refers to acid that is generated at mine sites, whereas acid-rock drainage or natural rock drainage is used to describe naturally occurring processes of acid generation.

The Río Grande de Arecibo watershed, which originates in the Cordillera Central of west-central Puerto Rico, is unique because it contains most of the known porphyry copper deposits in Puerto Rico. Investigations of the water chemistry in the area of porphyry copper deposits in Puerto Rico will help to understand natural rock-drainage processes that occur in unmined tropical terranes. The characterization of the natural background signatures in mineralized areas in Puerto Rico can provide realistic guidelines for the remediation of mine sites elsewhere in the world in tropical settings (Runnels et al., 1998). This study focuses on the porphyry copper deposits of the Río Viví and Río Pellejas watersheds, which drain into the Río Grande de Arecibo.

The history of the porphyry copper deposits on the Río Viví area began in 1957 when W.R. Bergey was searching for the source of copper and molybdenum anomalies in the stream sediments of the Rio Viví, which later lead to the discovery of mineralized porphyry in the walls of the river canyon. In 1960, a geochemical soil survey was conducted by Ponce Mining Company, which included drilling in the area. The result was the discovery of the subeconomic Sapo Alegre deposit. In contrast, the Piedra Hueca and Calá Abajo deposits

have reserves estimated at about 104 million tons with 0.82% Cu (Lutjen, 1971). At about the same time (1956), other porphyry copper deposits were discovered in the Río Tanamá watershed to the northwest of the study area; reserves were estimated at about 126 million tons with a copper grade of 0.64%.

In 1967, several mining companies presented a series of proposals to the government of Puerto Rico for the exploitation of these deposits. However, because a mining lease was never obtained, by 1987 the interest in mining was abandoned. In October 1992, the Department of Natural Resources of Puerto Rico gave Southern Gold Resources Inc. permission to explore the Calá Abajo deposit for evaluation for mining by open-pit methods. This sudden interest in the Puerto Rican porphyry deposits was triggered by the increasing gold prices and new techniques for gold recovering. A series of drill holes were completed in the area, which lead to a proposal to mine the deposit by open-pit methods.

The people of Puerto Rico protested the proposed mine because of the potential effects on the environment and on their lives. In June 1995, the Puerto Rican government amended Law number 9 of August 18, 1933 prohibiting open pit mining, strip mining, or any other method to extract metallic minerals that could significantly alter the natural background of the mining area. The area became a protected forest supported by the entity Casa Pueblo, which is a self management organization represented by all the people of Puerto Rico.

The purpose of this research is to document the geochemical signatures in water and stream sediments surrounding unmined porphyry copper deposits in the Río Viví and Río Pellejas watersheds, and to describe these signatures in

terms of the geochemical processes. The increased understanding of geochemical processes acting upon unmined porphyry copper deposits in tropical environments also will provide useful insights for the exploration for porphyry copper deposits in rugged, heavily vegetated terranes through the use of water and stream-sediment geochemistry.

For this purpose, the usefulness of remote sensing of the vegetated cover over these deposits is also evaluated. An anomalous substrate, such as a mineralized area, can cause taxonomic and vitality responses in the vegetation that can lead to differences in spectral signatures. Vegetation in other mineralized areas has been shown to have higher reflectance in the visible wavelengths and lower reflectance in the infrared wavelengths as compared to vegetation in non-mineralized areas (Carranza, 2002).

Chapter 2

Setting of the Study Area

The porphyry copper deposits near Adjuntas are located along the northern slope of the Cordillera Central in west-central Puerto Rico (Fig. 1). The factors affecting their weathering, including the physiography, hydrology, climate, and geology are summarized below.

Physiography, Hydrology, and Climate

Puerto Rico is the easternmost island of the Greater Antilles. The island is elongated in an east-west direction. The Cordillera Central forms its spine. The Río Grande de Arecibo is the main north-flowing drainage in the western part of the island. The porphyry deposits in the study occur in the Río Pellejas and Río Viví watersheds, which form part of the headwaters of the Río Grande de Arecibo. The area is characterized by a rough topography and dense vegetation (Fig. 2). The elevation ranges from 300 to more than 900 m above sea level. The highest peak in the area is on the southeastern boundary of the Río Viví watershed with an elevation of 937 m; the lowermost sampling points in the Río Pellejas watershed are at an elevation of 350 m. Forested areas and cultivated lands dominate both watersheds. The population is sparse and is distributed throughout the study area. Most houses rely on their septic tanks and sink pits to process the sewage. No significant industrial activity is found in the study area.

The part of the Río Pellejas watershed within the study area covers approximately 21.5 km^2, whereas the part of the Río Viví watershed within the

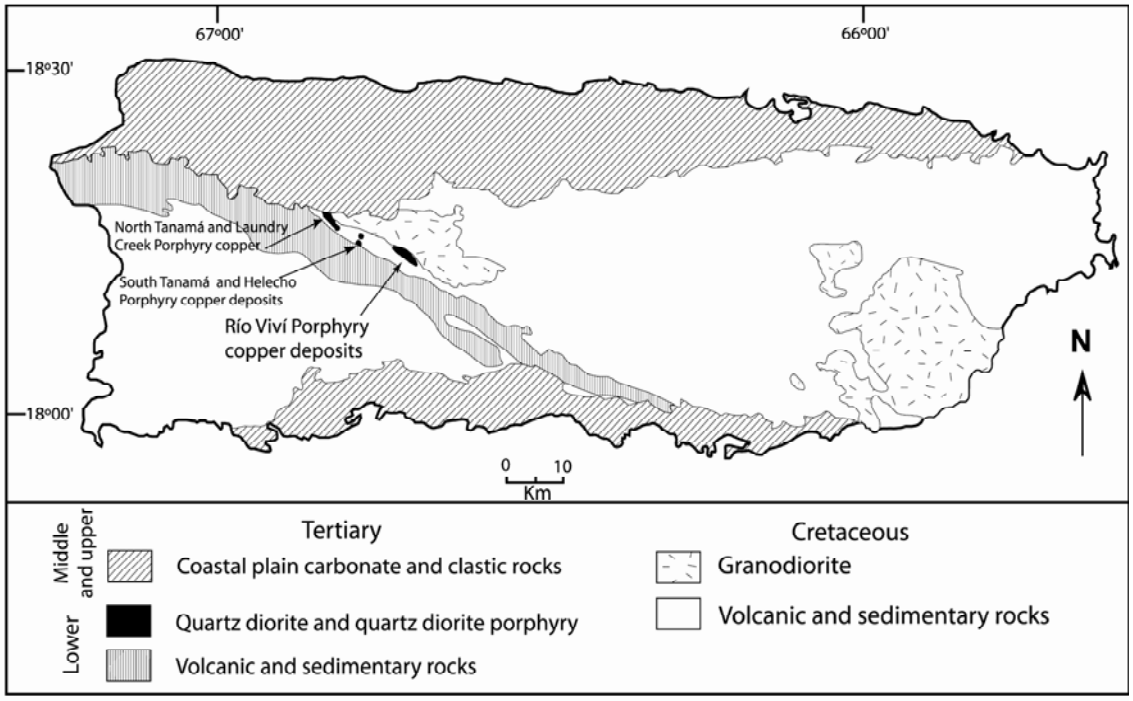

Figure 1. Generalized geologic map of Puerto Rico showing the location of the Río Viví and other Eocene porphyry copper deposits along the Utuado Batholith (based on Cox et al., 1973).

a.

b.

Figure 2. Photo showing the rough topography and dense vegetation in the Río Pellejas watershed area. **a.** View looking towards the north-east from road 521 close to sample site PRRP-5. **b.** View in the vicinity of sample site PRRP-1.

study area covers approximately 14.8 km^2. Both rivers have dams downstream of the study area, which connect them along a series of tunnels that supply water to a hydroelectric power plant on the Río Caonillas. Water is moved from the Lake Adjuntas Dam on the Río Grande de Arecibo eastward to Pellejas Dam, to Viví Dam and finally to Caonillas Dam, from where it is released to the hydroelectric plant. The Río Viví joins Río Grande de Arecibo approximately 5.7 km below the study area, in the town of Utuado; the Río Pellejas joins the Río Grande de Arecibo approximately 4 km upstream of Utuado and 3 km downstream of the study area (Fig. 3).

The general climate of the island is tropical marine. It is characterized by two seasons on the basis of precipitation - a wet season and a dry season. The dry season generally extends from January to June and the wet season extends from July to December. The wet season includes the hurricane season, which runs from July through November. Most of the rainfall on the island is orographic in origin. Moist air carried by trade winds comes from the east from the Atlantic Ocean, is forced to rise over the mountains in the center of the island, which causes cooling and the condensation of rain. Rainfall is low in the south in the orographic shadow of the Cordillera Central. Annual precipitation is highly variable across the island. For example, extremes in annual rainfall vary from 90 cm in the southwest to 600 cm in the northeast. The Río Viví area receives about 200 cm of rainfall annually, mostly between July and November (Learned 1972). Data for rainfall during the period of this study is shown in Figure 4.

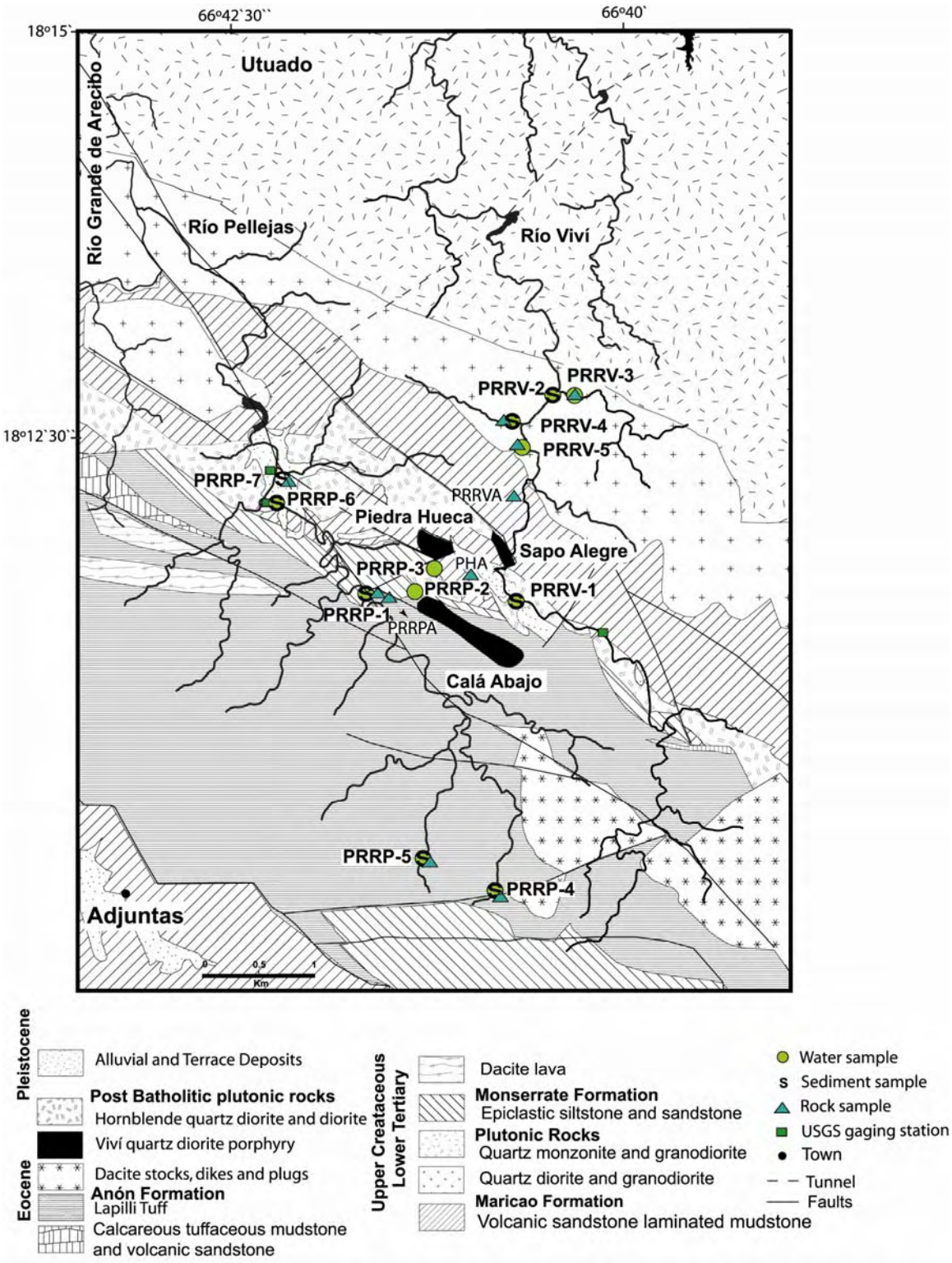

Figure 3. Lithologic map showing sample locations and the Río Viví porphyry copper deposits. Geology based on Mattson (1968), and Krushensky and Curet (1984).

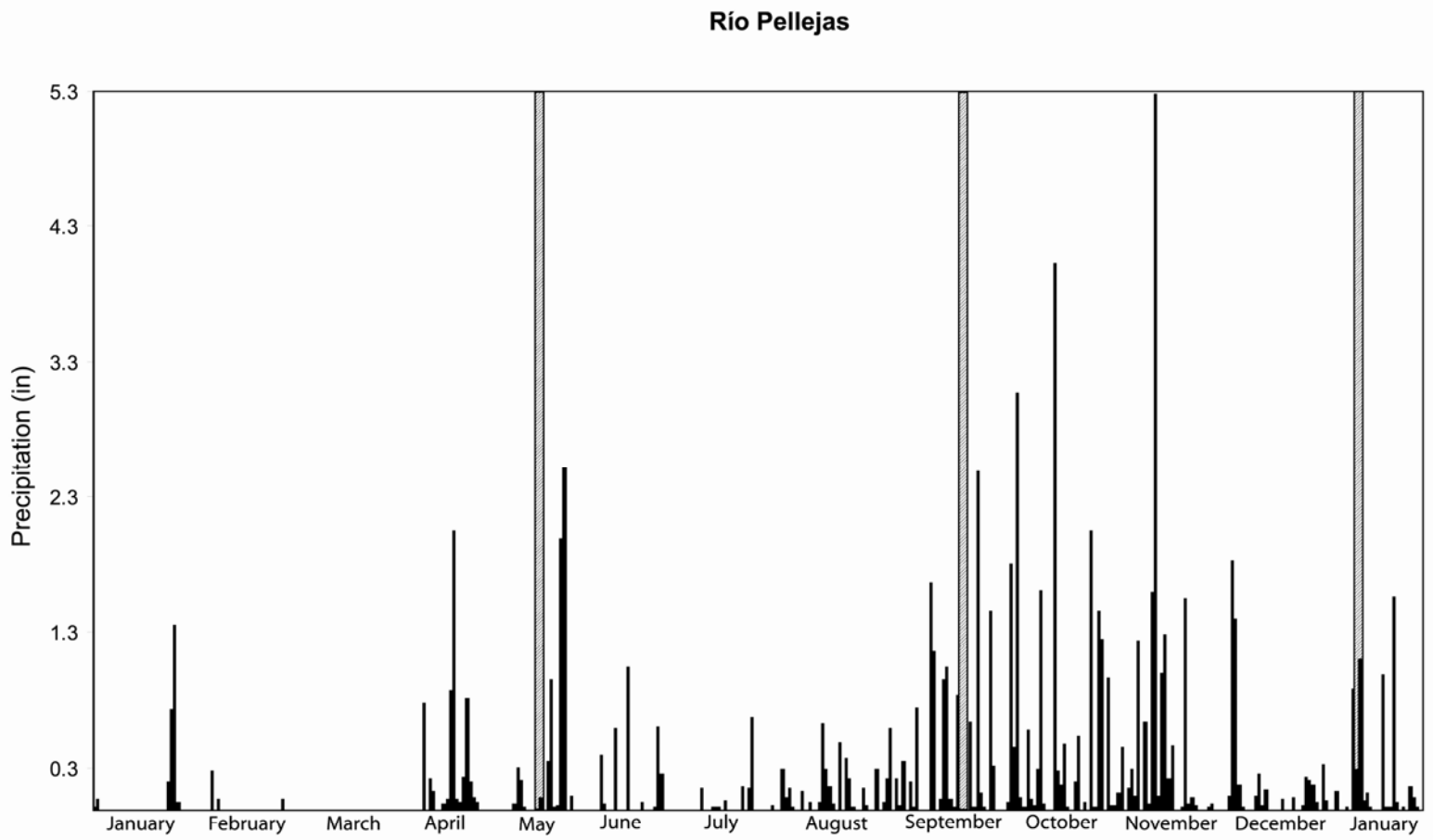

Figure 4a. Plot showing the average precipitation in the Río Pellejas area from January 2003 to January 2004. Columns with patterns represent the sample days. Data obtained from water gaging station 50021030 Río Pellejas above Central Pellejas, Puerto Rico (U.S. Geological Survey, Caribbean Water Science Center).

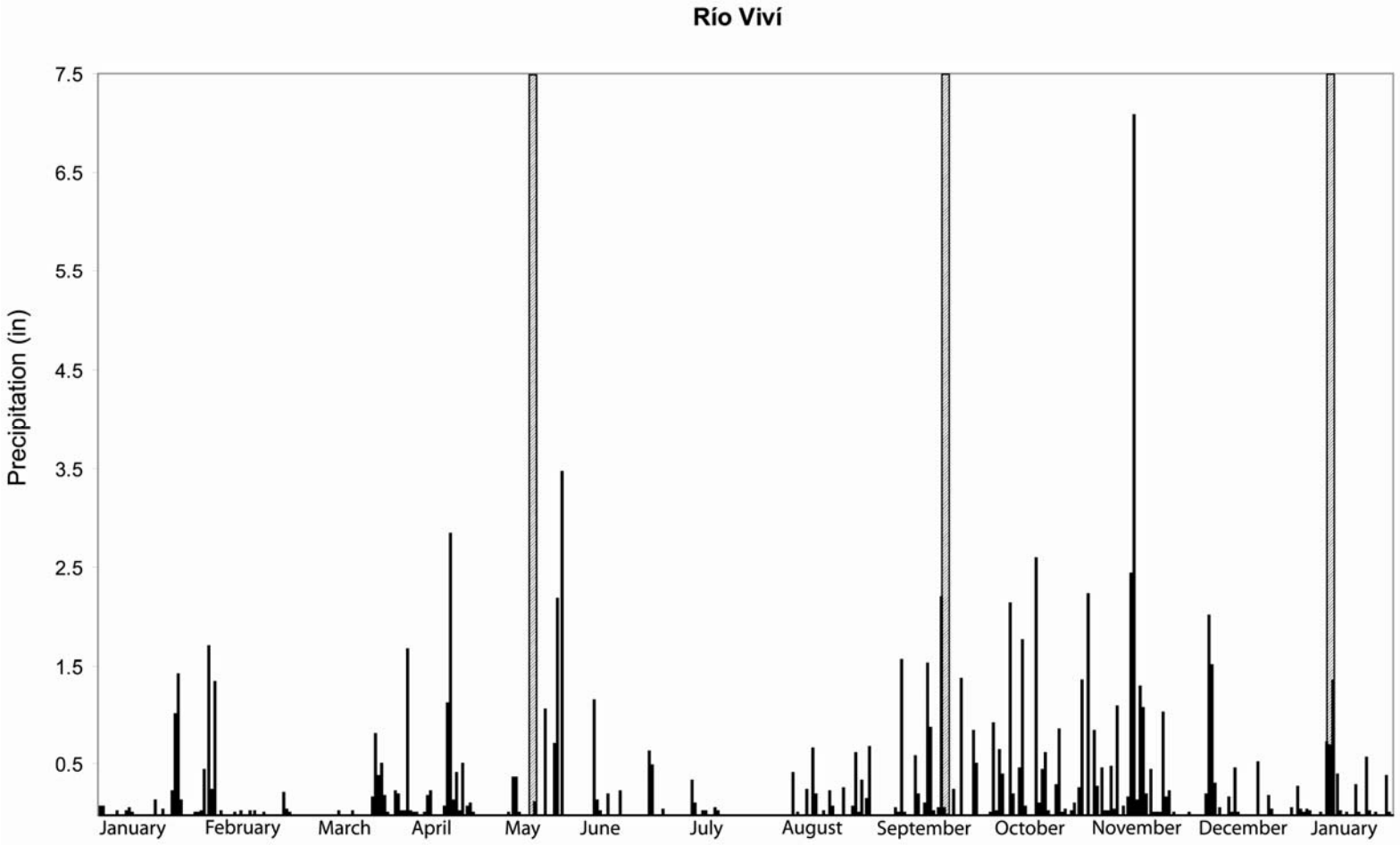

Figure 4b. Plot showing the average precipitation in the Río Viví area from January 2003 to January 2004. Columns with patterns represent the sample days. Data obtained from water gaging station 50022810 Río Viví below Hacienda el Progreso, Puerto Rico (U.S. Geological Survey, Caribbean Water Science Center).

Regional Geology

The Río Grande de Arecibo basin is underlain by Cretaceous and Lower to Middle Tertiary rocks (Fig. 3). The geology is dominated by volcanic rocks, subvolcanic intrusions, and related rocks. The oldest rocks in the study area are thermally metamorphosed basalts that were initially assigned to the Robles Formation (Mattson, 1968) but Krushensky and Curet (1984) correlated the northern basalts with the late Cretaceous Maricao Formation and the southern outcrop with Lago Garzas Formation of similar age. The formation consists chiefly of well bedded epiclastic sandstones and siltstones with subordinate lava and minor limestone. The Middle Eocene Monserrate Formation is composed of epiclastic siltstone and sandstone interbedded with tuff and conglomerate of andesitic composition. The Middle Eocene Anón Formation is chiefly lapilli tuff, and vitric tuff with trachytic fragments of andesite, dacite, and local diorite or gabbro.

The Cretaceous to Paleocene (70-55 Ma) Utuado pluton is composed mainly of tonalite and less commonly granodiorite and quartz diorite (Barabas 1982; Cox 1985). The batholith was intruded along the southwest margin by Eocene quartz diorite and tonalite intrusions. The porphyry copper mineralization including those of the study area, are associated with these Eocene intrusions.
The Sapo Alegre deposit is located in the Río Viví watershed, its host rock is epiclastic sandstones, mudstones and basaltic lava from the Maricao Formation. Upstream of Sapo Alegre, the country rocks belong mainly to the

Anón Formation. Most of the water samples were collected downstream of the Sapo Alegre porphyry, where the geology is limited to plutonic rocks associated with the Utuado Batholith, and consist of quartz monzonite, quartz diorite and granodiorite. Petrogaphic observations for rock samples of the Río Viví watershed shows moderate to high amounts of feldspars, chlorite and epidote, and minor biotite for the epiclastic siltstone and sandstone of the Monserrate Formation. Plutonic rocks that are part of the Utuado Batholith have high content of feldspars and quartz with minor biotite. Pyrite is a common minor phase. Chalcopyrite inclusions and veinlets in pyrite were locally observed in the batholithic and epiclastic rocks (Fig. 5).

The Calá Abajo deposit is located in the Río Pellejas watershed. Surrounding the deposit and upstream of it, the host rocks belong predominantly to the Anón Formation with some Eocene dioritic stocks. Downstream of the deposit occurs the Eocene Monserrate Formation. Upper Cretaceous to Lower Tertiary plutonic rocks, predominantly quartz diorite and granodiorite, underlie the northern sides of both watersheds until they join the main trunk of Río Grande de Arecibo. Petrographic examinations of rocks of both the Monserrate and Anón Formations from the Río Pellejas watershed reveal abundant plagioclase, moderate chlorite, epidote and quartz, and minor amounts of hornblende, biotite and pyrite (Fig. 6).

The Piedra Hueca deposit straddles the drainage divide between the two watersheds but lies mostly within the Río Pellejas watershed. The deposit is

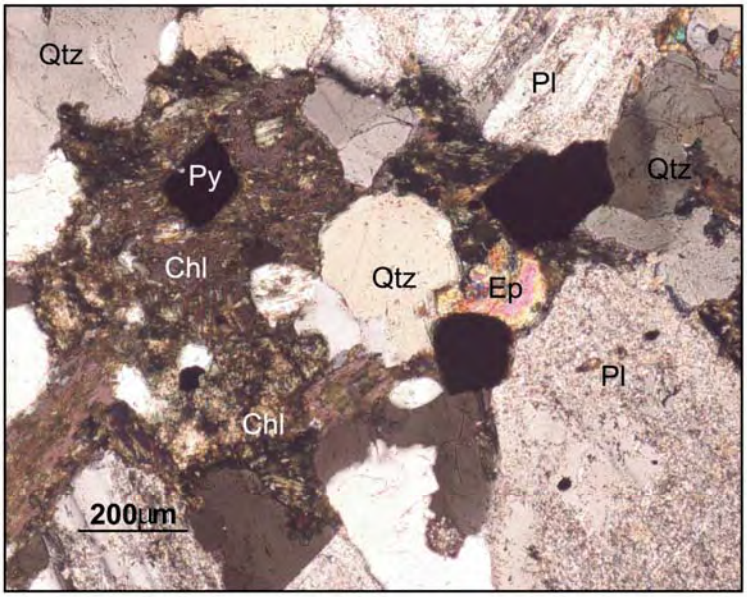

a.

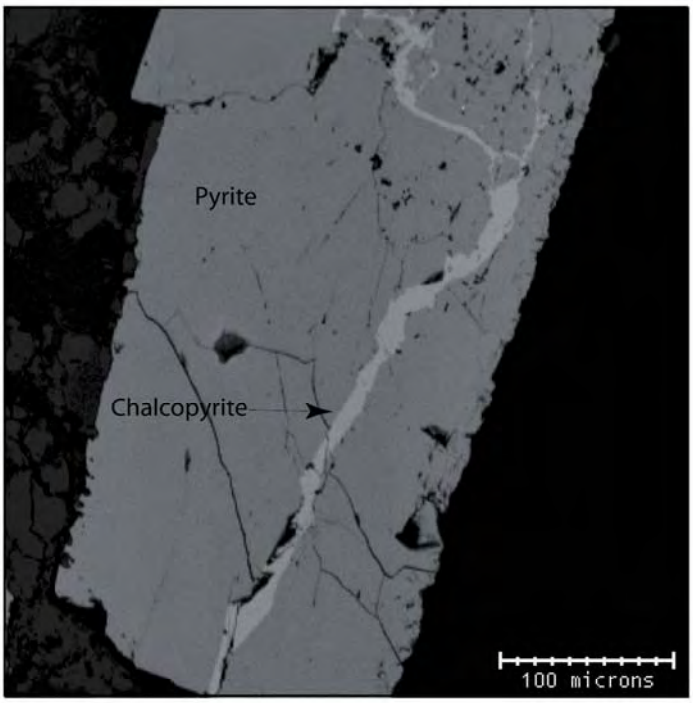

b.

Figure 5. Petrographic features of granodiorite from PRRV-4. ***a.*** Cross polarized light, quartz (Qtz), chlorite (Chl), plagioclase (Pl), epidote (Ep), and pyrite (Py). ***b.*** Backscattered - electron SEM image of sample site PRRV-A from the Monserrate formation showing a chalcopyrite veinlet in a pyrite grain.

hosted by the Maricao Formation. To the southwest of the deposit is the Monserrate Formation and to the east are Eocene hornblende – quartz diorites and diorites. The petrography of Piedra Hueca host rocks is dominated by moderate amounts of hornblende and quartz, and minor chlorite, biotite, and pyrite (Fig. 7).

Economic Geology

The copper deposits along the southwestern margin of the Utuado batholith display many of the characteristics that are typical of classic porphyry copper mineralization (Titley and Beane, 1981). They are associated with felsic stocks. The mineralization formed in stockworks of veinlets. The ore mineralogy is dominated by pyrite followed by chalcopyrite and minor molybdenite. Alteration zones include potassic, sericitic, argillic, and propylitic facies.

The deposits along the southwestern margin of the Utuado batholith occur in two areas separated by approximately 15 km (Fig. 1). The northwestern area is dominated by the Tanamá and Helecho deposits; two porphyry copper prospects, Copper Creek and Laundry Creek, are also found in the vicinity of Tanamá and Helecho. The southeastern area (the study area) includes the Calá Abajo, the Piedra Hueca, and the Sapo Alegre deposits.

Tanamá and Helecho are associated with tonalitic stocks composed of phenocrysts of calcic plagioclase, hornblende, and quartz in an aplitic textured

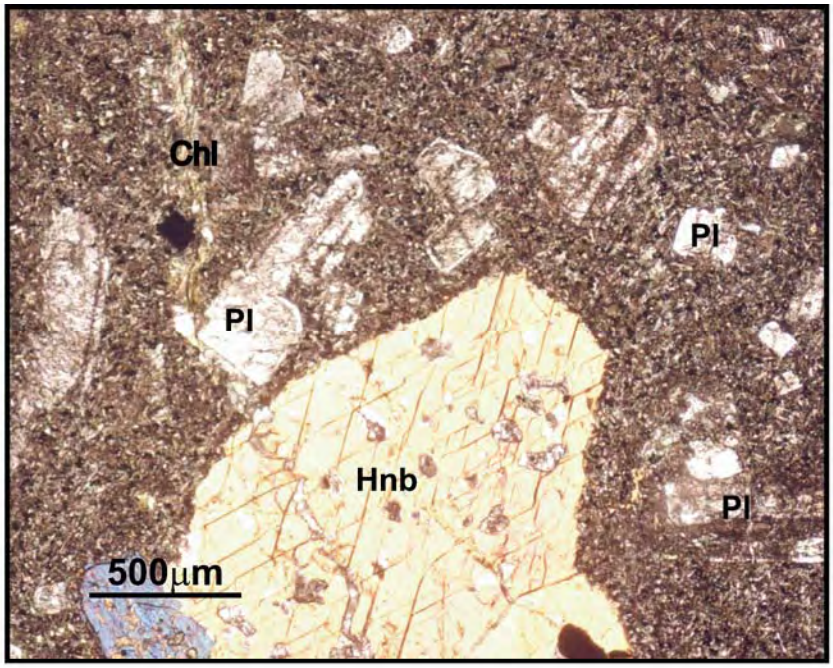

Figure 6. Photomicrograph in cross polarized light of the sample site PRRP-5 from the Anón Formation showing hornblende (Hnb), chlorite (Chl), and plagioclase (Pl).

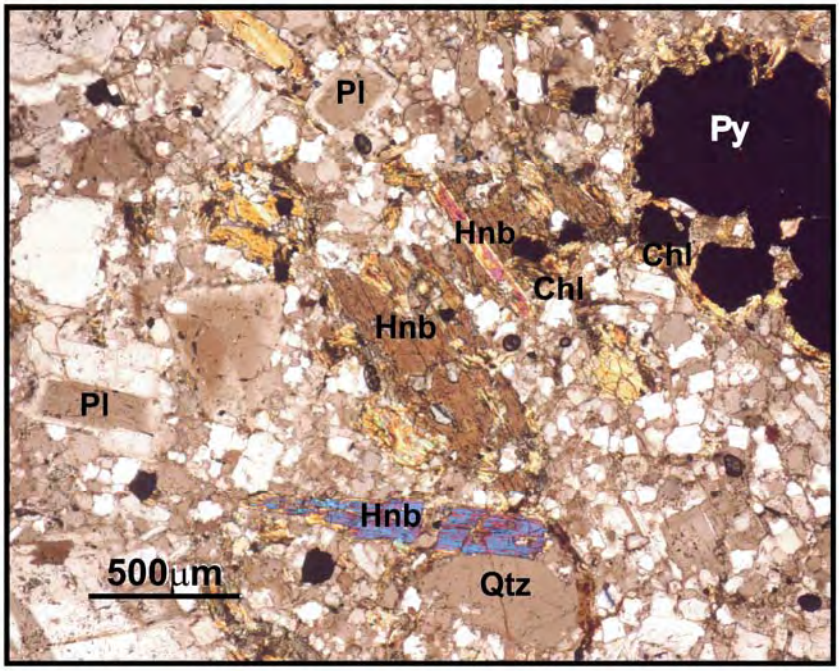

Figure 7. Photomicrograph of sample PH-A in cross polarized light from the Maricao Formation showing hornblende (Hnb), plagioclase (Pl), pyrite (Py), chlorite (Chl), and quartz (Qtz).

groundmass of quartz and sodic feldspar (Cox, 1985). The Tanamá deposit is hosted by a faulted tonalitic stock, with abundant quartz veins and disseminated chalcopyrite. Helecho is very similar to Tanamá. Reserves in the Tanamá deposit were estimated at approximately 126 million tons with 0.64% Cu (Table 1; Cox, 1985).

The largest deposit in the study area is Calá Abajo (1200 m x 200 m), followed by Piedra Hueca (450 m x 250 m), and Sapo Alegre (500 m x 100 m). The ages of the deposits are estimated to be between 35 to 43.1 Ma for Piedra Hueca, between 39.1 to 43.7 Ma for Calá Abajo, and between 41.8 to 42.1 Ma for Sapo Alegre (Barabas, 1982). Piedra Hueca is described as a strongly silicified porphyry; it contains chalcopyrite, pyrite, molybdenite, magnetite, potassium feldspars, and hydrothermal biotite, chlorite and laumontite. It is weakly fractured, and leaching and secondary enrichment are negligible (Bradley, 1971). The reserves of Piedra Hueca were estimated at about 33 million tons averaging 0.82% Cu (Lutjen, 1971).

Calá Abajo is associated with a tubular shaped intrusion that is highly fractured. It has been recrystallized, albitized, sericitized, chloritized, and pyritized, magnetite is abundant and both hydrothermal biotite and potassium feldspar are absent (Bradley, 1971). Reserves of Calá Abajo are about

Table 1. Characteristics of the Río Tanamá and Río Viví porphyry copper deposits.

Name	Map Area (m)	Tonnage and Grade	Host Rock	Assemblage Alteration
Piedra Hueca	450 x 250	33 million tons 0.82 % Cu (Cox et al., 1973)	Volcaniclastic sandstones, mudstones and basaltic lava	Chalcopyrite, pyrite, molybdenite magnetite, K-feldspars, hydrothermal biotite, chlorite and leonhardite, it is weakly fractured, strongly silicified; leaching and secondary enrichment are negligible (Bradley, 1971).
Calá Abajo	1200 x 200	71 million tons 0.82% Cu (Cox et al., 1973)	Lapilli tuff, and vitric tuff with trachitic fragments of andesite, dacite, and locally diorite or gabbro	Recristalized, albitized, sericitized, chloritized and piritized, magnetite is abundant and both hydrothermal biotite and K-feldspar are absent (Bradley, 1971).
Sapo Alegre	500 x100	Small	Volcaniclastic sandstones, mudstones and basaltic lava	Hydrothermally altered quartz diorite, varying amounts of pyrite, chalcopyrite and molybdenite (Cox et al., 1975).
Tanamá	750 x 800	126 million tons 0.64% Cu (Cox, 1985)	Lenticular flows of basalt interbedded with lenticular flows of andesite, volcanic sandstone and siltstone (Nelson et al.,1968)	Abundant quartz veins, disseminated chalcopyrite and a secondary-enrichment blanket containing various copper sulfide minerals (Cox, 1985).
Helecho	500 x 625	Small	Volcaniclastic breccia and tuffaceous sandstone siltstone and mudstone. Widely saprolitized (Krushensky et al., 1984)	Disseminated chalcopyrite associated with magnetite in feldspar-stable alteration assemblage (Cox,1985).

71 million tons with 0.82% Cu (Lutjen, 1971).

Sapo Alegre is a small porphyry copper-molybdenum prospect characterized by distinct zones of alteration and mineralization in a quartz diorite porphyry (Cox et al., 1975). At this deposit, a sericitic alteration zone with a low chalcopyrite to pyrite ratio and low copper values is adjacent to a biotitic alteration zone containing abundant chalcopyrite and molybdenite (Bradley, 1971).

Chapter 3

Sampling and Methods

In order to document and understand the geochemical signatures surrounding the unmined porphyry copper deposits near Adjuntas samples of representative rock types, stream sediments, and waters were collected. The water was sampled from surface waters, shallow ground-water seeps, and springs. Satellite-based spectral images (IKONOS) of the area were also examined.

Sampling Sites

Sample sites for waters, stream sediments, and rocks were selected throughout the Río Viví and Río Pellejas watersheds to provide a representative characterization of the region within and downstream of the area affected by hydrothermal activity and outside the area. Sample sites are shown in Figure 3.

A total of 39 water samples were collected from eleven sites from the watersheds during May 2003, September 2003, and January 2004, to contrast base and peak-flow conditions. In addition duplicate samples and field blanks were collected to monitor the quality of the data and sampling methods. Eight stream-sediment samples were collected in May 2003. Ten samples of major rock types were collected in the study area.

The water-sampling field methods are based on those outlined by Ficklin and Mosier (1999) which are consistent with EPA approved protocols. Water samples were collected in one liter polyethylene bottles that were first doubly

rinsed with sample water. Each water sample was divided into four splits: two for cation analysis (one filtered and one unfiltered), one for anion analysis, and one for alkalinity. Samples were filtered on site through 0.45 μm nitrocellulose filters. Cation samples were stored in acid washed polyethylene bottles and were preserved by acidification using ultra pure, concentrated nitric acid. Anion and alkalinity water samples were stored in non-acid washed polyethylene bottles and refrigerated until the analyses were performed. On-site measurements including water and air temperature, specific conductance, pH, dissolved oxygen, dissolved ferrous iron and total iron, dissolved nitrate and water flow. Sample sites are described below.

Description of the sample sites

Water and sediment samples of PRRV-1 of Río Viví were obtained from the main channel near a small bridge at Hacienda la Esperanza, this sample site is upstream of the Sapo Alegre deposit (Figs. 3 and 8a). Sample site PRRV-2 is located downstream of the Sapo Alegre and Piedra Hueca deposits; the water and sediment samples were collected from the main channel (Figs. 3 and 8b) upstream of its confluence with a small tributary entering from the east. PRRV-3 is located in a tributary to the east of PRRV-2, where water, sediment and rock samples were collected (Figs. 3 and 8c). Water, sediment and rock samples PRRV-4 were collected from a tributary that is downstream of Sapo Alegre and upstream of sample sites PRRV-3 and PRRV-2 (Figs. 3 and 8d). PRRV-5 was obtained along Road 605 from the southern of two small PVC pipes installed by

local people to collect potable water from a ground-water seepage (Figs. 3 and 8e). This sample site is located downstream of the Sapo Alegre deposit.

Water, sediment, and rock samples were collected from the main stem of the Río Pellejas downstream of the Calá Abajo deposit at PRRP-1 (Figs. 3 and 9a). At sample site PRRP-2, downstream of Calá Abajo and upstream of Piedra Hueca, a water sample was obtained from a pipe along a dirt road off PR 605 which passes very close to Piedra Hueca, (Figs. 3 and 9b). Water sample PRRP-3 was collected from a shallow spring, flowing to a pipe. This site is located upstream of Piedra Hueca along a dirt road close to sample site PRRP-2 and to the Piedra Hueca deposit (Figs. 3 and 9c). Sample sites PRRP-4 and PRRP-5 are in the most southern tributaries of the Río Pellejas and are upstream of the Calá Abajo and Piedra Hueca deposits. At PRRP-4 water, sediment, and rock samples were collected from a tributary close to PR Road 521 in the town of Adjuntas (Figs. 3 and 9d). Sample site PRRP-5 is located to the west across PR Road 521, where water, sediment, and rock samples were collected (Figs. 3 and 9e). PRPP-6 was collected from the main channel of the Río Pellejas, downstream of the Calá Abajo and Piedra Hueca deposits, close to a dirt road connected to PR Road 524 near Central Pellejas (Figs. 3 and 9f).

Geochemistry and Mineralogy

The pH was measured using a Thermo Orion 230 pH meter calibrated against buffer solutions of pH 7 and pH 4. Conductivity was measured using an

a. PRRV -1, May 13, 2003

b. PRRV-2, May 13, 2003

c. PRRV-3, September 16, 2003

d. PRRV-4, September 16, 2003

e. PRRV-5, September 16, 2003

Figure 8. Sample sites in the Río Viví area. **a.** Río Viví near Hacienda la Esperanza looking upstream. **b.** Río Viví upstream of confluence with tributary (PRRV-3). **c.** Small tributary of Río Viví, looking upstream. **d.** Tributary of Río Viví down side Road 605, looking upstream. **e.** Río Viví, pipes along Road 605 in the town of Utuado.

Orion Model 115 conductivity meter calibrated with a standard with a conductivity of 1413 µS/cm. Dissolved oxygen concentration was obtained using Chemetrix high-range colorimetric ampoules. The concentrations of dissolved ferrous and total iron were determined using a phenanthroline (5144-81-8) indicator with a Hach DR2000 spectrophotometer. Nitrate was measured using a Hach DR2000 spectrophotometer with the cadmium-reduction indicator technique. Alkalinity was determined by the Gran titration using 0.18N H_2SO_4. Cations were analyzed at the U.S. Geological Survey (Central Mineral Resources Team) laboratories in Denver, CO, by inductively-coupled plasma mass spectrometry (ICP-MS; Lamothe et al., 2002) and by inductively-coupled plasma atomic emission spectroscopy (ICP-AES; Briggs and Meier, 2002). Cation data for 44 elements were obtained, including all of the major elements (Na, K, Ca, Mg, Mn, Al, Fe), most of the trace metals (except Hg), and the rare earth elements (La, Ce, Pr, Nd, Sm, Eu, Gd, Tb, Dy, Ho, Er, Tm and Yb). In general, ICP-MS is more useful for determining trace-element concentrations in the parts per billion range (ppb), whereas ICP-AES is more accurate for major elements that are in parts per million (ppm). Anions including sulfate, chloride and fluoride were analyzed using ion chromatography at the U.S. Geological Survey Laboratories in Ocala, Florida.

Stream-sediment samples collected at water-sampling sites, and rock samples collected in the study area, were analyzed with X -ray diffraction (XRD), optical microscopy, scanning electron microscopy (SEM), electron microprobe, and by bulk geochemical analytical techniques (ICP-AES). Sediment samples

Figure 9. Sample sites in the Río Pellejas watershed. **a.** Río Pellejas, looking downstream. **b.** Pipe at Río Pellejas, close to Piedra Hueca deposit. **c.** Shallow spring in Río Pellejas that flows into a pipe. **d.** Most southern tributary of Río Pellejas; sample was obtained close to Road 521. **e.** Río Pellejas, sample obtained close to Road 521, looking upstream. **f.** Río Pellejas, looking downstream of the main channel, close to Hacienda Pellejas.

were obtained from seven locations (Fig. 3). Thin sections were also prepared from the rock samples described in the previous section. For the XRD analysis,sediment samples were dried, sieved (80-mesh), and pulverized to 1 to 5 micrometers in a McCrone micronizer. Samples were processed using a Scintag X1 automated powder diffractometer equipped with a Peltier detector and CuKα radiation. Patterns were analyzed using the Material Data Inc.'s JADE software. The scanning electron microscope used was a JEOL JSM-840 equipped with a back-scattered electron (BSE) detector, a secondary electron (SE) detector, and a PGT X-ray energy-dispersive system (EDS). Samples were carbon coated and examined at a voltage of 15 kV and a specimen current of 1 to 2 nA. For microprobe analysis, the samples were first carbon coated and then analyzed using a JEOL-JSX8900 at the USGS laboratories in Reston, VA. This microprobe has five wavelength-dispersive spectrometers, and is operated at 15 kV for silicate minerals and at 20 kV for sulfide minerals.

The software PHREEQC was used to model the equilibrium speciation and saturation state of the waters (Parkhurst and Appelo, 1999). This computer program simulates chemical reactions and transport processes in both natural and contaminated water. The program is based on equilibrium chemistry of aqueous solutions interacting with minerals, gases, and solid solutions; it is capable of modeling exchange and sorption reactions. It also includes the capability for inverse modeling of water chemistry.

Remote Sensing

The IKONOS satellite image used in this study was collected on 2001 and is part of the Adjuntas quadrangle (Fig.10). This image was pre-processed by the company to generate four spectral bands with 1 meter of spatial resolution. The Image was processed with the software ENVI 3.6 at the Geological and Environmental Remote Sensing Laboratory (GERS Lab) of the University of Puerto Rico, Mayagüez, Department of Geology. ENVI (Environment for Visualizing Images) is a processing system designed to provide comprehensive analysis of satellite and aircraft remote sensing data (RSI, Inc., 2004).

The Normalized Difference Vegetation Index (NDVI) was used to measure the vigor of vegetation. It is obtained using the algorithm:

$$NDVI = \frac{(NIR - R)}{(NIR + R)} \quad \textbf{(1)}$$

Where NIR is the near-infrared value and R is the value for the red band.

Good values of NDVI result in a number that ranges from zero (0) to one (1). Values close to 0.8 - 0.9 indicate increasing amounts of green vegetation. Values near zero indicate low vegetation or non- vegetated features such as rock, soil, water, snow, ice, and clouds. NDVI is a useful technique because it provides a crude approximation of vegetation health and a means of monitoring changes in vegetation.

The first step with the image was the radiometric calibration. This was performed using a specific coefficient for each of the IKONOS bands; for blue 728, green 727, red 949 and near infrared 843 (Space Imaging, 2001).

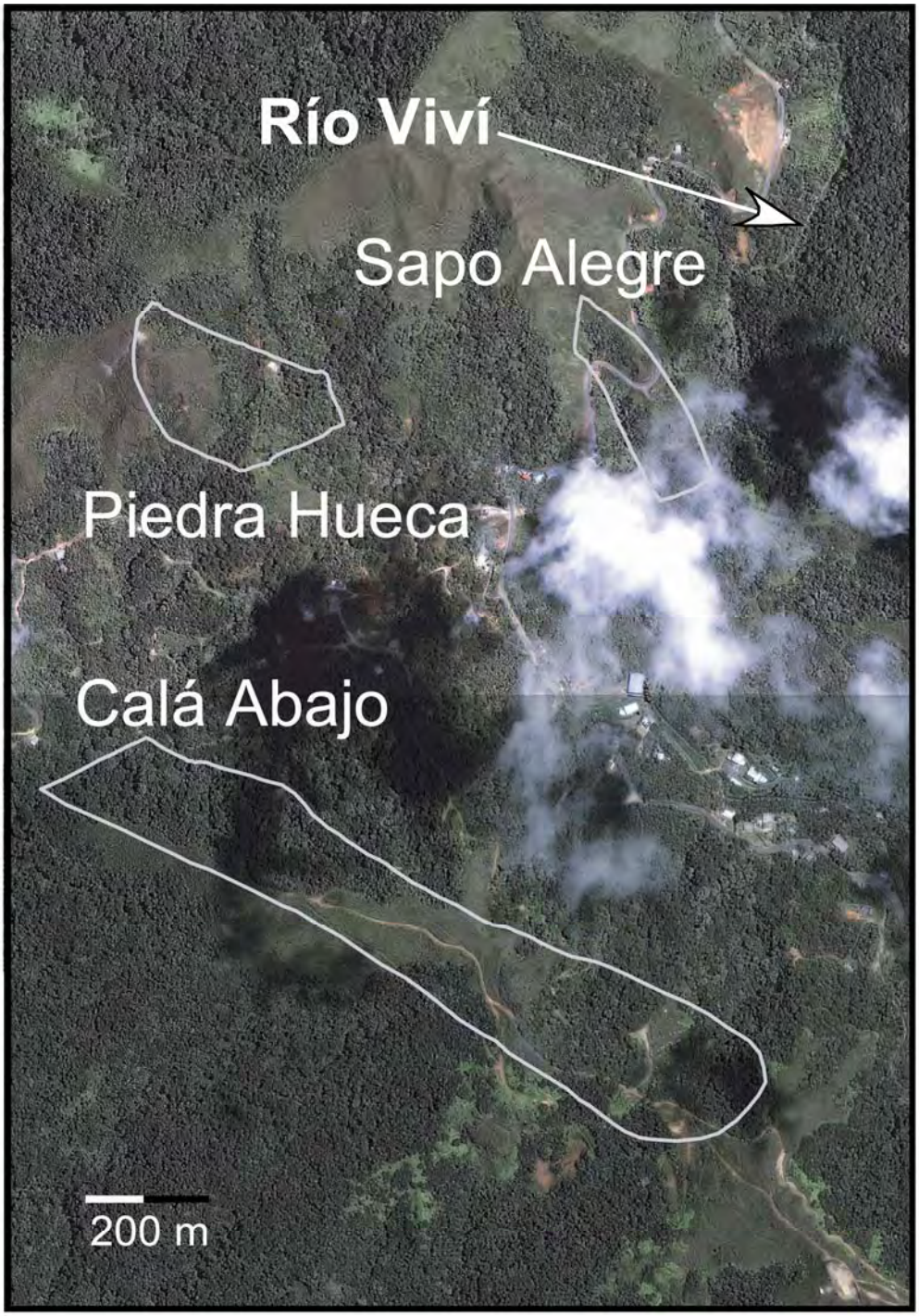

Figure 10. IKONOS image of the studied area, displaying the three porphyry copper deposits.

$$Band\ radiance = \frac{Float(b1)}{Coefficient} \quad \textbf{(2)}$$

where (b1) is the band and coefficient unit is DN*cm2*sr/mW.

An atmospheric correction was performed as second step using the dark pixel subtraction method. After processing the image, several regions of interest were created. Each region of interest measured 900 m^2 or 30 m x 30 m. The purpose of the selection process was to obtain from each region a characteristic value of (NDVI). Regions of interest were located within the boundaries of the deposits and outside of the deposits to establish a relationship between mineralized and non-mineralized areas (Fig. 11).

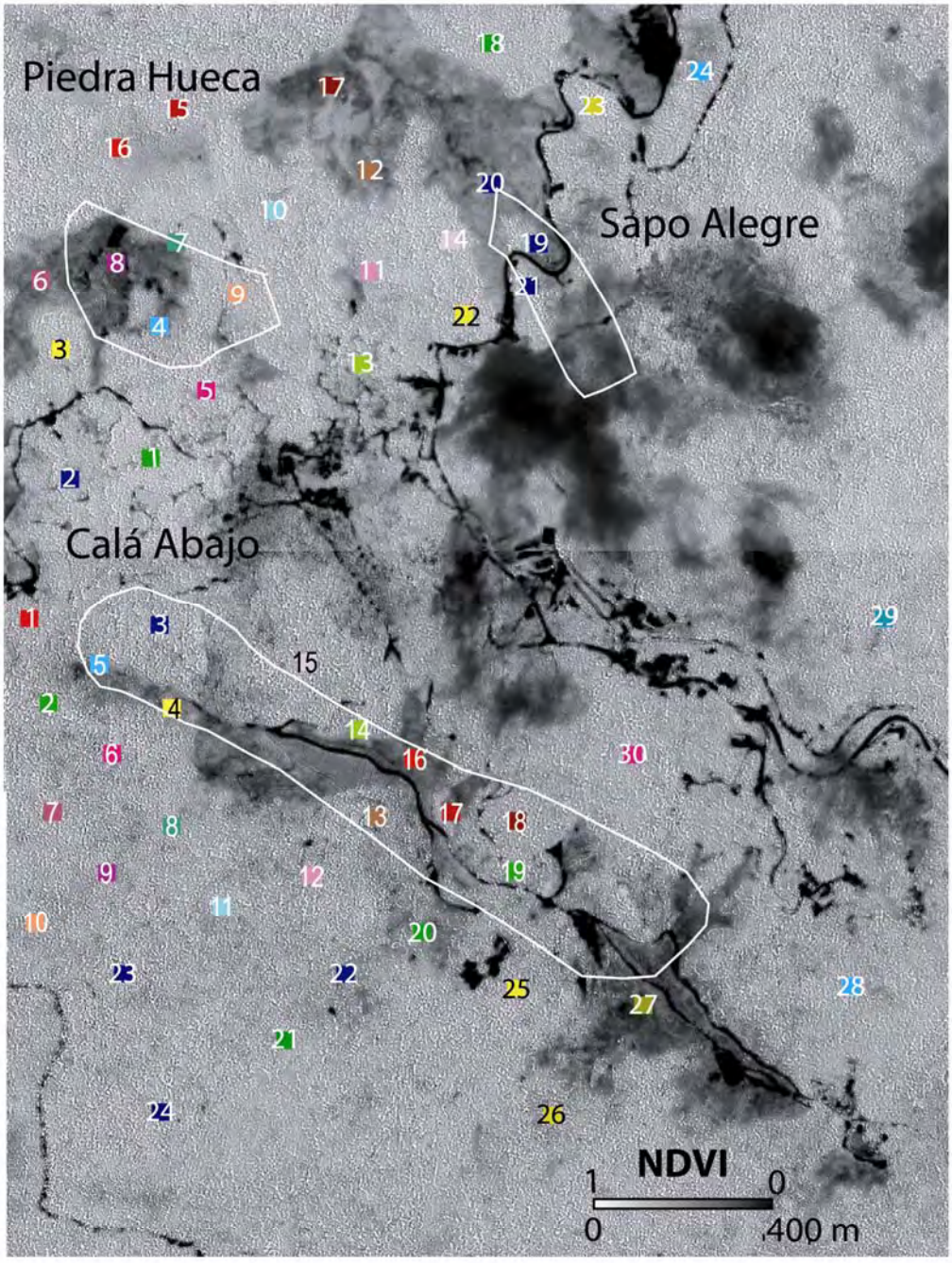

Figure 11. NDVI image showing the deposits and the regions of interest represented by the polygons.

Chapter 4

Results

This chapter will present the results for the water chemistry, stream-sediment chemistry, stream-sediment mineralogy, mineral chemistry, and remote sensing**.** Complete bulk chemical analysis for water samples can be found in Appendices IA-IC, Tables 2, 5 and 6 summarize the ranges for selected variables of the watersheds during the three sampling periods.

Water chemistry

Upstream samples

There are two upstream sites in the Río Pellejas watershed, PRRV-4 and PRRP-5, which are distant from the porphyry copper deposits: there is only one sample site upstream of the deposits in the Río Viví watershed, PRRV-1. This site is relatively close to the deposits as compared to those in the Río Pellejas watershed. The pH for upstream samples for both rivers ranged uniformly from 7.5 to 8.4, and conductance values ranged from 119 to 236 µS/cm (Table 2). Dissolved oxygen concentrations of unfiltered water samples, in Río Pellejas ranged from 7 to 10 mg/kg; this constitutes conditions that ranged from 80 to more than 100% saturation (Ficklin and Mosier, 1999). Río Viví has dissolved oxygen values for unfiltered samples, which ranged from 7 to 8 mg/kg; which ranged from 80 to 91% saturation. Upstream sample sites from Río Pellejas and Río Viví are dominated mostly by calcium, sodium and chloride. Other important cations for the upstream sites include Mg and K, which along with

Table 2 a. Field parameters and major anions and cations for to sample sites upstream of the porphyry copper deposits for the Río Pellejas and Río Viví watersheds.

Site	Parameter	May 2003	September 2003	January 2004	Site	May 2003	September 2003	January 2004
Río Pellejas					**Río Viví**			
PRRP-4	*pH*	7.95	7.48	7.5	**PRRV-1**	8.41	7.64	7.74
	SC(µS/cm)	144	119	139		236	197	207
	DO(mg/L)	7	9	10		8	7	7
	Alkalinity(mg/L)	40.3	34.6	37.2		64.41	33.4	28.81
	SO_4 (mg/L)	0.80	2.2	1.6		31	28	26
	F (mg/L)	<0.1	<0.1	<0.1		<0.1	<0.1	<0.1
	Cl (mg/L)	2.30	4.9	5.1		8	7	7.7
	Al (mg/L)	0.004	0.013	0.007		0.014	0.023	0.042
	Ca (mg/L)	16.6	13.7	14.9		25.2	19.5	19.4
	Cd (mg/L)	<0.00002	<0.00002	<0.00002		<0.00002	<0.00002	<0.00002
	Cu (mg/L)	<0.0005	<0.0005	<0.0005		0.0019	0.0024	0.0143
	Fe (mg/L)	0.0069	<0.001	<0.05		0.0072	0.018	<0.05
	K (mg/L)	1.3	1.4	1.1		1.5	1.8	1.4
	Mg (mg/L)	3.9	3.2	3.5		7.2	5.9	6.3
	Mn (mg/L)	0.00029	0.00036	0.0005		0.0033	0.0065	0.009
	Na (mg/L)	7.6	6.4	7.2		10.8	7.9	9.2
	Si (mg/L)	14.7	12.9	14.5		13.4	13	14.9
	Zn (mg/L)	0.0016	0.00052	<0.0005		0.0011	0.0014	0.0082

Table 2 b. Field parameters and major anions and cations for to sample sites upstream of the porphyry copper deposits for the Río Pellejas and Río Viví watersheds.

Sites	Parameter	May 2003	September 2003	January 2004
Río Pellejas PRRP-5	pH	7.72	7.79	7.67
	SC(µS/cm)	218	216	208
	DO(mg/L)	7	5	8
	Alkalinity(mg/L)	75.1	59.9	39.3
	SO_4 (mg/L)	2.7	5	3.7
	F (mg/L)	<0.1	<0.1	<0.1
	Cl (mg/L)	4.5	7.3	7.5
	Al (mg/L)	0.006	0.0076	0.009
	Ca (mg/L)	23.3	22	20.9
	Cd (mg/L)	<0.00002	<0.00002	<0.00002
	Cu (mg/L)	<0.0005	<0.0005	<0.0005
	Fe (mg/L)	0.0084	0.0088	<0.05
	K (mg/L)	0.89	1.1	0.96
	Mg (mg/L)	6.8	6.4	5.8
	Mn (mg/L)	0.00063	0.0012	0.0034
	Na (mg/L)	9.1	8.4	8.3
	Si (mg/L)	16.4	15.6	15.4
	Zn (mg/L)	0.0023	0.00055	0.0011

Ca and Na had the highest concentration in the study area in Río Viví during May 2003. In Río Pellejas, the water hardness ranged from 47.4 to 86.1 mg/L $CaCO_3$ equivalent, in Río Viví the range was between 76.5 to 105 mg/L $CaCO_3$ equivalent (Fig. 12). Arsenic, Cd, Cr, and Pb, were mostly below the detection limits for both rivers during the three sampling periods. Copper and nickel had concentrations below the detection limits for Río Pellejas during the three sampling periods, but Río Viví had Cu values that ranged from 0.0019 to 0.0143 mg/L, and Ni values that ranged from <0.0001 to 0.0004 mg/L for May 2003, September 2003, and January 2004.

In general, upstream concentrations of Fe, Al, Mn, Co, and Mo were higher in Río Viví than in Río Pellejas (Fig. 12). In the Río Pellejas, Fe ranged from <0.001 to 0.0088 mg/L, in the Río Viví it ranged from <0.05 to 0.018 mg/L. Aluminum concentrations in Río Pellejas ranged from 0.004 to 0.013 mg/L; in Río Viví, they ranged from 0.014 to 0.042 mg/L. Manganese concentrations in Río Pellejas ranged from 0.00029 mg/L to 0.0034 mg/L; in Río Viví, concentrations varied from 0.0033 to 0.009 mg/L. Cobalt concentrations in Río Pellejas were below detection limits during all three sampling periods. Cobalt concentrations in Río Viví were below detection limits during May and September but reached 0.00017 mg/L during January. Finally, molybdenum concentrations in Río Pellejas and Río Viví ranged, during May and September from 0.000075 to 0.00024 mg/L, and from 0.00019 to 0.00032 mg/L, respectively. For both rivers, molybdenum concentrations in January were below detection. Zinc contents

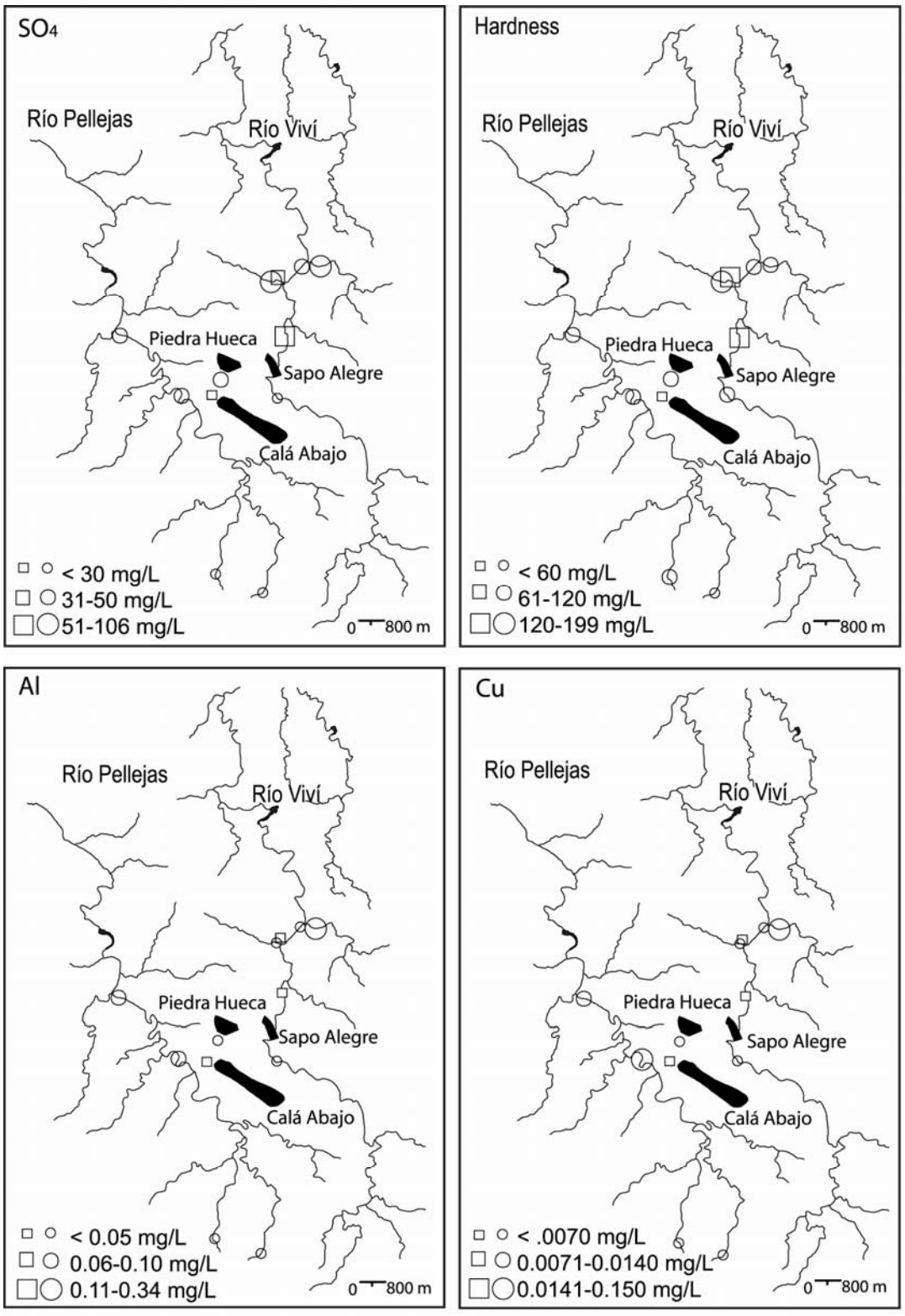

Figure 12. Maps showing concentrations of some cations, anions and hardness of water for surface (circles) and groundwater sites (squares).

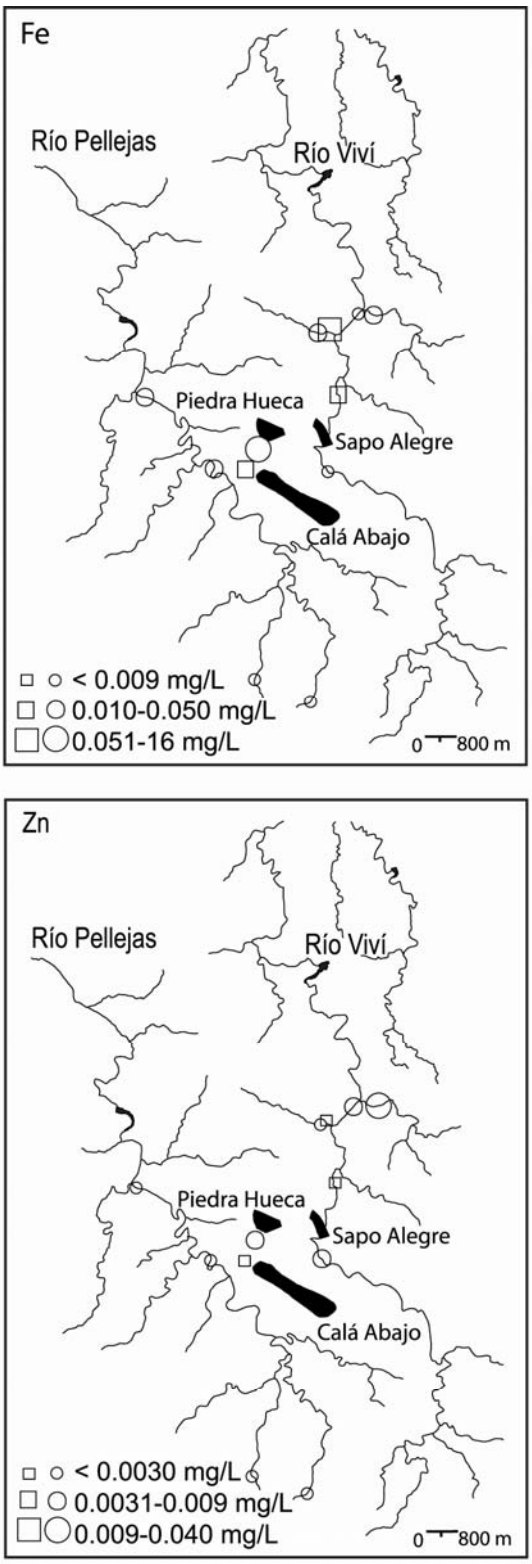

Figure 12 Cont. Maps showing concentrations of selected cations, anions and hardness of water for surface (circles) and groundwater sites (squares).

were higher in Río Pellejas only during May; in September and January, samples with higher concentrations of zinc were collected in Río Viví (Table 2, Fig. 12).

The anionic species analyzed included alkalinity, sulfate, chloride, and fluoride. Alkalinities ranged from 34.6 to 75.1 mg/L $CaCO_3$ in the Río Pellejas, and in the Río Viví from 28.8 to 64.4 mg/L. Among the analyzed anions, fluoride was below the detection limits during the three sampling periods for both watersheds. Sulfate and chloride concentrations were notably higher in Río Viví than in Río Pellejas. For Río Pellejas sulfate values fluctuated between 0.80 and 5 mg/L, whereas for Río Viví they varied between 26 and 31 mg/L (Fig. 12). Chloride in Río Pellejas ranged from 2.30 to 7.5 mg/L, in Río Viví the range was between 7 and 8 mg/L (Table 2). It is important to recall that the Río Pellejas upstream samples are closer to the source area, compared to the Río Viví water sample, which is far from the starting point and closer to the deposits; this in part may relate to the higher concentration of dissolved solids in Río Viví at the samples sites.

Water samples were obtained from the main trunk of the river channels, from small tributaries and from pipes tapping shallow ground waters. Analytical results are presented in Appendix IA-IC. As discussed previously, Puerto Rico has two main seasons, the dry and rainy periods.

None of the element concentrations of the upstream samples of both watersheds exceeded the water-quality criteria (Table 4), but the closest value to these parameters was found in sample site PRRV-1 for Al, with a concentration of 0.041 mg/L; the water-quality standard establishes that the Al concentration

Table 3. Flow measurements obtained during the three sample periods. Blank spaces (/) were values not obtained.

Samples	Description	May flow 2003 *(L/s)*	September flow 2003 *(L/s)*	January flow 2004 *(L/s)*
PRRP-4	Upstream Calá Abajo and Piedra Hueca deposits	0.50	2.95	1.33
PRRP-5	Upstream Calá Abajo and Piedra Hueca deposits	24.8	11.28	35.1
PRRP-1	Downstream Calá Abajo deposit	/	414	479
PRRP-2	Groundwater	/	0.10	/
PRRP-3	Downstream Calá Abajo deposit	/	0.16	/
PRRP-6	Downstream Calá Abajo and Piedra Hueca deposits	540	306	483
PRRV-1	Upstream Sapo Alegre	194	262	234
PRRV-5	Groundwater	0.02	.02	0.02
PRRV-4	Downstream Sapo Alegre and Piedra Hueca	/	5.25	87.3
PRRV-4SP	Downstream Sapo Alegre and Piedra Hueca	/	/	/
PRRV-2	Downstream Sapo Alegre and Piedra Hueca	/	167	451
PRRV-3	Downstream Sapo Alegre and Piedra Hueca	56.46	46.25	136

.

range must be less than 0.05 mg/L.

Downstream samples

The pH of the downstream samples of the Río Pellejas watershed ranged from 7.2 to 8.5 and from 7.1 to 8.0 for the groundwater sites (Tables 5 and 6). The pH for the Río Viví ranged from 5.1 to 8.9 and from 6.5 to 7.9 for the groundwater sites downstream of the porphyry copper deposits. Specific conductance for Río Pellejas ranged from 221 to 298 µS/cm and from 102 to 121 µS/cm for the groundwater sites in the watershed, whereas that for Río Viví ranged from 198 to 390 µS/cm and from 412 to 475 µS/cm for the groundwater sites in the watershed. Dissolved oxygen for surface waters in Río Pellejas ranges from 3 to 10 mg/L, this is a saturation that ranged from 35% to more than 100%. For the groundwater sites the range is between 7 and 8 mg/kg, which is 80 to 90% of saturation. In the Río Viví dissolved oxygen ranged from 7 to 10 mg/L, which represents saturation of 80 to 100%. Groundwater sites in Río Viví had dissolved oxygen concentrations that range from 2 to 8 mg/L, which represents saturation of 23 to 90%. The most extreme pH measurements were found in a single site, PRRV-3; this site had the lowest pH during the three sample periods, 6.0 in May, 5.7 in September and 5.1 in January.

Table 4. Water-quality data for Río Viví and Río Pellejas during the three sampling collection. Values selected were the highest from the dissolved data of each river. Values in bold italics exceed water-quality standards.

Constituent	Río Pellejas May mg/L	Río Viví May mg/L	Río Pellejas September mg/L	Río Viví September mg/L	Río Pellejas January mg/L	Río Viví January mg/L	Drinking Water Standard* mg/L
Sulfate	62.0	110	61.0	120	54.0	90.0	500
Aluminum	***0.10***	***0.56***	***0.07***	***0.09***	***0.13***	***0.90***	0.05-0.02
Arsenic	<0.002	<0.002	0.0004	0.003	<0.001	0.003	0.01
Barium	0.02	0.047	0.01	0.04	0.02	0.19	2
Beryllium	<0.00005	0.0001	<0.00005	0.0001	0.00005	.0001	0.004
Cadmium	<.00002	0.0002	<.00002	0.0003	0.0001	0.0002	0.005
Chromium	0.001	0.001	<0.001	<0.001	0.001	<0.001	0.1
Copper	0.01	0.13	0.01	0.09	0.02	0.20	1.3
Fluoride	0.10	0.10	0.10	0.20	0.10	0.10	4
Iron	***0.14***	0.02	0.02	0.05	0.05	***15.9***	0.3
Lead	0.00006	0.0002	<0.00005	0.00007	<0.000005	0.0001	0
Manganese	0.05	***0.13***	0.007	***0.14***	0.02	***5.73***	0.05
Nickel	<0.0001	0.002	<0.0001	0.0024	0.0004	0.0026	0.1
Selenium	0.00024	0.0005	<0.0002	<0.0002	0.002	<0.001	0.05
Silver	0.00004	<0.00001	<0.00001	<0.0001	<0.003	<0.003	0.1
Thallium	0.00008	<0.00005	<0.00005	<0.00005	<0.0001	<0.0001	0.0005-0.002
Zinc	0.004	0.03	0.002	0.04	0.02	0.03	5

*Water quality criteria after U.S. EPA 2005, values are used by the Puerto Rico Department of Health (PRDOH).

Table 5 a. Field parameters and major anions and cations (dissolved) from samples sites downstream of the porphyry copper deposits in Río Pellejas and Río Viví.

Site	Parameter	May 2003	September 2003	January 2004	Site	May 2003	September 2003	January 2004
Río Pellejas					**Río Viví**			
PRRP-1	*pH*	8.57	7.74	7.82	**PRRV-4**	8.01	7.66	7.76
	SC(µS/cm)	298	233	221		377	390	200
	DO(mg/L)	9	7	10		7	7	8
	Alkalinity(mg/L)	68.2	39.36	27.39		39.42	47.89	22.31
	SO_4 (mg/L)	51	35	26		96	99	60
	F (mg/L)	<0.1	<0.1	<0.1		0.1	0.1	0.1
	Cl (mg/L)	9.1	7.5	8.6		12	11	9.9
	Al (mg/L)	0.052	0.07	0.126		0.0025	0.007	0.0202
	Ca (mg/L)	35.8	25.5	20.9		41.1	42.2	24.6
	Cd (mg/L)	<0.00002	<0.00002	<0.00002		<0.00002	0.00002	0.00003
	Cu (mg/L)	0.01	0.011	0.024		0.0024	0.0028	0.0052
	Fe (mg/L)	0.036	0.018	<0.05		0.022	0.042	<0.05
	K (mg/L)	1.6	2	1.8		2.6	3.1	2.6
	Mg (mg/L)	8.5	6.6	5.9		10.9	11.2	7.2
	Mn (mg/L)	0.0058	0.0068	0.0143		0.019	0.038	0.0553
	Na (mg/L)	12	9.4	9.1		15.8	15.1	12.8
	Si (mg/L)	17	14.6	13.8		16.8	15.7	16.7
	Zn (mg/L)	0.004	0.0014	0.0033		0.0018	0.0014	0.0008
PRRP-3	*pH*	7.54	7.79	7.27	**PRRV-2**	8.86	7.61	7.95
	SC(µS/cm)	272	255	239		246	198	222
	DO(mg/L)	3	7	8		10	7	8
	Alkalinity(mg/L)	48.13	31.93	23.6		64.1	27.9	33.5
	SO_4 (mg/L)	62	61	54		42	34	37
	F (mg/L)	0.1	0.1	0.1		<0.1	<0.1	<0.1

Table 5 b. Field parameters and major anions and cations (dissolved) from samples sites downstream of the porphyry copper deposits in Río Pellejas and Río Viví.

Site	Parameter	May 2003	September 2003	January 2004	Site	May 2003	September 2003	January 2004
Río Pellejas	*Cl (mg/L)*	6.3	6	6	*Downstream*	8.1	7.1	7.9
PRRP-3	*Al (mg/L)*	0.1	0.0017	0.0038	**PRRV-2**	0.026	0.037	0.103
	Ca (mg/L)	26.6	26.4	22.4		25.7	20.3	19.3
	Cd (mg/L)	<0.00002	<0.00002	0.00005		<0.00002	0.00002	0.00003
	Cu (mg/L)	*0.0032*	0.002	0.0083		0.0037	0.0048	0.0118
	Fe (mg/L)	*0.14*	<0.001	<0.05		0.012	0.015	<0.05
	K (mg/L)	2.9	2.6	2.4		1.7	1.9	1.6
	Mg (mg/L)	*7.8*	8	6.6		7.7	6.3	6.9
	Mn (mg/L)	*0.05*	0.00027	0.0031		0.0017	0.0065	0.0187
	Na (mg/L)	*9.3*	9.3	8.3		10.7	8	9.3
	Si (mg/L)	*17.6*	18.3	16.4		12.8	12.2	14.2
	Zn (mg/L)	*0.0021*	0.0017	0.071		0.00083	0.0017	0.0026
PRRP-6	*pH*	*8.34*	7.93	7.83	**PRRV-3**	6.04	5.68	5.12
	SC(µS/cm)	*298*	272	260		296	303	244
	DO(mg/L)	*7*	8	8		8	7	8
	Alkalinity(mg/L)	*63.4*	52.72	36.5		64.4	-2.37	-0.71
	SO_4 (mg/L)	*50*	42	40		110	120	90
	F (mg/L)	*<0.1*	<0.1	<0.1		0.1	0.1	0.1
	Cl (mg/L)	*8.4*	8.2	8.6		7.7	7.8	7.7
	Al (mg/L)	*0.058*	0.06	0.123		0.056	0.089	0.895
	Ca (mg/L)	*35.7*	29.2	24		41.1	28.2	19.6
	Cd (mg/L)	<0.00002	<0.00002	0.00005		<0.00002	0.00029	0.00015
	Cu (mg/L)	*0.0059*	0.0052	0.015		0.0024	0.088	0.204
	Fe (mg/L)	*0.039*	0.026	0.052		0.022	0.046	0.088

Table 5 c. Field parameters and major anions and cations (dissolved) from samples sites downstream of the porphyry copper deposits in Río Pellejas and Río Viví.

Site	Parameter	May 2003	September 2003	January 2004	Site	May 2003	September 2003	January 2004
Río Pellejas	*K (mg/L)*	*1.8*	2.1	1.5	*Downstream*	2.6	1.9	1.8
PRRP-6	*Mg (mg/L)*	*9.2*	7.8	7.2	**PRRV-3**	10.9	6.8	5.4
	Mn (mg/L)	*0.0053*	0.0059	0.0158		0.019	0.14	0.113
	Na (mg/L)	*12.2*	10.4	9.9		15.8	11.1	10.6
	Si (mg/L)	*16.1*	15.4	15.6		16.8	15.2	17.1
	Zn (mg/L)	*0.0023*	0.0016	0.0046		0.034	0.04	0.028

Table 6 a. Field parameters and major anions and cations (dissolved) related to groundwater sites for Río Pellejas and Río Viví downstream of the porphyry copper deposits.
*Sample collected during January only

Site	Parameter	May 2003	September 2003	January 2004	Site	May 2003	September 2003	January 2004
Groundwater					*Groundwater*			
PRRP-2	*pH*	7.82	7.95	7.06	**PRRV-5**	7.83	7.93	7.54
	SC(µS/cm)	121	110	102		412	432	411
	DO(mg/L)	8	7	7		8	6	7
	Alkalinity(mg/L)	/	15.4	5.86		123	104	82.3
	SO_4 (mg/L)	22	21	16		60	66	54
	F (mg/L)	<0.1	<0.1	<0.1		0.1	0.2	0.1
	Cl (mg/L)	6.3	6.2	6.3		8.9	10	8.8
	Al (mg/L)	0.0013	0.0031	0.007		<0.0001	0.0007	<0.002
	Ca (mg/L)	8	8.2	8		50.2	53.9	49.2
	Cd (mg/L)	<0.00002	<0.00002	<0.00002		<0.00002	0.00003	<0.00002
	Cu (mg/L)	0.0032	0.004	0.0043		0.0019	0.003	<0.0005
	Fe (mg/L)	0.006	<0.001	<0.05		0.0072	0.048	<0.05
	K (mg/L)	1.1	1.5	1.1		0.58	0.6	0.47
	Mg (mg/L)	3.4	3.2	3.4		13.1	14.1	12.5
	Mn (mg/L)	0.00047	0.00027	0.0009		0.0033	0.00006	<0.0002
	Na (mg/L)	7.3	6.6	7.3		16	16.2	15.4
	Si (mg/L)	14.2	13.5	14.2		11.9	11.3	11.7
	Zn (mg/L)	0.0014	0.0018	0.0024		0.0016	0.0014	0.001
	pH				**PRRV-4sp***			6.5
	SC(µS/cm)							475
	DO(mg/L)							2
	Alkalinity(mg/L)							123
	SO_4 (mg/L)							38

Table 6 b. Field parameters and major anions and cations (dissolved) related to groundwater sites for Río Pellejas and Río Viví downstream of the porphyry copper deposits.
*Sample collected during January only

Site	Parameter	May 2003	September 2003	January 2004	Site	May 2003	September 2003	January 2004
	F (mg/L)				*Groundwater*			0.1
	Cl (mg/L)				**PRRV-4sp**			11
	Al (mg/L)							<0.002
	Ca (mg/L)							62.8
	Cd (mg/L)							<0.00002
	Cu (mg/L)							<0.0005
	Fe (mg/L)							15.9
	K (mg/L)							5.8
	Mg (mg/L)							17
	Mn (mg/L)							5.73
	Na (mg/L)							14.4
	Si (mg/L)							15.3
	Zn (mg/L)							0.0008

The next site with the lowest pH is sample site PRRV-4sp with a pH of 6.5; this water was only sampled in January.

Complete chemical analyses are presented in Appendixes IA-IC. Most of the major cation concentrations between the two watersheds were similar during the three sampling periods. Calcium, Mg, Na and Si had the highest concentration in both rivers. In terms of base metals in the Río Pellejas watershed, Fe had concentrations of up to 0.052 mg/L in surface waters and up to 0.006 mg/L in shallow groundwater sites; Fe in the Río Viví watershed reached 0.088 mg/L and as high as 15.9 mg/L in groundwater seep PRRV-4sp. Iron was found mostly below the detection limits during January. Manganese concentrations in the Río Pellejas watersheds ranged to up to 0.05 mg/L in surface waters and 0.0009 mg/L for the groundwater site, whereas the Mn content in Río Viví was up to 0.113 mg/L in surface waters and for the groundwater sites, the highest concentration was 5.73 mg/L (PRRV-4sp). Lead concentrations were generally below the detection limit for both rivers, the highest concentration in Río Pellejas was 0.00006 mg/L and the highest for Río Viví was 0.00023 mg/L. The highest concentration of zinc in the Río Pellejas watershed was 0.071 mg/L for surface waters and 0.0024 mg/L for the groundwater site. In the Río Viví watershed, the Zn concentration reached 0.034 mg/L in surface water and 0.0016 mg/L for the groundwater sites. Molybdenum concentrations in the Río Pellejas watershed were generally low and mostly below the detection limit during January; values ranged up to 0.017 mg/L and 0.0005 mg/L at the groundwater site. In the Río Viví watershed, the highest Mo

concentration was 0.002 mg/L in surface waters and 0.0025 mg/L for the groundwater site. Aluminum in the Río Pellejas watershed ranged from 0.001 to 0.126 mg/L in surface waters, and from 0.0013 to 0.007 mg/L at the groundwater sites whereas in Río Viví ranged from 0.0025 to 0. 895 mg/L at site PRRV-3 in the Río Viví watershed. Values for the groundwater sites in the Río Viví watershed range from below detection up to 0.0007 mg/L. Copper concentrations in Río Pellejas samples ranged from 0.002 to 0.024 mg/L in surface waters and to 0.0038 mg/L for the groundwater site. Concentrations of copper for Río Viví were from 0.002 to 0.204 mg/L, whereas for the ground-water sites, the values ranged from below detection up to 0.001 mg/L. Nickel concentrations in Río Pellejas were mostly below detection for all the sample sites except for PRRP-3 in January with a Ni concentration of 0.0004 mg/L. Río Viví shows slightly higher Ni values, but concentrations below detection limits are common. Nickel concentrations ranged up to 0.0026 mg/L in surface water, whereas all the ground-water sites remained below detection limits. Similar to Ni, Co concentrations in Río Pellejas were low; many sites have values below the detection limits, for example all the groundwater sites. The highest concentration was found at site PRRP-6 with 0.00036 mg/L in January. In the Río Viví watershed, all ground-water sites have concentrations below detection limits; the highest concentration of Co among all the sites during the three periods was of 0.0067 mg/L at site PRRV-3 in September. Cadmium concentrations in Río Pellejas were below the detection limits for all sites during May and September whereas in January, two sites (PRRP-3 and PRRP-6) had the highest values of

0.00005 mg/L. Río Pellejas also had several sites with values below detection limits, but in general, the concentration of Cd in the Río Viví watershed was higher than that in the Río Pellejas, with values reaching to 0.00029 mg/L for surface waters and 0.000026 mg/L for groundwater.

The anionic species analyzed included alkalinity, sulfate, chloride, and fluoride. Alkalinity values as $CaCO_3$ equivalent for the Río Pellejas watershed ranged from 48.13 to 68.22 mg/L in May 2003, from 31.93 to 52.72 mg/L in September 2003, and from 23.57 to 39.87 mg/L in January 2004 (Table 5). In general, site PRRP-1 had the highest alkalinity values for surface water in Río Pellejas. The highest alkalinity value in groundwater sites in the Río Pellejas was found in September with a value of 15.4 mg/L at PRRP-2. For the Río Viví, the alkalinity values in surface waters ranged in May from 39.42 to 64.41 mg/L, in September from 27.99 to 47.89 mg/L, and in January from 22.31 to 33.5 mg/L. The highest alkalinity value for surface waters was at site PRRV-4 during September. For the groundwater, alkalinity ranged during the three periods from 82.19 mg/L in site PRRP-5 in January to 122.9 mg/L in sample site PRRP-5 in May. Sulfate concentrations in Río Pellejas ranged from 26 to 62 mg/L. This last value is from PRRP-3. For the groundwater site the sulfate concentration ranged from 16 to 22 mg/L. Sulfate concentrations in Río Viví were higher than in Río Pellejas. The concentration ranged from 34 to 120 mg/L in surface waters, whereas at the groundwater sites, the range was from 38 to 66 mg/L. The highest sulfate concentration was for site PRRV-3 during September. Chloride concentrations during the three sampling periods in Río Pellejas ranged from 6 to

9 mg/L for the surface water sites and from 6.2 to 6.3 mg/L for the groundwater sites. The highest concentration of chloride for surface waters was at site PRRP-1 in May. In Río Viví, chloride concentrations ranged from 7 to 12 mg/L in surface water and from 8.8 to 11 mg/L in the groundwater. The highest Cl concentration was for PRRV-4 in surface water and for PRRV-4sp in groundwater. Fluoride concentrations for the surface and groundwater in the Río Pellejas watershed was mostly below the detection limits except for sample site PRRP-3, which contained 0.1 mg/L. The concentration of fluoride in Río Viví watershed was below detection limit for the three sampling periods at the site PRRV-2; for the other surface-water sites and for the groundwater sites the fluoride concentration was 0.1 mg/L.

Relationship to Water-Quality Guidelines

Water quality is defined by the physical, chemical, biological and aesthetic characteristics of water. The importance of water quality is not only limited to human health, but also for other social and economical values, such as farming, fishing, tourism, recreation, and mining. Aquatic ecosystems can be severely impacted by acid-mine and acid-rock drainage. The solubility of some metals increases with lower pH, for example Cu, Zn, Cd, Co, Ni, and Pb, but other metals, such as Al and Fe^{3+}, are more soluble at both lower and higher pH with solubility minima at intermediate pH (Nordstrom and Alpers, 1999).

Water-quality standards are set to protect of both human health and aquatic ecosystems. The U.S. Environmental Protection Agency (EPA) has

established drinking water standards, known as Maximum Contaminant Levels (MCL), for various metals and other compounds such as Pb, Cu, Zn, Ni, Hg, Sb, As, and cyanide, among others. The EPA also established Secondary Maximum Contaminant Levels (MCLs), these are related to aesthetic aspects, such as taste, odor, or color (Smith and Huyck, 1999) and only applied to few compounds (Fe, Mn, Al, SO_4). These parameters are used by the Puerto Rico Department of Health (PRDOH). The toxicity to aquatic ecosystems of most divalent metals, such as Pb, Cu, Zn, and Cd, is dependent on the water hardness (Table 7, Smith and Huyck, 1999). Aquatic organisms are able to tolerate higher concentrations of metals in waters with higher hardness values. Water hardness expressed in mg/L $CaCO_3$ equivalent, is described by the formula:

$$Hardness = 2.5\,(Ca\ mg/L) + 4.1\,(mg/L)$$

In terms of the water quality of the Río Pellejas upstream from the deposits, during May 2003, three surface waters sites had values that exceeded the primary and secondary water-quality criteria for Al (0.05 - 0.02 mg/L); values ranged from 0.052 to 0.1 mg/L (Table 4). Site PRRP-3 was the one with the highest concentration. During September 2003 and January 2004, Al values also exceeded the primary and secondary water-quality parameters for two of the three upstream surface-water sites (PRRP-1 and PRRP-6), with values of 0.07 and 0.06 mg/L, respectively, for September, and 0.126 and 0.123 mg/L, respectively, for January. Aluminum concentrations also exceeded the water-quality parameters for some of the downstream surface-water samples from Río Viví. During May and September, site PRRV-3 exceeded the guideline with

Table 7. Acute and chronic water quality criteria based on average hardness of Río Viví and Río Pellejas downstream of the porphyry copper deposits.

Parameter	Human Health	Freshwater Aquatic Life					
	Drinking Water	Acute Toxicity[2] µg L^{-1}			Chronic Toxicity[2] µg L^{-1}		
	(MCL or MCLG[3]) µg L^{-1}	Acute Criterion[1]	X	Y	Chronic Criterion[1]	X	Y
Aluminum		750					
Antimony	50	9,000					
Arsenic	10	360					
Cadmium[1]	5	3.84	1.128	-3.828	1.11	0.7852	-3.490
Copper[1]	1300*	17.43	0.9422	-1.464	11.6	0.8545	-1.464
Iron					1,000		
Lead	15*	79.82	1.273	-1.460	3.11	1.273	-4.705
Mercury	2	2.4			0.012		
Nickel[1]	100	1,395	0.8460	3.3612	155	0.8460	1.1645
Selenium	50	20			5		
Silver[1]		3.93	1.72	-6.52	0.12		
Thallium	2	1,400			40		
Zinc[1]	5000	115	0.8473	0.8604	104	0.8473	0.7614

[1]Acute and chronic criteria are dependent on hardness. Example values were based on the average hardness of Río Viví and Río Pellejas downstream of the deposits, H = 98.24 mg L^{-1} $CaCO_3$

[2]Acute and chronic criteria are calculated using the equation: Criterion (µg L^{-1}) = $e^{(X\,[\ln(\text{hardness})] + Y)}$. Acute refers to one hour exposure; chronic refers to four-day average exposure.

[3]MCL: maximum contaminant limit; MCLG (*): maximum contaminant limit goal.

0.056 and 0.089 mg/L, respectively; during January, this site exceeded the water-quality guideline with a value of 0.895 mg/L, which is the highest for all the sites in both watersheds. During January, site PRRV-2, also exceeded the standard with a value of 0.103 mg/L. None of the groundwater sites of the two watersheds exceeded the water quality standard for Al (Table 6). Iron was another metal that exceeded the secondary water quality standards for the downstream sites. The iron concentration must be below 0.3 mg/L (Table 2 and Table 4). This occurred only in the groundwater site PRRV-4sp with a Fe concentration of 15.9 mg/L. The surface-water site closest to the standard was PRRP-3 in May with a concentration of 0.14 mg/L.

Manganese surpassed the secondary water-quality standards in several Río Viví sites; the standard is established at 0.05 mg/L as the maximum concentration. During May 2003, sample site PRRV-3 had a manganese concentration 0.13 mg/L, in September 2003 this site had 0.14 mg/L, and in January 2004 it had 0.11 mg/L. Site PRRV-4 also had high manganese during this period. The highest concentration of manganese among the two watersheds was found at site PRRV-4sp with a concentration of 5.73 mg/L. The closest value to the water-quality standard in Río Pellejas was at site PRRP-3 with 0.05 mg/L.

In general, the most extreme values in pH, conductance, dissolved oxygen, and cations and anion concentrations were found in Río Viví watershed. However, some sample sites in the Río Pellejas watersheds, such as PRRP-3, which receives water draining from Piedra Hueca and Calá Abajo, had the higher

concentrations of iron (0.14 mg/L) and aluminum (0.1 mg/L) for May, compared to values from the Río Viví watershed, such as <0.05 mg/L Fe in sites PRRV-4 and PRRV-2, and <0.002 mg/L Al in PRRV-4sp and 0.002 mg/L in site PRRV-4.

Stream Sediments

Stream-sediment samples were obtained from eight localities that coincide with some of the water-sample sites (Fig. 3). Mineralogy, determined by X-ray diffraction, shows that the principal minerals in the samples are quartz, plagioclase (albite and anorthite), and minor micas. All stream-sediment results are presented in Appendix ID. Figure 13 shows selected stream-sediment geochemical data for both watersheds. Table 8 presents selected stream-sediment data for Río Pellejas and Río Viví and compares it with stream-sediment data for porphyry and other copper deposits around the world.

In general, for the two upstream sediment samples of Río Pellejas, the concentrations of several metals are slightly higher at PRRP-5 than in PRRP-4. The iron content in PRRP-5 is 7.84 weight %, it is of 6.3 % weight in PRRP-4. Copper content in PRRP-5 is 79 mg/kg, whereas in PRRP-4, it is 64 mg/kg; the manganese concentration in PRRP-5 is 1340 mg/kg and in PRRP-4 it is 1180 mg/kg. Other metals show similar behavior. For the upstream site in Río Viví, (PRRV-1), values greater than those for the upstream sites in the Río Pellejas watershed were found. The iron concentration in Río Viví was 9.83 weight %, Cu was 235 mg/kg, and Mn was 1630 mg/kg; other elevated concentrations in this

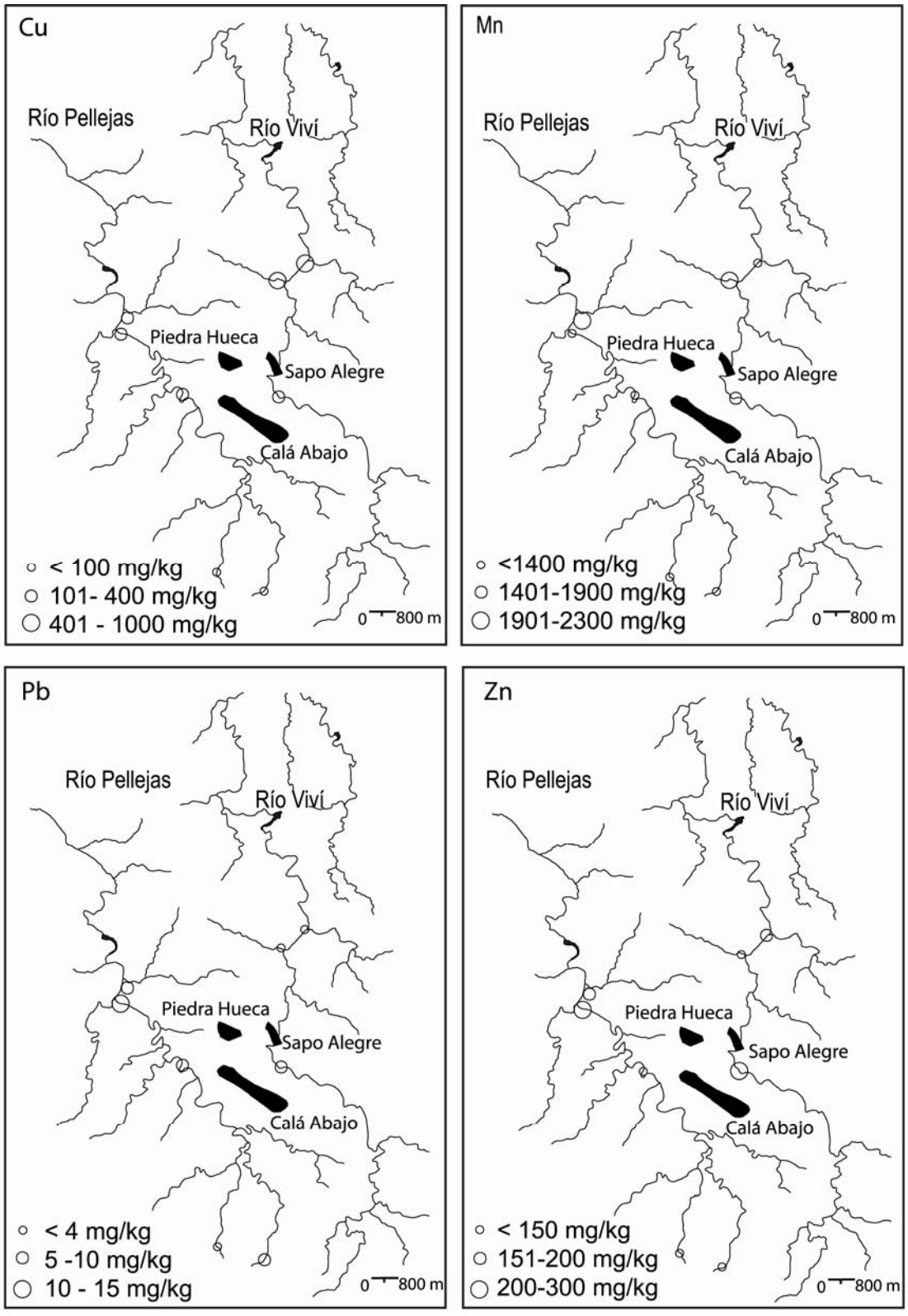

Figure 13. Stream-sediment geochemistry for Cu, Mn, Pb and Zn for Río Pellejas and Río Viví.

Table 8 a. Stream-sediment data for the Puerto Rican porphyries and other sites around the world.

Site	Sample	Al Wt %	Fe Wt %	As mg/kg	Cd mg/kg	Co mg/kg	Cr mg/kg	Cu mg/kg	Mn mg/kg	Ni mg/kg	Pb mg/kg	Sn mg/kg	Zn mg/kg
Río Pellejas	PRRP 1 - 1	8.145	7.89	<10	<2	20	45	364	1100	21	6	<50	132
	PRRP 4 - 1	6.71	6.3	<10	<2	18	17	64	1180	10	9	<50	109
	PRRP 5 -1	10.11	7.84	<10	<2	26	45	79	1340	28	<4	<50	104
	PRRP 6- 1	8.223	8.05	<10	<2	23	50	331	1390	32	14	<50	217
	PRRP 7 - 1	9.064	9.46	<10	<2	26	75	190	2290	41	6	<50	152
Río Viví	PRRV 1 - 1	7.734	9.83	<10	<2	24	29	235	1630	20	8	<50	291
	PRRV 2 - 1	8.462	7.28	<10	<2	20	26	410	1300	23	<4	<50	166
	PRRV 4- 1	8.221	7.29	<10	<2	23	26	804	1850	22	<4	<50	150
Fontana Copper Mine[1]	FM-97-1- SS	3.1	3.2	10	<2	15	20	19	1520	16	22	67	78
	FM-97-2 - SS	4.3	8	15	<2	19	37	6280	1020	17	223	111	795
	FM-SS- 97 - 3	5.6	9.8	<10	<2	252	25	5420	13600	24	79	56	824
	FM-SS- 97 - 4	5.2	8.1	17	<2	55	3.7	10200	4830	23	169	78	1300
	FM-98-1- SS	5.3	8.9	<10	5	75	76	8900	8140	23	157	<50	1380
	FM-98-2 - SS	7.7	5.23	<10	<2	20	101	1510	956	30	50	<50	547
	FM-98-3 - SS	5.9	4.24	13	<2	17	62	469	852	27	16	<50	231
	FM-98-4	4.0	3.44	11	<2	13	50	35	1530	25	<4	<50	134

Table 8 b. Stream-sediment data for the Puerto Rican porphyries and other sites around the world.

Site	Sample	Al Wt %	Fe Wt %	As mg/kg	Cd mg/kg	Co mg/kg	Cr mg/kg	Cu mg/kg	Mn mg/kg	Ni mg/kg	Pb mg/kg	Sn mg/kg	Zn mg/kg
Hazel Creek Copper mine[1]	HCM-97-1-SS	3.3	2.9	<10	<2	10	9	36	1310	10	26	42	93
	HCM-97-2-SS	4.4	4.2	<10	<2	12	25	3400	1290	10	210	86	1640
	HCM-97-2-SS	5.2	6.1	<10	5	14	24	5090	1210	13	509	58	4450
	SF-97-SS -1	3.1	2.6	<10	<2	6	29	10	1170	8	22	50	86
Orange Hill Creek[2]*			64	57	1.6			1100	1300		130		500
The Casino[3]**								30-50			30-50		
Yandera[4]**								10 - 1070	0 - 150				

[1] Besshi-type massive sulfide deposit, North Carolina USA
[2] Unmined porphyry copper-molybdenum deposit, Wrangell-St. Elias National Park and Preserve, Alaska
[3] Unmined porphyry copper-molybdenum deposit, Yukon, Canada
[4] Unmined porphyry copper-molybdenum deposit, Yandera, Papua New Guinea
* Mean values
**Values presented as ranges

site included 291 mg/kg Zn, which was the highest value for all upstream and downstream sites. The concentrations of metals among the downstream sites of the two rivers are mostly similar except for some specific metals. For example, Cu concentrations in Río Pellejas ranged between 190 to 364 mg/kg, whereas for Río Viví, the range was between 410 and 804 mg/kg; Cr in Río Pellejas ranged from 45 to 75 mg/kg, whereas for both sites in Río Viví, the concentration was 26 mg/kg. Molybdenum in Río Pellejas was <2 mg/kg and in Río Viví the range was between 4 and 10 mg/kg.

Table 8 presents geochemical data for metals associated with a variety of types of copper deposits including Besshi-type massive deposits in North Carolina (Hammarstrom et al., 2003), and also unmined porphyry copper deposits in Alaska (Eppinger et al., 2000), Canada (Gleeson and Brummer, 1976) and New Guinea (Fleming and Neale, 1979). Stream-sediment data for Fontana and Hazel Creek Copper deposits in North Carolina are arranged from upstream to downstream of the mine workings; for the other deposits, this information is not specified. Iron content associated with the Fontana (North Carolina), Hazel Creek (North Carolina), and Orange Hill (Alaska) deposits are basically similar to the values obtained for the study area in Puerto Rico. Iron concentrations at the Fontana Mine ranged from 3.2 to 9.8 weight %, from 3.1 to 5.5 weight % in Hazel Creek, and from 6.3 to 10.6 weight % in Puerto Rico. Copper concentrations associated with the Fontana and Hazel Creek mines are considerably higher than those found in Río Viví and Río Pellejas. Similarly, at the Orange Hill deposit, the Cu concentration is high but closer to the highest

values found in Río Viví. Copper concentrations at the Casino (Canada) deposit are lower than those in Río Pellejas and Río Viví. The value is similar to the concentration of the upstream sites in Río Pellejas. In the Yandera (New Guinea) deposit, the copper concentration range is broad (10 to 1070 mg/kg). The average value of 540 mg/kg is similar to the downstream Cu concentration values in Río Viví. The higher copper concentrations associated with the Fontana and Hazel Creek deposits undoubtedly reflect the fact that these deposits are mined and abandoned massive sulfide deposits with higher copper grades than the Adjuntas porphyry deposits (Hammarstrom et al., 2003).

Manganese concentrations at Fontana generally were higher values than those for Río Viví and Río Pellejas, whose range is from 1100 to 2290 mg/kg. Hazel Creek had manganese values similar or even lower than those associated with the Adjuntas porphyry deposits. The Orange Hill deposit had the same concentration (1300 mg/kg) of Mn as sample PRRV-4. The Yandera deposit had very low concentrations of Mn (0 to 150 mg/kg) when compared to the Río Pellejas and Río Viví porphyry copper deposits. Lead concentrations ranged from <4 to 14 mg/kg in Río Pellejas and from <4 to 8 mg/kg in Río Viví. In all of the other deposits presented in Table 8, lead concentrations are very high compared to the Puerto Rican porphyries. For example at Fontana, lead concentrations vary from <4 to 223 mg/kg, at Hazel Creek the range is between 22 and 509 mg/kg, at Casino, it is between 30 and 50 mg/kg, and finally, at Orange Hill the Pb content is 130 mg/kg. In general, the most similar values to

those from Puerto Rico are those from unmined deposits, especially in Wrangell-St Elias National Park and Preserve in Alaska (Eppinger et al., 2000).

Sediment-quality guidelines developed by MacDonald et al., (2000) are listed in Table 9. These guidelines are based on two parameters: the threshold effect concentration (TEC) and the probable effect concentration (PEC). The TEC is a parameter for predicting the absence of sediment toxicity, whereas the PEC is a parameter for predicting the presence of sediment toxicity (MacDonald et al., 2000). Values for copper for most of the sample sites exceeded the sediment-quality parameters, especially for sample site PRRV-4 which is downstream of Sapo Alegre; the lowest values are from PRRP-4 (64 mg/kg) and PRRP-5 (79 mg/kg), which are upstream and most distant of the deposits.

Minerals

Knowledge of the compositional variations of the rock-forming minerals in the vicinity of the Río Pellejas and Río Viví porphyry copper deposits will facilitate the understanding of the weathering processes that are occurring and therefore affecting the water and sediment compositions. Weathering reactions involving rock-forming minerals are particularly important for determining the major-element chemistry of the watersheds.

Plagioclase was one of the most abundant minerals. The samples analyzed by electron microprobe were from the Maricao Formation, the Anón Formation, and the plutonic rocks associated with the Utuado batholith. The

Table 9. Selected elements from ICP-AES data for sediments compared to threshold effect concentration (TEC) and probable effect concentration (PEC) (MacDonald et al., 2000)

Sample	As (mg/kg)	Cd (mg/kg)	Cr (mg/kg)	Cu (mg/kg)	Pb (mg/kg)	Ni (mg/kg)	Zn (mg/kg)
PRRP-1-1	<10	<2	45	364	6	21	132
PRRP-4-1	<10	<2	17	64	9	10	109
PRRP-5-1	<10	<2	45	79	<4	28	104
PRRP-6-1	<10	<2	50	331	14	32	217
PRRP-7-1	<10	<2	75	190	6	41	152
PRRP-7Dup	<10	<2	82	155	5	35	146
PRRV-1-1	<10	<2	29	235	8	20	291
PRRV-2-1	<10	<2	26	410	<4	23	166
PRRV-4-1	<10	<2	26	804	<4	22	150
TEC[1]	9.79	0.99	43.4	31.6	35.8	22.7	121
PEC[2]	33	4.98	111	149	128	48.6	459

[1] Below which harmful effects are unlikely to be observed.
[2] Above which harmful effects are likely to be observed.

composition of plagioclase for all the units ranged from andesine to anorthite (Fig. 14, Table 10). Samples from the Maricao Formation are mostly andesine and labradorite with Na_2O contents up to 5.9 weight %, and CaO contents up to 17.2 weight %. Two plagioclase-bearing samples were analyzed from the Anón Formation (PRRP-5 and PRRP-A). Plagioclase from PRRP-5 is classified as bytownite with CaO contents of 16.5 weight % and Na_2O up to 2.4 weight %. Plagioclase in PRRP-A was mostly labradorite; its CaO content reached 14 weight % and Na_2O reached 6.9 weight %. Plagioclases from the plutonic rocks were mostly andesine with up to 7 weight % Na_2O and 10.7 weight % CaO.

Chain silicates in the rocks include both pyroxenes and amphiboles. Pyroxenes were found only in sample site PH-A from the hornblende quartz diorite and diorite of the post-batholitic rocks. Its composition was dominantly augitic but ranged to diopsidic (Fig. 15, Table 10); it contains up to 5.82 weight % Al_2O_3, 0.36 weight % MnO, 15.8 weight % MgO, and 0.76 weight % TiO_2. Amphiboles analyzed from the Maricao Formation were found to be magnesio-hornblende (Fig. 16) with up to 14 weight % of MgO and 14.9 weight % FeO. Amphiboles from the Anón Formation from PRRP-5 and PRRP-A were found to be hornblendes. Hornblende from sample PRRP-5 was classified as tschermakite; its Al_2O_3 content was up to 13.8 weight %, and FeO reached 13.1 weight %. The amphibole in sample PRRP-A is magnesio-hornblende with an MgO content of 15.9 weight % and FeO up to 14.3 weight %.

Sheet silicates include primary biotite and secondary chlorite. Biotite was only found in the plutonic rocks (quartz diorite and granodiorite) of sample PRRV-

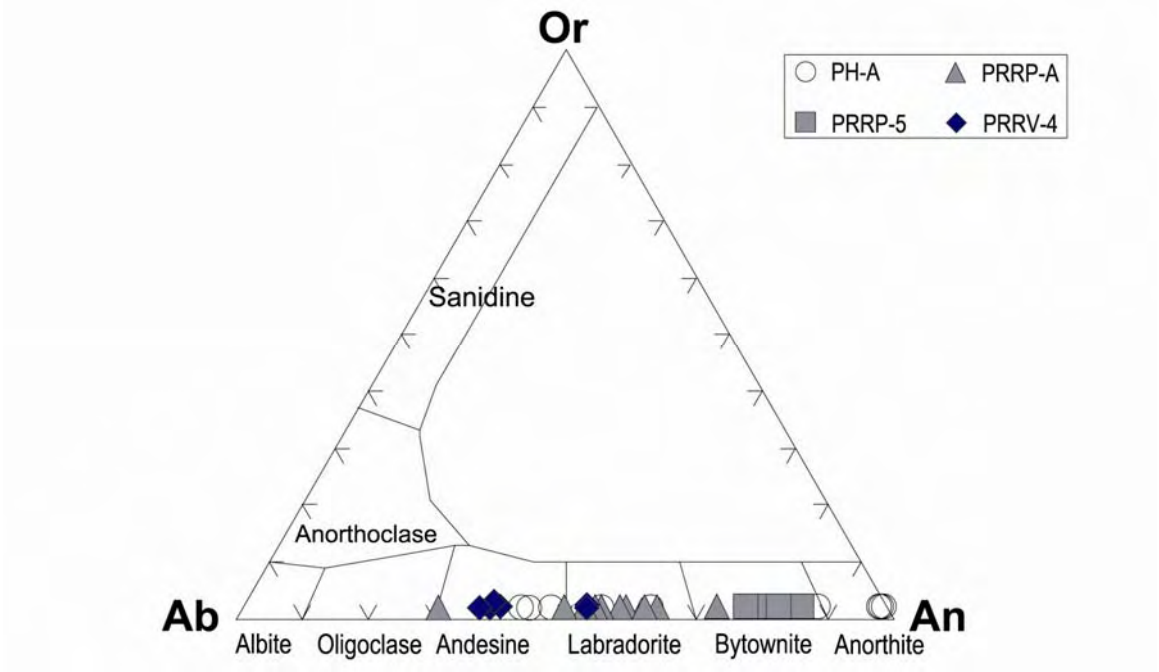

Figure 14. Feldspar compositions for the Maricao Formation (PH-A), Anón Formation (PRRP-5, PRRP-A), and plutonic rocks associated with the Utuado batholith. Diagram by Minpet 2.02 (1988).

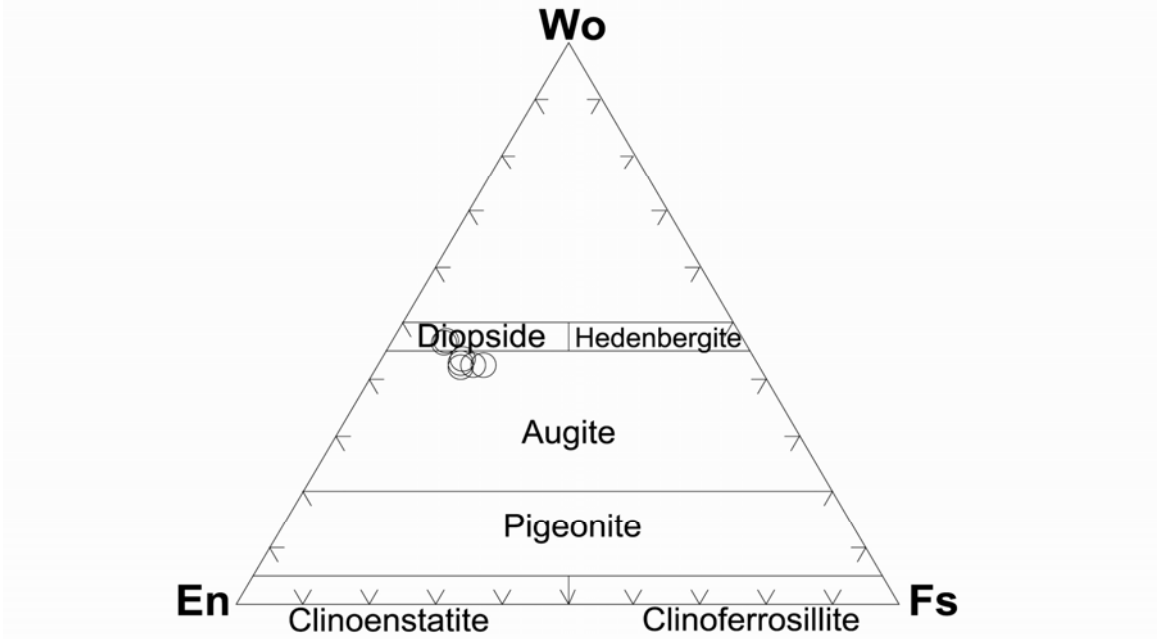

Figure 15. Pyroxene compositions from sample site PH-A, from the Maricao Formation. Diagram by Minpet 2.02 (1988).

Table 10. Average formula for major minerals from the Eocene Anón Formation, Cretaceous plutonic rocks, and Maricao Formation.

Maricao Formation		
Chlorite	*PH-A*	$(Si_{5.8}, Al_{2.16})\ Al_{2.43}, Fe_{3.41}, Mn_{0.43}, Mg_{5.6}\ Ca_{0.1}\ Na_{0.03}\ O_{20}\ OH_{16}$
Epidote	*PH-A*	$Ca_{1.8,}\ Fe^{3+}{}_{0.7}, Al_{2.\ 3,}\ Mn_{\ 0.12}\ [Si_2\ O_7]\ [Si\ O_4]$
Hornblende	*PH-A*	$(Ca_0, Na_{0.03}, K_{0.06})_{0.09}\ (Ca_{1.6}, Na_{0.41})_2\ (Al_{0.13}, Cr_0, Fe^{3+}{}_{1.2}, Ti_{0.16}, Mg_{2.9}, Fe^{2+}{}_{0.53}, Mn_{0.42})_{5.34}\ (Si_{\ 6.7}, Al_{1.31})_8\ O_{22}\ (OH)_2$
Plagioclase	*PH-A*	$Na_1,\ Ca_{2.4}, K_{0.24}, (Si_{9.6}, Al_{6.5})_{16}\ O_{32}$
Anón Formation		
Plagioclase	*PRRP-5*	$Na_{0.78},\ Ca_{3.1},\ K_{0.01}\ (Si_{8.8}, Al_{7.2})_{16}\ O_8$
Plagioclase	*PRRP-A*	$Na_{1.6}, Ca_{2.1},\ K_{0.02}\ (Si_{9.8}, Al_{6.2})_{16}\ O_8$
Pyroxene	*PRRP-5*	$(Fe^{2+}{}_{0.13}, Ca_{0.83}, Na_{0.02})_{0.98}\ (Si_{1.9}, Al_{\ 0.63})_{2.53}\ O_6$
Hornblende	*PRRP-5*	$(Ca_{0.55}, Na_{0.38}, K_{0.07})_1\ (Ca_{1.7}, Na_{0.33})_2\ (Al_{0.24}, Cr_0, Fe^{3+}{}_{1.1}, Ti_{0.26}, Mg_3, Fe^{2+}{}_{0.37}, Mn_{0.20})_5\ (Si_{\ 6}, Al_2)_8\ O_{22}\ (OH)_2$
Hornblende	*PRRP-A*	$(Ca_0, Na_0, K_{0.03})_{0.03}\ (Ca_{1.5}, Na_{0.35})_{1.85}\ (Al_{0.90}, Cr_{0.01}, Fe^{3+}{}_{1.3}, Ti_{0.13}, Mg_{3.1}, Fe^{2+}{}_{0.26}, Mn_{0.68})_{6.3}\ (Si_{\ 6.8}, Al_{1.1})_8\ O_{22}\ (OH)_2$
Plutonic Rocks		
Biotite	*PRRV-4*	$K_{1.4}\ (Mg_{3.8}, Fe^{2+}{}_{1.9})_{3.7}\ (Al_{2.2}, Fe_0)_{2.2}\ Si_{5.8}\ O_{20}\ (OH_{1.9}\ F_{1.4})_{3.3}$
Plagioclase	*PRRV-4*	$Na_{2.2},\ Ca_{1.6}, K_{0.04}\ (Si_{10.3}, Al_{5.7})_{16}\ O_8$

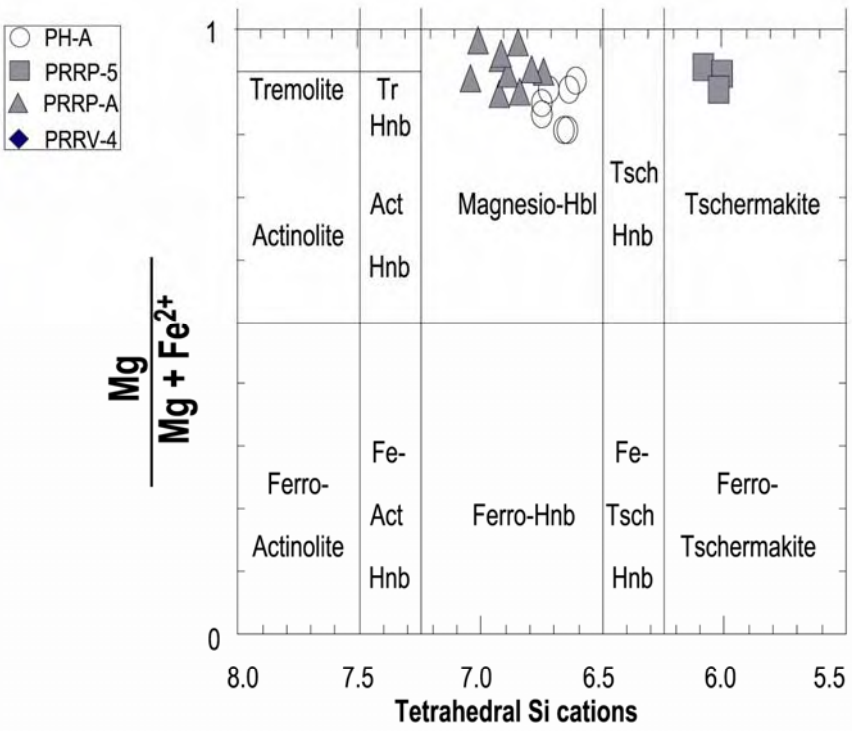

Figure 16. Hornblende (Hnb) compositions for the Maricao Formation, (PH-A), and Anón Formation (PRRP-5, PRRP-A). Abbreviations are for actinolite (Act), tschermakite (Tsch), tremolite (Tr), and ferro (Fe). Diagram by Minpet 2.02 (1988).

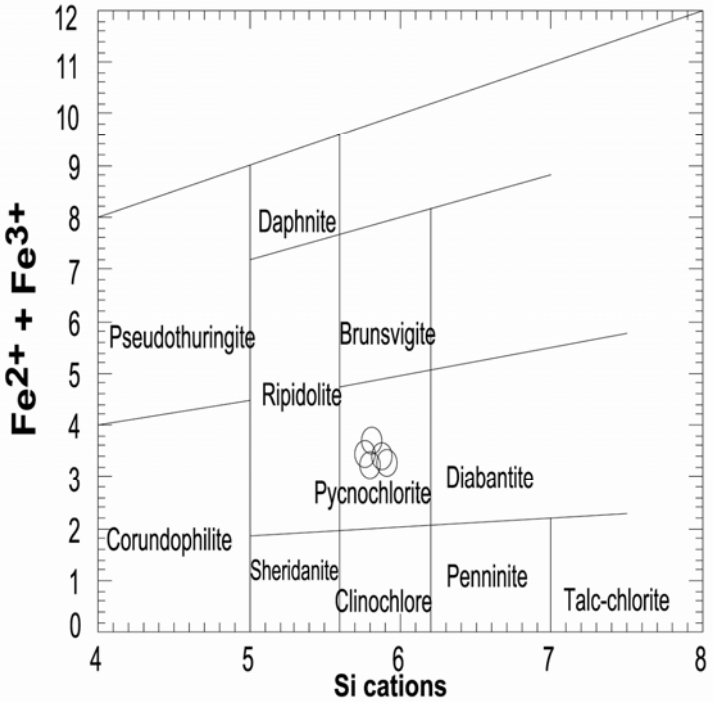

Figure 17. Chlorite compositions from the Maricao Formation (site PH-A). Diagram by Minpet 2.02 (1988).

4. Its composition ranged up to 18.3 weight % Al_2O_3, 18.3 weight % MgO and 15.5 weight % FeO. Secondary chlorite was analyzed for sample site PH-A from the Maricao Formation. All chlorites can be classified as pycnochlorite, which is an iron clinochlore (Fig. 17, Table 10). Its Al_2O_3 content ranged up to 18.6 weight %, MgO content up to 19 weight %, and its FeO content up to 20.2 weight %. Secondary epidote was found in samples from the Maricao Formation. It has concentrations of up to 12.3 weight % of Fe_2O_3, and 25.2 weight % of Al_2O_3.

Remote Sensing

Figure 11 shows the NDVI for the study area generated by the software ENVI 3.6. Light grey areas represent vegetation-index values of approximately 0.50. As the area becomes darker, the index value diminished to zero or become a negative number. Black areas in the image represent water, clouds, roads, houses, or rivers and streams. The NDVI image displays a series of mixed values for areas inside and outside the mineralized regions; thus, there is not a constant set of values for each of the areas (mineralized and unmineralized) (Tables 11 to 13).

For the Piedra Hueca porphyry copper deposit, a broad range of NDVI values are observed. For the center of the deposit exposure, the average value is 0.45 with individual values ranging from 0.16 to 0.59 (Fig. 18, Table 11). The average value for the outer part is 0.48 with a range of values from 0.26 to 0.59 showing small differences from the average value of the center. In the

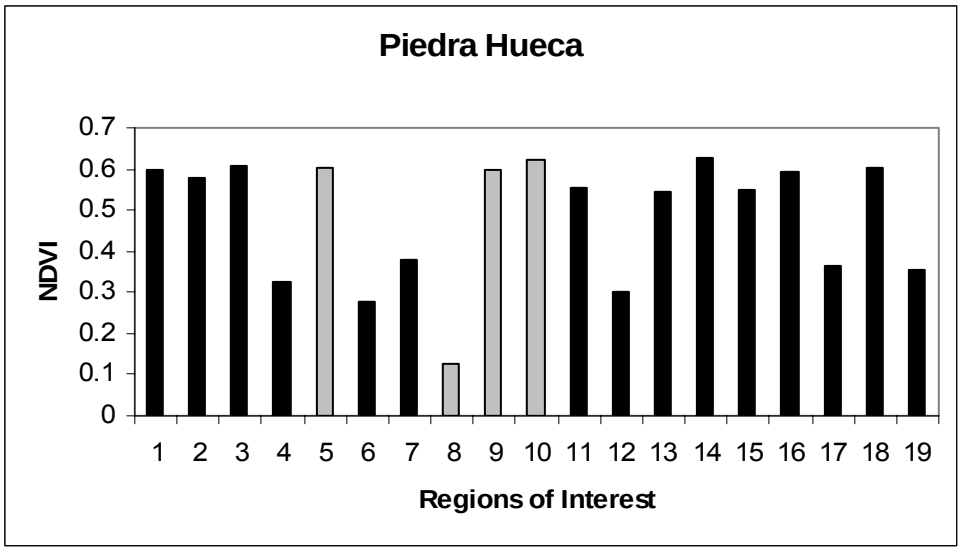

a.

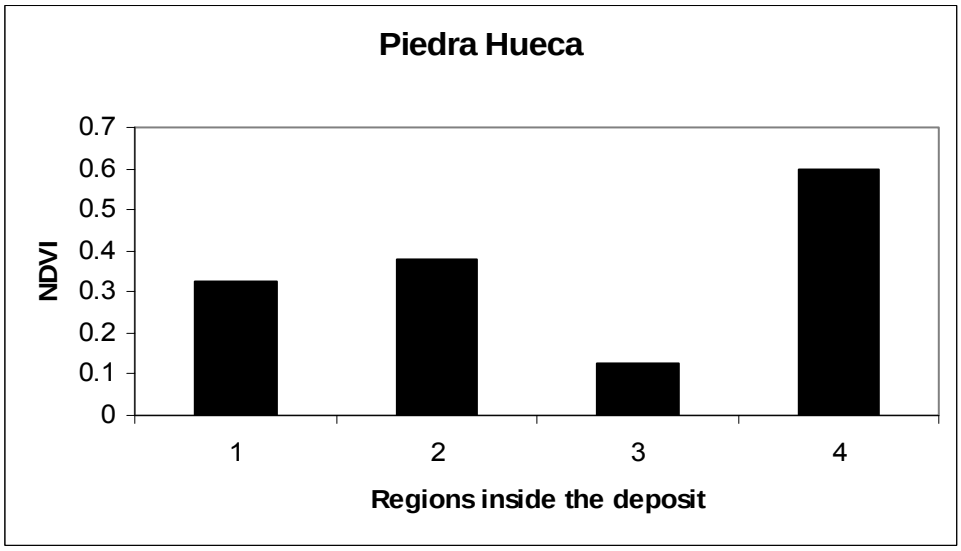

b.

Figure 18 a. Graphs showing the NDVI for all the regions of interests of the Piedra Hueca deposit, light grey areas represent the NDVI inside the deposits. b. NDVI for the regions inside the deposit.

Table 11. General statistics of NDVI for the Piedra Hueca deposit.

Region	Latitude	Longitude	Min	Max	Mean	Std. Deviation
1	18º 11’26.16	66º 41’11.28”	0.084204	1.000000	0.596254	0.241082
2	18º 11’31.42”	66º 41’13.19”	0.143875	1.000000	0.578125	0.177704
3	18º 11’38.61”	66º 41’13.75”	0.211119	1.000000	0.607870	0.194721
4	18º 11’39.92”	66º 41’08.00”	0.024000	1.000000	0.323959	0.178895
5	18º 11’36.38”	66º 41’05.27”	0.186842	1.000000	0.600493	0.179512
6	18º 11’42.58”	66º 41’14.94”	0.117424	0.555556	0.277226	0.064088
7	18º 11’44.64”	66º 41’07.05”	0.084976	1.000000	0.377092	0.165426
8	18º 11’43.49”	66º 41’10.59”	-0.161731	0.745902	0.124395	0.103592
9	18º 11’41.81”	66º 41’03.48”	0.284929	1.000000	0.595882	0.145804
10	18º 11’46.40”	66º 41’01.37”	0.184303	1.000000	0.623226	0.189838
11	18º 11’43.09”	66º 40’55.75”	0.279102	1.000000	0.553461	0.146006
12	18º 11’48.65”	66º 40’55.90”	0.145889	0.570595	0.299492	0.061114
13	18º 11’37.82”	66º 40’56.22”	0.123391	1.000000	0.542854	0.148892
14	18º 11’44’79”	66º 40’51’06”	0.137212	1.000000	0.628459	0.207842
15	18º 11’49’90”	66º 41’10.43”	0.155486	1.000000	0.548904	0.192221
16	18º 11’52’.08”	66º 41’06.96”	0.165616	1.000000	0.592434	0.207631
17	18º 11’53’40”	66º 40’58.05”	0.148618	0.741546	0.366433	0.078593
18	18º 11’55’75”	66º 40’48.79”	0.267416	1.000000	0.603523	0.170534

NDVI image, the western part of the deposit is enclosed by a dark color that designates areas without vegetation. The vegetation index for this area is very low, with values being mostly negative numbers. These altered areas are probably part of the extension of the typical alterations zones contained in the porphyry copper deposits. The graph resulting for the Sapo Alegre deposit shows that the NDVI average value for the inner part of the deposit is 0.42 and the average value for the area outside of the deposit is 0.53 (Fig. 19, Table 12). Inside the deposit values of 0.30 and 0.50 were commonly observed but unfortunately due to a cloud located just at the south side of the deposit no additional regions of interest were included in the image. In this small deposit, there are areas in which bare rock surfaces are observed. These areas have the lowest NDVI values for this deposit.

The Calá Abajo image has a problem similar to that for Sapo Alegre; in this image, a nearby cloud is shadowing a significant part of the deposit. As in the Sapo Alegre image, only those values not affected by the clouds or the shadow were considered. The average value for the center part of the deposit is 0.47 and for the outer part is 0.55 (Fig. 20, Table 13). Values in the center of the deposits range from 0.34 to 0.58 and those for the outer part from 0.35 to 0.62. In this deposit, as in Piedra Hueca, the lowest NDVI values probably correspond to alteration zones associated with the deposits.

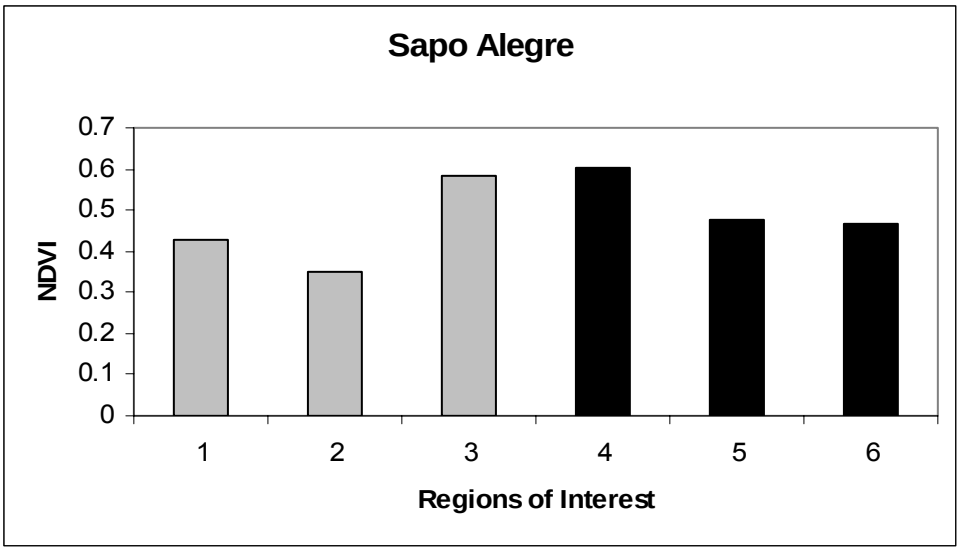

a.

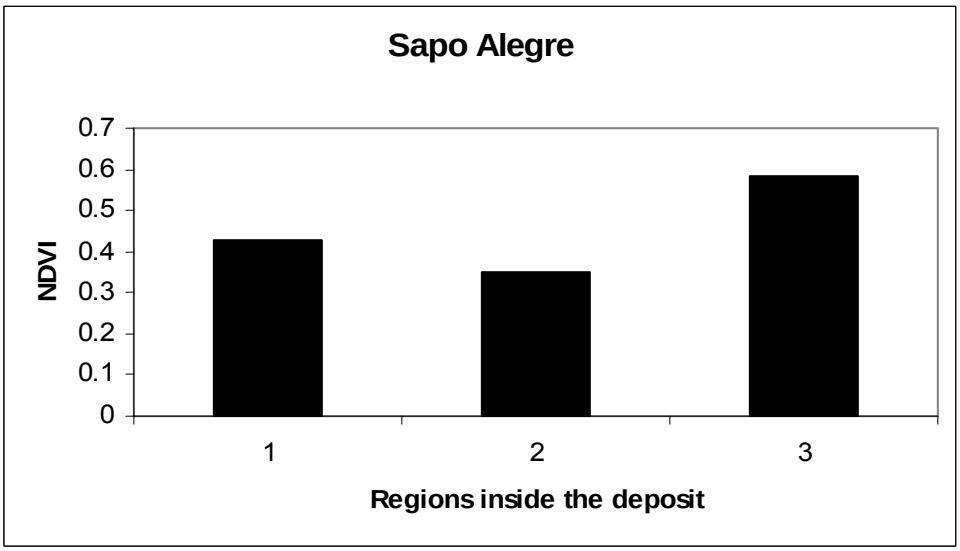

b.

Figure 19 a. Graph showing the normalized difference vegetation index (NDVI) of the regions of interests of Sapo Alegre porphyry copper deposit, light grey areas represent the regions inside the deposits. b. NDVI for the regions inside the deposits.

Table 12. General statistics of NDVI for the Sapo Alegre deposit

Region	Latitude	Longitude	Min	Max	Mean	Std. Deviation
19	18º 11’44.63”	66º 40’45.89”	0.114617	1.000000	0.427034	0.162894
20	18º 11’42.22”	66º 40’46.49”	0.173356	1.000000	0.581512	0.197807
21	18º 11’47.91”	66º 40’48.68”	0.190341	0.527321	0.351107	0.054722
22	18º 11’52.25”	66º 40’42.73”	0.280757	1.000000	0.601383	0.172517
23	18º 12’00.05”	66º 40’43.32”	0.254457	1.000000	0.474510	0.110726
24	18º 11’54.21”	66º40”36.54”	0.192403	1.000000	0.465751	0.147923

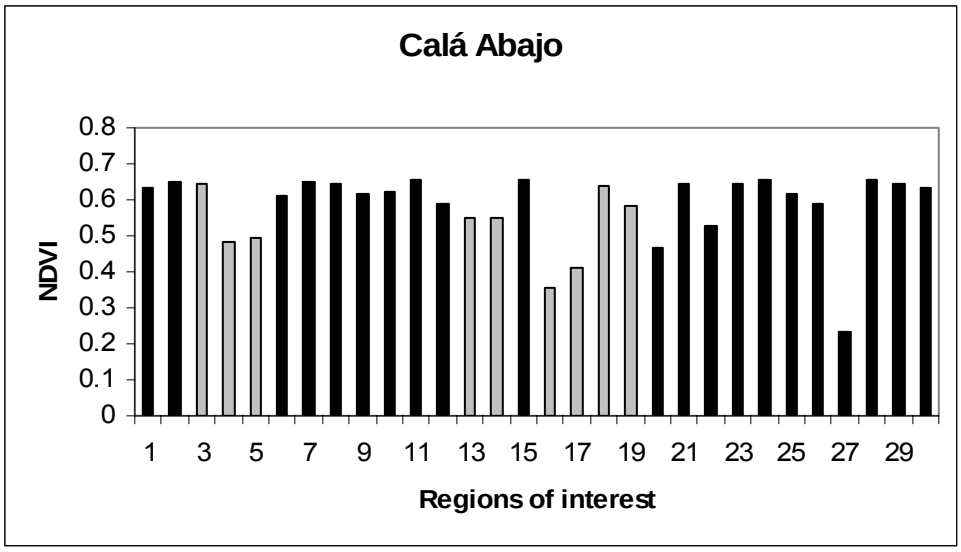

a.

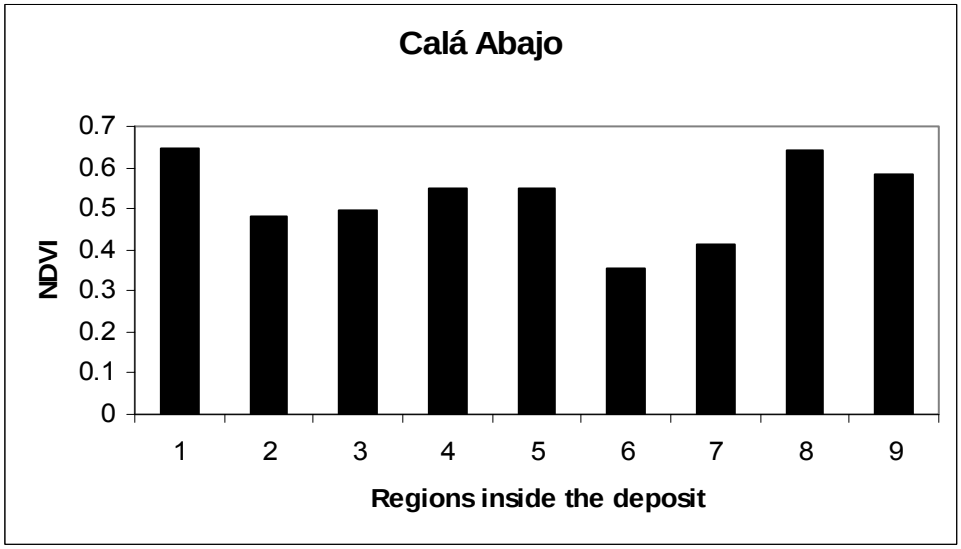

b.

Figure 20. a. Graphs showing the NDVI for all the regions of interests of the Calá Abajo deposit, light grey areas represent the regions inside the deposits b. NDVI for the regions inside the deposit.

Table 13 a. General statistics of NDVI for the Calá Abajo deposit.

Region	Latitude	Longitude	Min	Max	Mean	Std. Deviation
1	18º11’24.07”	66º 41’15.77”	0.263533	1.000000	0.635405	0.174996
2	18º11’19.29”	66º 41’14.60”	0.240753	1.000000	0.651163	0.199329
3	18º 11’27.72”	66º 41’18.15”	0.208208	1.000000	0.646002	0.191851
4	18º 11’19.07”	66º 41’07.42”	0.150192	1.000000	0.482082	0.164927
5	18º 11’21.54”	66º 41’11.65”	0.190582	1.000000	0.495255	0.159309
6	18º 11’16.59”	66º 41’10.93”	0.149722	1.000000	0.611411	0.210975
7	18º 11’13.27”	66º 41’14.13”	0.216911	1.000000	0.649715	0.189459
8	18º 11’12.57”	66º 41’07.41”	0.219254	1.000000	0.645730	0.209955
9	18º 11’9.89”	66º 41’11.22”	0.192157	1.000000	0.614654	0.192566
10	18º 11’7.19”	66º 41’15.37”	0.140938	1.000000	0.620142	0.195454
11	18º 11’8.08”	66º 41’04.48”	0.239799	1.000000	0.652780	0.172907
12	18º 11’9.81”	66º 40’59.28”	0.191926	1.000000	0.590990	0.187973
13	18º 11’13.04”	66º 40’55.47”	0.206840	1.000000	0.550922	0.178405
14	18º 11’17.91”	66º 40’56.53”	0.206840	1.000000	0.550922	0.178405
15	18º 11’21.62”	66º 40’59.57”	0.266557	1.000000	0.656401	0.177529
16	18º 11’16.26”	66º 40’53.37”	0.227957	0.657503	0.353616	0.047607
17	18º 11’13.37”	66º 40’51.18”	0.209928	0.971936	0.411572	0.096619
18	18º 11’12.82”	66º 40’47.30”	0.219294	1.000000	0.640126	0.176810

Table 13 b. General statistics of NDVI for the Calá Abajo deposit.

Region	Latitude	Longitude	Min	Max	Mean	Std. Deviation
19	18º 11’10.05”	66º 40’47.40”	0.200316	1.000000	0.581568	0.162249
20	18º 11’6.60”	66º 40’52.84”	0.253380	0.969116	0.468235	0.093722
21	18º 11’00.57”	66º 41’00.80”	0.281959	1.000000	0.641938	0.174246
22	18º 11’04.32”	66º 40’57.30”	0.262915	1.000000	0.529831	0.140261
23	18º 11’04.30”	66º 41’10.19”	0.163685	1.000000	0.643543	0.212847
24	18º 10’56.59”	66º 41’08.04”	0.196657	1.000000	0.655333	0.212783
25	18º 11’03.48”	66º40’47.36”	0.254250	1.000000	0.616883	0.189084
26	18º 10’56.43”	66º 40’45.24”	0.203703	1.000000	0.588939	0.179512
27	18º 11’02.55”	66º 40’39.94”	0.077223	0.824763	0.235170	0.062140
28	18º 11’03.67”	66º 40’27.90”	0.303233	1.000000	0.656471	0.176167
29	18º 11’24.13”	66º 40’25.95”	0.254949	1.000000	0.645180	0.162052
30	18º 11’16.54	66º 40’40’57”	0.371703	1.000000	0.635469	0.122538

Chapter 5

Discussion

This chapter will present a general discussion of the effect of the unmined porphyry copper deposits on the watersheds in the study area. To accomplish this task, several topics must be addressed. First it will be important to understand the relationship of the effects of weathering in the unmineralized bedrock on water quality and the stream sediments as a basis for understanding the additional effects of the porphyry deposits. Results from the geochemical modeling software PHREEQC, including molalities, activities of dissolved species, saturation indices for various minerals and other compounds of all the water samples will be used in conjunction with data from electron microprobe analysis of minerals from country rocks, and bulk geochemical data from the stream-sediment samples to assess qualitatively the mass balance of weathering reactions and its relations to water quality. The discussion will be constructed on an element by element basis, including major cations (K, Na, Ca, Mg, Si) and anions (SO_4^{2-} and HCO_3^-), minor elements (Al, Fe, Mn), and trace elements (Cu, Zn, Cd, As, among others). In terms of remote sensing, this chapter will make a final comparison between the normalized differenced vegetation index values for mineralized and unmineralized areas around the porphyry copper deposits. Together all these results will help improve our understanding of weathering processes operating around porphyry copper deposits in tropical terranes and their implications for environmental geochemistry and mineral exploration.

Weathering

Chemical weathering is strongly affected by climate, with moisture and temperature being the most important factors (White and Blum, 1995). Several factors such as bedrock, soil composition, chemical composition of precipitation, and vegetation can also affect the water chemistry (Ginés Sánchez et al., 1986). The Adjuntas porphyry copper deposits are located in a heavily vegetated and humid area, characteristics that should enhance a number of processes related to weathering. The water composition from the upstream sites of both watersheds begins an evolution as it traverses the different geologic units, including the porphyry copper deposits. When water finally flows into the Río Grande de Arecibo, its composition is very different from its starting composition. The resulting water composition is a combination of several types of reactions, particularly those of dissolution and precipitation. Some of the dissolution reactions can be incongruent, others congruent. Incongruent dissolution reactions lead to the precipitation of secondary phases at the source site, whereas congruent reactions do not. Both incongruent and congruent dissolution reactions may ultimately also lead to later precipitation of secondary phases. Thus, precipitation reactions can take place near the site of dissolution, within the streams, and also during oxidation of anoxic groundwater; it can also occur when waters with different pH are mixed. Another chemical process that can take place in the waters is sorption of major and trace elements, which can occur on Fe, Al, or Mn hydroxides and also on clay minerals (Smith and Huyck, 1999). All of these chemical processes can occur in the study area and under different

conditions for the different elements. The variety of processes, which vary on an element by element basis results in some elements behaving conservatively once they go in solution, and others behaving nonconservatively.

Calcium

Calcium is one of the most abundant metals in the Earth's crust and it is an essential element for human health (Smith and Huyck, 1999). In terms of aquatic ecosystems, it has an important role as the cation that contributes most to water hardness: as hardness increases, the concentrations of divalent metals, such as copper, and zinc, needed to produce toxic effects increases. The weathering of minerals such as plagioclase, amphibole, and clinopyroxene, which were found in rocks from both watersheds, is the most likely source of Ca in the streams in the study area.

Amphiboles found in the samples were magnesio-hornblendes and tschermakites, which are part of the calcic amphiboles group as described in Chapter 4 (Fig.16). Magnesio-hornblendes were found in rock samples from the Anón Formation, which consists of rhyodacitic lapilli tuffs. This sample (PRRP-A) was collected in the Río Pellejas watershed. Magnesio-hornblende was also found in the hornblende quartz diorite and diorite from the post-batholitic rocks (PH-A); this sample was collected from the Río Viví watershed. The sample with tschermakite was found in the Río Pellejas watershed (PRRP-5) in the Anón Formation. Amphiboles constitute about 15 % of the modal mineralogy of these rocks. Pyroxenes were only found in one sample in Río Viví (PH-A) and are

augitic to diopsidic in composition. The pyroxene content constitutes about 5% in the rock sample.

Plagioclase feldspars were abundant in the rocks of both watersheds. The most common plagioclase compositions found in the Río Pellejas watershed were labradorite and bytownite (Fig. 14). In the Río Viví watershed, most of the feldspars range in composition from andesine to anorthite, the calcium-rich end members (Fig. 14). Feldspars constitute approximately 40 % of the rocks in the Río Pellejas watershed and 35 % in the Río Viví watershed. Plagioclase feldspars were found in Río Pellejas watershed in the alluvial and terrace deposits (PRRP-7), in the lapilli tuffs (PRRP-4, PRRP-5, PRRP-A), and in epiclastic siltstones and sandstones (PRRP-A), whereas in the Río Viví watershed, plagioclase was observed in epiclastic siltstones and sandstones (PRRV-5, PRRV-A), in hornblende quartz diorites and diorites (PHA), and in quartz diorites and diorites (PRRV-3, PRRV-4). For the sedimentary rocks, it is more difficult to estimate the calcium content on the basis of rock classification but for the plutonic rocks in the Río Viví watershed, it is clear that the calcium content should be high in rocks with granodioritic compositions.

Calcium fluxes can originate from any of these minerals. The main source of calcium is probably the plagioclases because the modal abundances of pyroxenes and amphiboles are low, compared to plagioclase. For plagioclases the rate of dissolution increases with increasing anorthite content from An_0 to ~An_{80} (Blum and Stillings, 1995). Thus, most of the calcium concentration in both rivers could be the result of dissolution of feldspar with observed anorthite

contents ranging from An_{50} to An_{90} for Río Pellejas, and from An_{30} to An_{100} for Río Viví. It is important to recall that bedrock geology of the Río Pellejas watershed is simpler than that of the Río Viví watershed. Most of the rock samples from Río Pellejas are volcanic rocks, whereas most of the rocks in the Río Viví watershed are plutonic in origin. The relative role of plagioclase as the dominant source of calcium in the watersheds can be semi-quantitatively assessed by comparing the Ca/(Ca+Na) ratio of the water samples with that of plagioclase feldspars from various rock units in the study area. In Figure 21, the histogram shows that the Ca/(Ca+Na) ratios of water and the feldspars in the rock units agree well, suggesting that the calcium and sodium are generally behaving conservatively downstream of the source rocks. Secondary calcite has been shown to play an important, but localized role in the calcium budget of watersheds draining granitic terranes; weathering of plagioclase feldspars results in the formation of minor amounts of secondary calcite that can locally buffer water compositions (White and Blum, 1999). Although calcite was not found megascopically in the rock samples, microprobe analysis confirmed two grains of calcite in sample PH-A. The potential role of secondary calcite in controlling water chemistry in the study can be evaluated by examining its calculated saturation indices for the water samples from the study. The saturation indices for calcite during the lowest flow period (May 2003, Table 3) suggest its saturation with values that range from -0.79 to 0.56 for Río Pellejas and from -0.19 to 0.64 for Río Viví. Figure 22 shows the saturation indices for calcite going from upstream to downstream during

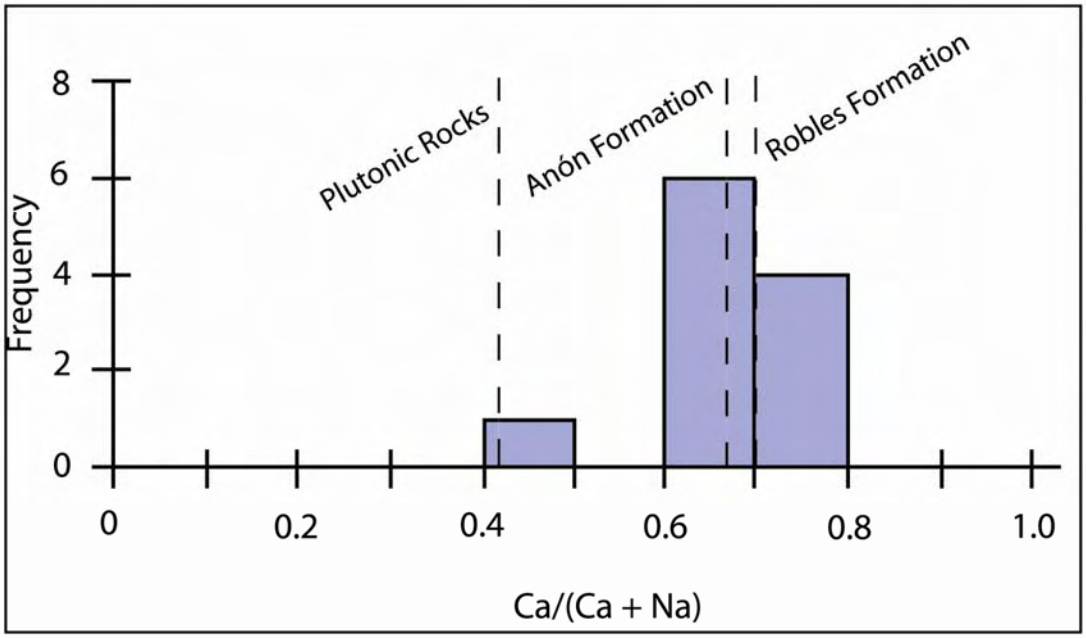

Figure 21. Histogram showing the relationship of the Ca/Ca+Na ratio from the streams (bars) and the rock samples from microprobe analyses of feldspars (dashed lines).

the different collection periods. The May 2003 sampling had the lowest flows, and thus probably represents conditions closest to base flow. Modeling indicates that most of the reach of Río Viví is saturated or nearly saturated with respect to calcite, but Río Pellejas only reached saturation with respect to calcite for two sites during low flow conditions. Based on the localized saturation with respect to calcite, the bedrock geology must be exerting the dominant control in the calcium concentration. The abundance of calcium in the plutonics rocks of the Río Viví watershed compared to that in Río Pellejas watershed is reflected in the saturation index values and in the water chemistry. Nevertheless, the amount of calcium removed from the watershed due to secondary calcite precipitation in the Río Viví, is probably insufficient to alter significantly the Ca/(Ca+Na) ratio of the waters inherited from the source plagioclase. During the high flow periods (September and January), calcium was probably affected by dilution because the saturation indices of calcite were mostly below zero, indicating undersaturation, for both watersheds (Fig. 22). White et al. (1999) reached similar conclusions that most of the mass of the calcium in granitoid rocks resides predominantly in plagioclase feldspars, and that trace amounts can also be found in disseminated secondary calcite. Thus, these two minerals also appear to be the main sources of calcium in the study area, as indicated by the geologic setting, mineralogical data, and modeling results.

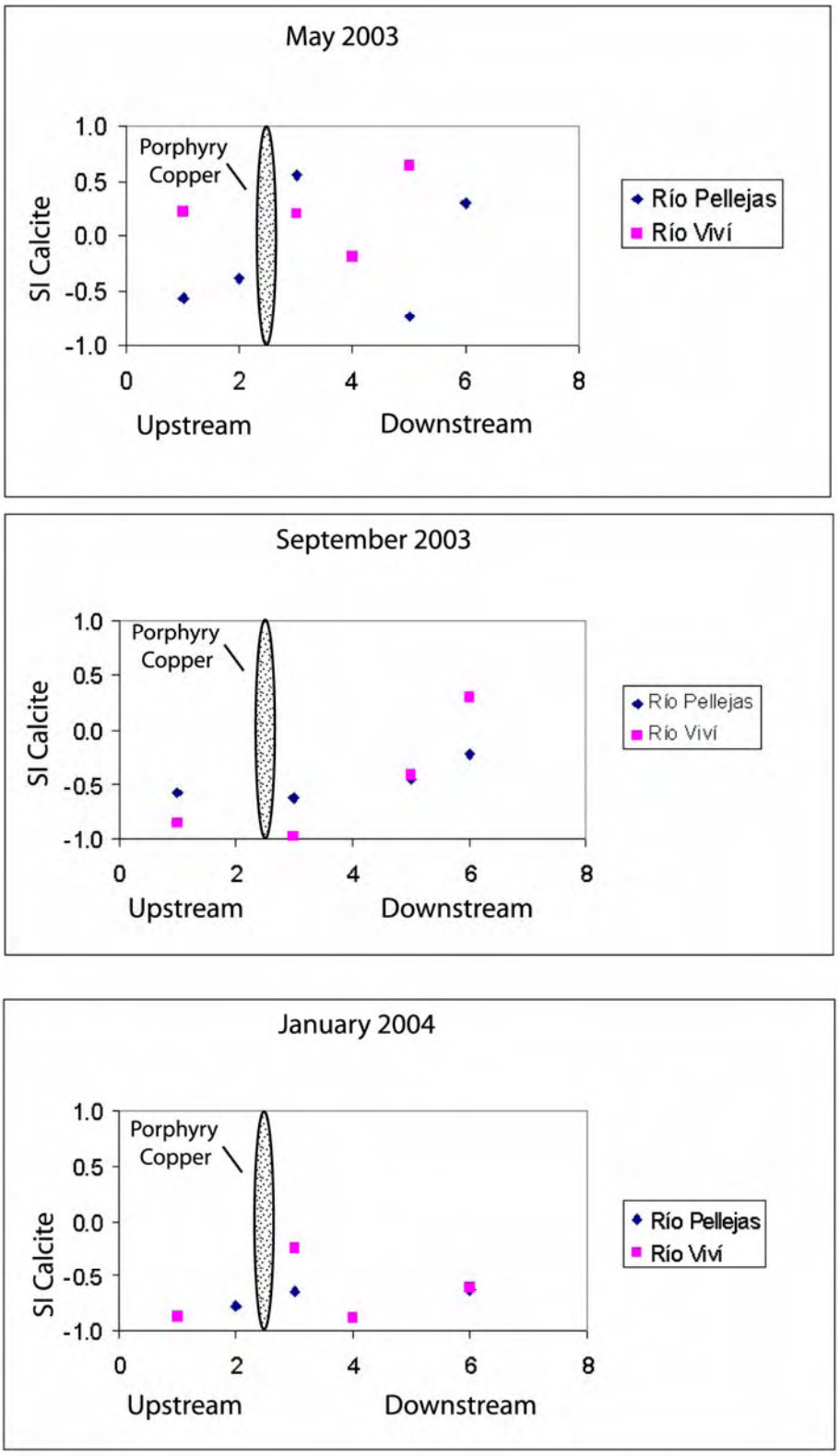

Figure 22. Saturation indexes of calcite from upstream to downstream during the three sampling periods.

McDowell (1990) also suggested that during summer, aeolian transport of Saharan dusts makes significant contribution to the Ca, K, Mg, and sulfate budgets of a tropical rainforest in Puerto Rico to the east of the study area. However, these contributions are generally less than 1 mg/L, and thus do not represent a significant portion of the budget of these elements in the study area.

With respect to the role of the porphyry deposits in the calcium budget of the study area, it appears that the calcium concentration of the watersheds is mostly controlled by the unmineralized bedrock geology rather that the porphyry copper deposits. The propylitic alteration associated with the deposits was probably essentially an isochemical processes. Even though the sericitic and argillic alterations would have leached Ca, Mg, K, and Na, these ancient processes do not appear to be reflected in the water chemistry. Highly soluble anhydrite ($CaSO_4$), which is commonly found in porphyry copper deposits (Titley and Beane, 1981) has not been identified in the Adjuntas deposits.

Sodium

Sodium is the fourth most abundant element in the earth`s crust, comprising about 2.6% of its composition; it is the most abundant of the alkali group of metals (Lide, 2004). Sodium is not considered to be harmful to freshwater organisms, unless concentrations reach extreme levels at which freshwater organisms cannot survive. High sodium concentration can be derived from agricultural runoff from residues of fertilizers (Florida LAKEWATCH, 1999). Similar to calcium, possible sources of sodium in the watersheds are feldspars,

amphiboles, and pyroxenes. The amphiboles identified in the study area, tschermakite and magnesio-hornblende, have low Na content. Pyroxenes, found only in one sample PH-A, vary between augitic to diopsidic compositions; diopside lacks Na, whereas Na is present in augite only in low concentrations (Table 6). The plagioclase feldspars are generally more calcic than sodic. The highest concentrations of sodium were found in sample PRRV 4 (Fig. 13), which is a quartz diorite or granodiorite.

Figure 23 shows the different concentrations of sodium in both watersheds during the three sampling periods. As is observed, there is not a significant difference between the concentrations of the upstream samples and the downstream samples. Modeling results indicate that the most abundant dissolved sodium species is the free ion Na^+ and that no sodium-bearing mineral phases are near saturation. As with calcium, the general correspondence of the Ca/(Ca+Na) of the waters with that from the plagioclase analyses suggests that sodium was derived from the dissolution of feldspars (Fig. 21) and that it behaves conservatively once in solution. Sodium is not a major component of either river and its input to the stream waters comes mostly from plagioclase feldspars. Figure 23 suggest that the porphyry copper deposits are not making a major contribution of sodium in the waters. Sea salt aerosols are another possible source of sodium in the area (McDowell, 1990), but as with calcium, their potential contribution is minor compared to the total concentrations in waters in the study area.

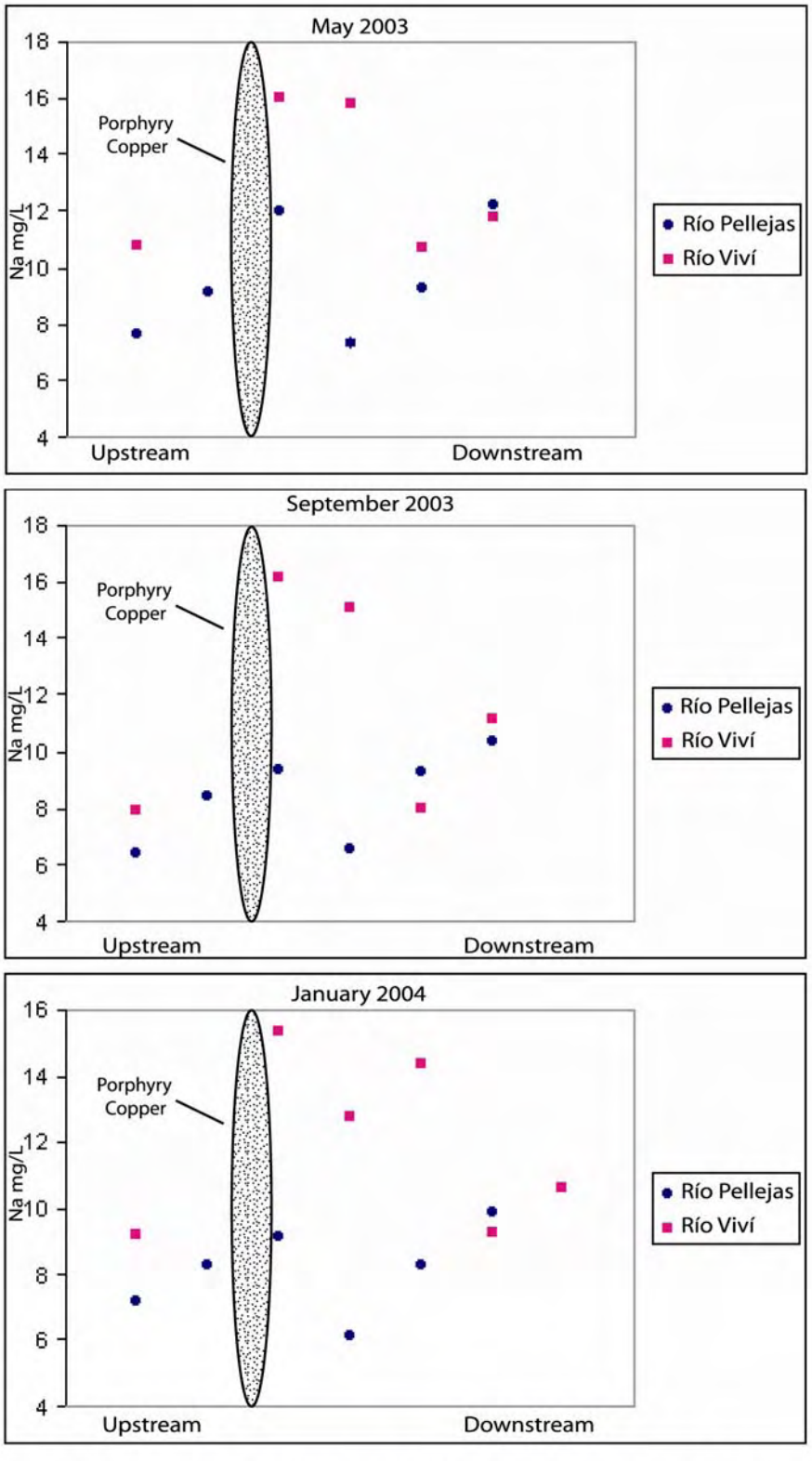

Figure 23. Sodium concentration in the Río Pellejas and Río Viví watershed and their relation to the porphyry copper deposits. Values are presented from upstream to downstream including the groundwater sites.

Potassium

Potassium is the seventh most abundant metal, and makes up about 2.4% by mass of the Earth's crust (Lide, 2004). It is considered an essential element for human health and plays an important role in the plant development, hence, its wide use in for plant fertilizers. Likely sources of potassium in both watersheds include biotites, amphiboles, and feldspars. Biotite was found only in sample site PRRV-4; which is a quartz diorite/granodiorite from the Río Viví area. Biotite is common in quartz diorite and granodiorite, but in minor quantities. These biotites are Mg-rich and their potassium content averages of 1.4 wt. % (Table 6), which categorize them as phlogopitic to eastonitic in composition. Potassium concentrations in all the observed amphiboles were small, but were higher in the tschermakites (PRRP-5) compared to the magnesio-hornblende (PRRP-A, PH-A). Low potassium content in the rocks and minerals indicates the scarcity of K-feldspars in the rock units of the study area.

The very high saturation indices of K-mica (Fig. 24), suggest that it is not playing a major role in controlling the water chemistry of both watersheds, because they suggest extreme supersaturation. The closest values to zero in Río Pellejas were those from the groundwater site PRRP-2 for May and September and from site PRRP-3 in January. In Río Viví, the closest values to equilibrium (i.e., zero) were from the downstream sites PRRV-3 and PRRV-4 during January and May and for the groundwater site PRRV-5 in September. According to the PHREEQC results, the most abundant potassium species is the free ion K^+.

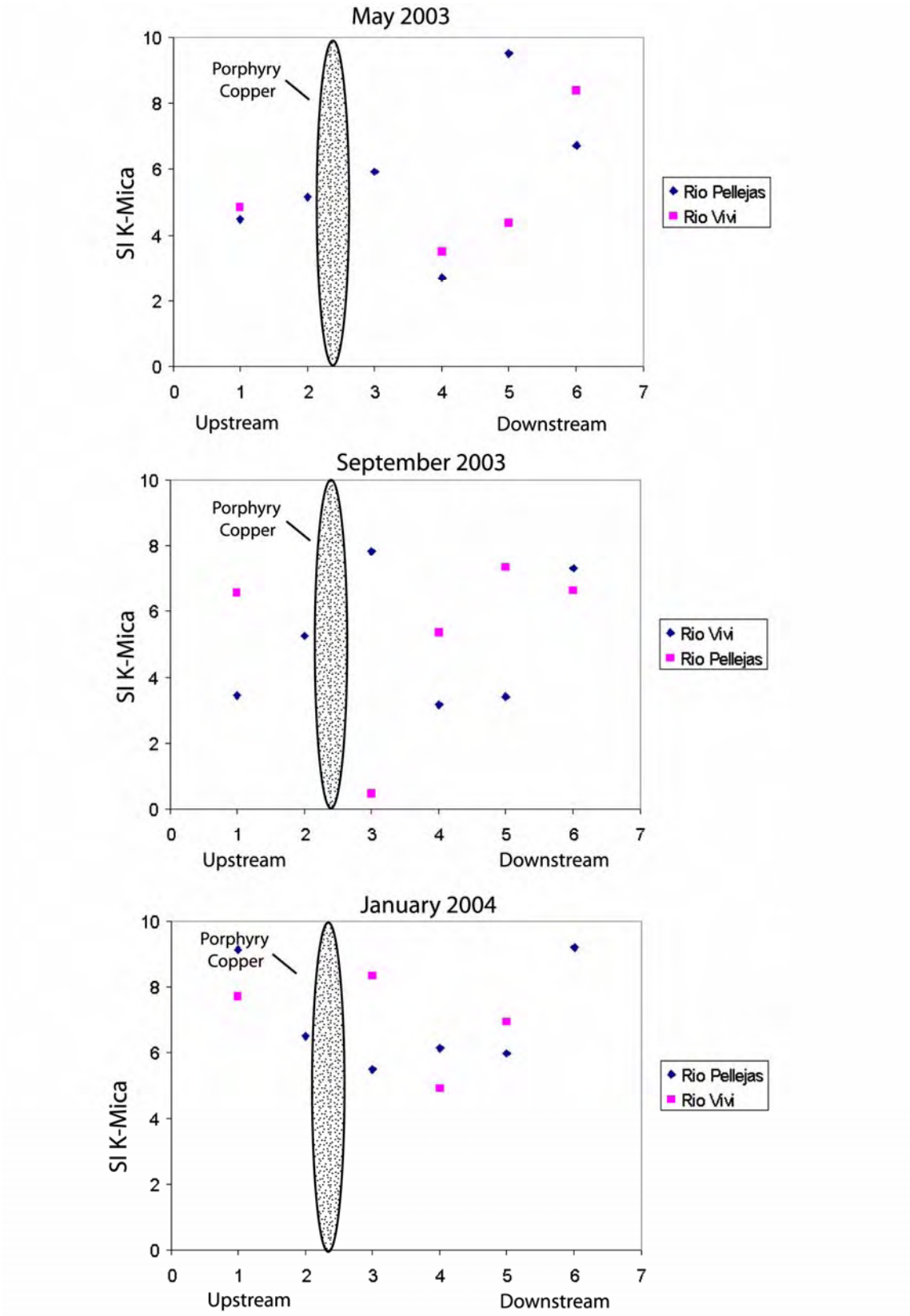

Figure 24. Saturation indices of K-mica in Río Pellejas and Río Viví during May, September and January.

Minor potential contributors of potassium in the streams are sea-salt aerosols and the Saharan dusts (McDowell, 1990).

Magnesium

Magnesium is the eighth most abundant element in the Earth's crust (Lide, 2004). It is an essential nutrient to humans and other organisms. It is found naturally in water and is highly soluble; if it is in high concentrations it causes hard water. Weathering of pyroxenes and amphiboles is the principal source of magnesium (Brantley et al., 1995), but it can also be derived from chlorite and biotite. Chlorite was found in most of the rock samples from both watersheds, which indicates that the processes of hydrothermal alteration and low-temperature weathering of pyroxenes and amphiboles have been important processes in both watersheds. The chlorite from sample PH-A is pycnochlorite (iron clinochlore) (Fig. 17). The magnesium content in biotites from plutonic rocks is high because they are phlogopitic to eastonitic in composition (PRRV-4; Table 6). The amphibole with the highest content of Mg is magnesio-hornblende from sample sites PRRP-A and PH-A. In most geologic settings, hornblende is the principal source of Fe, Mg, and some trace metals, due to its abundance, variable composition and its instability under weathering conditions (Brantley and Chen, 1995). Other possible sources with lesser amounts of magnesium are the sea-salt aerosols and the Saharan dust. According to McDowell (1990), studies performed at the El Yunque forest, east of the Adjuntas porphyry copper area, suggest that most of the Mg, Cl, Na and K founded in wet and bulk precipitation

is contributed by sea-salt aerosols. The significance of these elements there is greatly influenced by the proximity of El Yunque to the sea (20 km). The porphyry copper deposits are located about 30 km south of the north coast of the island and approximately 100 km west of El Yunque. Thus, sea salts and other aerosols may contribute to the magnesium budget of the study area, but no studies have been made in the area.

Sulfate

Sulfate is a chemical compound widely distributed in nature and can be dissolved into water bodies in significant amounts. Sulfate in drinking water has a secondary maximum contaminant level (SMCL) of 250 mg/L, based on aesthetic effects (taste and odor) (EPA, 2002). There are a variety of potential sources for sulfate in water bodies. Sulfate concentrations in a water body are influenced primarily by natural deposits of minerals and organic matter in its watershed (Florida LAKEWATCH, 1999). Sulfate, like Cl, Na and Mg, can be supplied to the air in large amounts from sea spray (Gorham, 1971). Precipitation, ground, and surface water can contain sulfate not only from natural sources such as sea salts, bedrock, soils, and volcanic emissions, but also from industrial and domestic pollution. According to McDowell, (1990) sulfate in precipitation in Puerto Rico can be derived from long-range transport of air masses of European or African origin, and it is also associated with wintertime movement of cold fronts from the North American continent into the Caribbean.

Unfortunately no studies of aerosols and their impact in central Puerto Rico have been done.

In the study area, the oxidation of sulfide minerals in the mineralized area is likely the main source of sulfate. Sulfide minerals, such as pyrite and pyrrohotite, when exposed to atmospheric oxygen or oxygenated ground or surface waters can cause acid-rock drainage (Plumlee, 1999). Although none of the water samples exceeded the water-quality guidelines in the study area, the SO_4 concentration varies from upstream to the downstream sites, with the highest concentrations from the sites downstream of the porphyry deposits in the Río Viví watershed (Fig. 25, Tables 7, 8, and 9). Based on Figure 25, it is observed that for Río Pellejas, the lowest SO_4 concentration, excluding the upstream sites, was for the groundwater site PRRP-2 (16 mg/L, January 2004) and for the downstream sites PRRP-1 (26 mg/L, January) and PRRP-6 (40 mg/L, January 2004); the highest concentration was for PRRP-3 (62 mg/L). The low concentrations of SO_4 at the ground-water sites are probably because little or no oxidation of sulfide minerals is occurring upgradient from the sample site. Low concentrations in the downstream sites (PRRP-1, PRRP-6) are probably related to dilution, because both sites are located in the main stem of the river (Fig. 3). High concentrations of SO_4 at sample site (PRRP-3) could be explained by its proximity to Piedra Hueca porphyry copper deposit with limited dilution because the sampling point is at the source of a stream. For the Río Viví, the behavior is similar to that for Río Pellejas, but the concentrations are higher. The upstream site (PRRV-1) had the lowest SO_4 concentration (26 mg/L, January 2004),

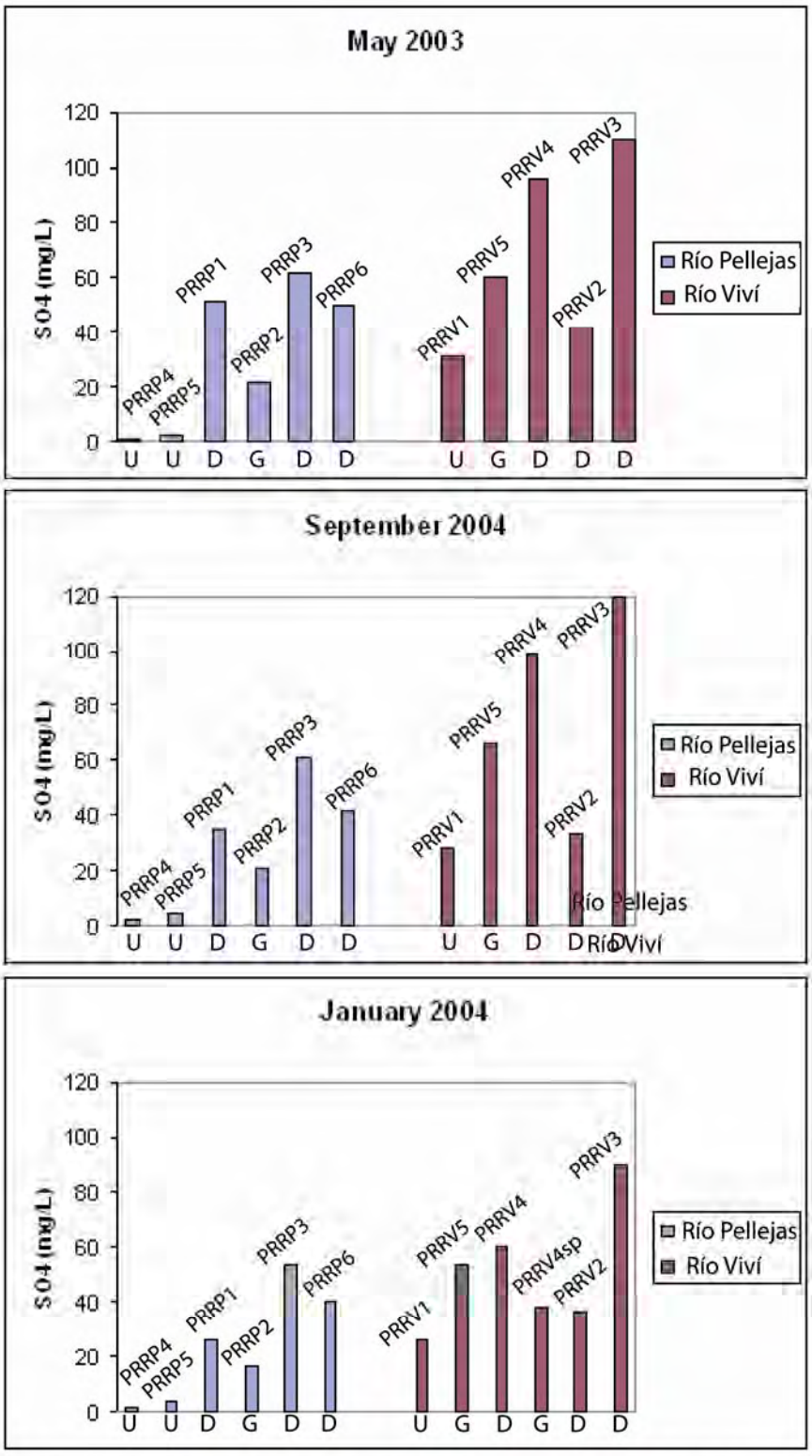

Figure 25. Sulfate concentrations in both watersheds during the three sampling periods. Values are displayed from upstream (U) to downstream (D) including the groundwater (G) sites.

followed by the downstream site PRRV-2 (34 mg/L, September 2003) and then the ground-water site PRRV-5 (54 mg/L, January 2004), which in contrast to the groundwater site in Río Pellejas, had a higher SO_4 content than some of the downstream sites. Finally, sample sites PRRV-4 and PRRV-3 had the highest concentrations (99 mg/L and 120 mg/L in September 2003, respectively). Ground-water site PRRV-5 is probably reflects greater oxidation of sulfides compared to sample sites PRRV-4sp and PRRP-2. Sample sites PRRV-4 and PRRV-3 are sites located in streams away from the main channel of the river where less dilution is occurring. In contrast, sample site PRRV-2 is located in the main trunk of the river and receiving all waters from a variety of streams in addition to those where sample sites PRRV-4 and PRRV-3 are located.

Small concentrations of pyrite and traces of pyrrhotite were found is most of the rock samples. It is assumed that the oxidation of these minerals is the main, the major source of SO_4. In terms of saturation indices, none of the sulfate minerals (especially less soluble barite and gypsum) reach saturation suggesting that SO_4 behaves conservatively throughout the watersheds.

Sulfate, in addition to Cu and Zn, are potential pathfinders to target porphyry copper deposits. All the results suggest that the concentrations of sulfate throughout the sample sites reflect the location of the porphyry copper deposits. This fingerprint is observed in the differences between the sulfate concentrations of the surface water upstream and downstream of the deposits and also in the ground-water composition.

Silica

Silicon is second most abundant element in Earth's crust, only exceeded by oxygen. Silica is the name given to silicon dioxide (SiO_2). Silica is found in every water body and in freshwater. Its concentration can vary widely. Under humid tropical conditions, surface waters are characterized by high proportions of silica. Silicon is relatively insoluble at low pH but becomes more soluble at high pH (Smith and Huyck, 1999). Silica is not considered harmful for the environment and is a nutrient for some microorganisms, but in general is not considered a major biological nutrient.

There are many potential sources of silicon. Virtually all of the minerals described in the rocks contain it. Because the plutonic rocks contain more silica than the volcanic rocks it was assumed that high dissolved silica concentrations would be found in the watershed where the bedrock is dominantly composed of plutonic rocks. However, as is observed in Figure 26, the silica concentration is very similar in both watersheds, but is locally higher in the non-plutonic parts of Río Pellejas. In general, the highest dissolved silica concentration was for May, which is the time with the least flow of the three sampling periods; it is assumed that more dilution occurred during January and September causing lower silica concentrations to be observed. Minerals like amphiboles and feldspars could be sources of aqueous silica because their dissolution could liberate silica, whereas quartz, the main detrital mineral in the streams, is more resistant to weathering, and thus less probable to contribute to the aqueous silica in the streams. This

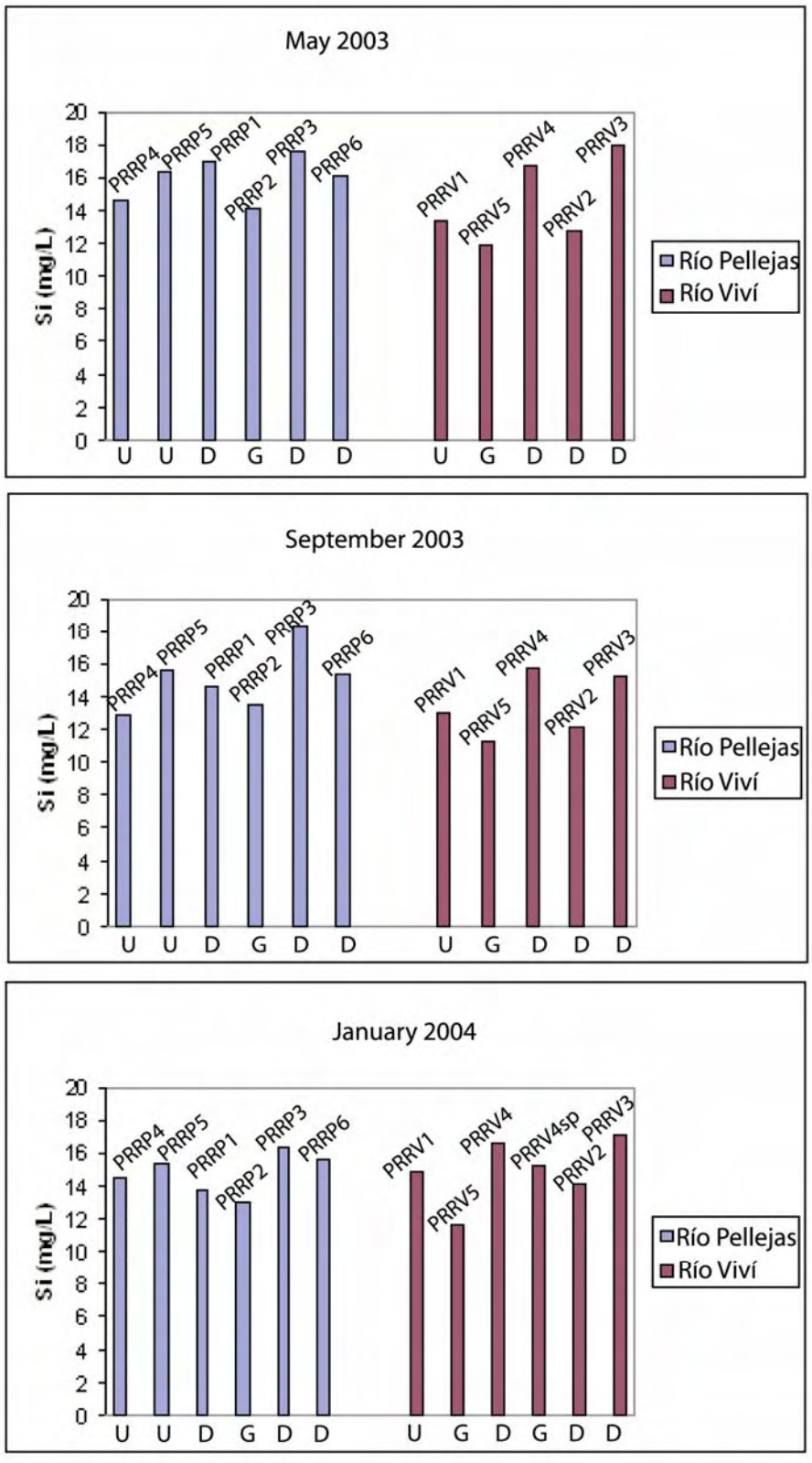

Figure 26. Silica concentration in the two watersheds during the three sampling periods. Values are presented from upstream (U) to downstream (D) including the groundwater sites

can be an explanation for the lack of correlation between the high-silica rocks (plutonic rocks) and the concentration of silica in the streams. Other important sources of silica are soils. Thick soils, typical of tropical environments, are generally depleted in major cations because they are mainly composed of secondary minerals, such as clays (kaolinite) and oxy-hydroxides (gibbsite, goethite), and primary phases (quartz), which may serve to buffer the concentrations of these elements in the watersheds (Oliva et al., 2003). Figure 27 shows the saturation index of chalcedony for the three sampling periods. Chalcedony is near or at saturation because most of the saturation index values ranged from -0.18 to 0.25.

Iron

Iron is the fourth most abundant element in the Earth's crust and is an essential element for humans and plants, although it can become toxic if present in excessive amounts. Natural waters can contain variable amounts of Fe. It can occur in waters as ferric (Fe^{3+}) or ferrous (Fe^{2+}) iron depending upon redox conditions. The EPA has established a maximum secondary contaminant limit for iron, which is related to aesthetic aspects such as taste and appearance rather than toxic effects (Smith and Huyck, 1999).

Iron sources in the watershed are numerous. In the study area, iron was found in, amphiboles, chlorites and biotites, and in minor concentrations in the observed pyroxenes and epidotes (Table 6). The amphiboles are magnesio-hornblende and tschermakite (Fe = 0.07 to 0.8 atoms per unit formula; Fig. 16,

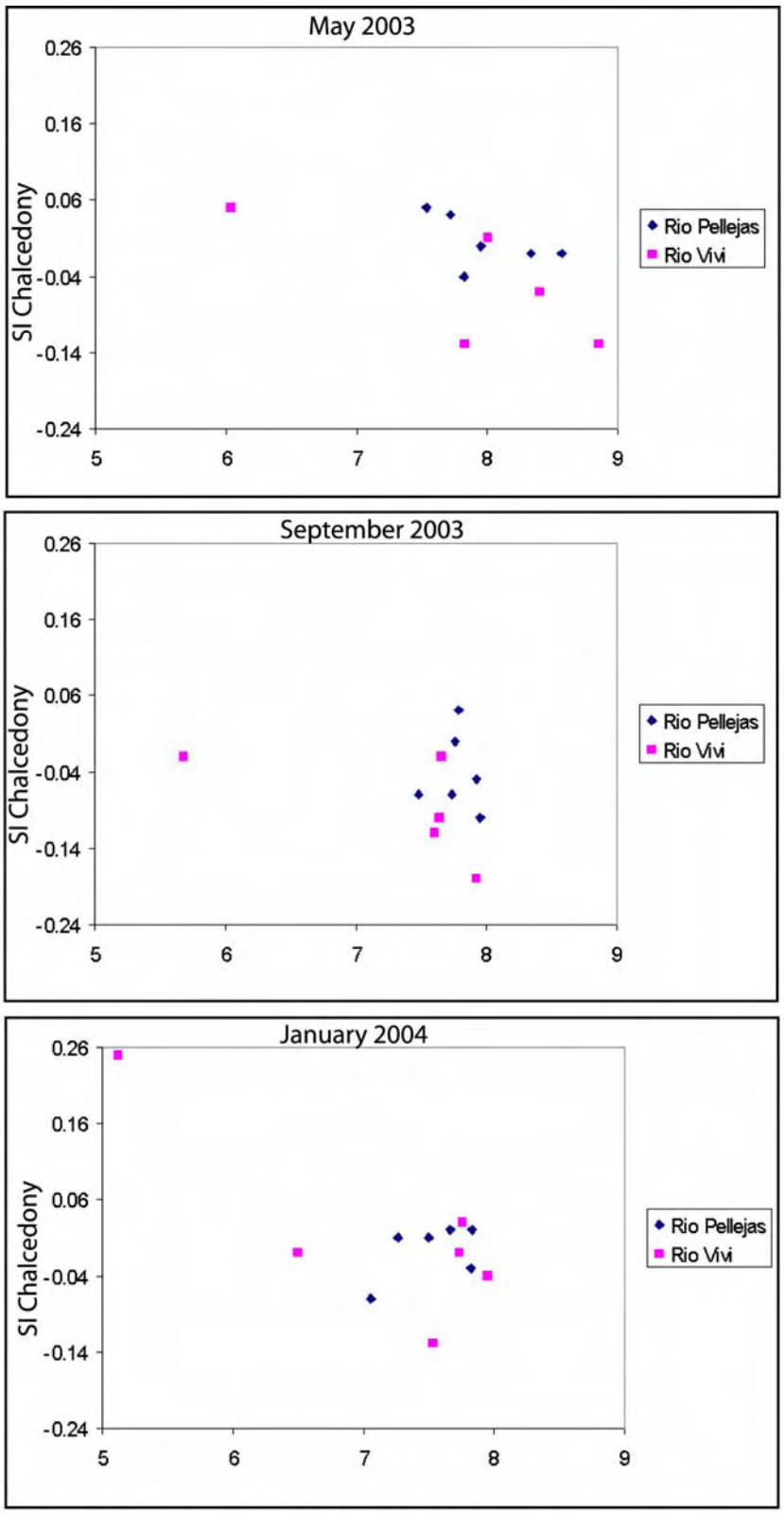

Figure 27. Graphs showing the saturation indexes of chalcedony versus pH of the Río Pellejas and Río Viví during the three sampling periods.

Table 6). The chlorite, pycnochlorite, as was discussed previously is an iron clinochlore (Fe = 3.41 to 5.0 atoms per unit formula; Fig 17, Table 6). The biotites are phlogopitic to eastonitic composition (Fe = 0.33 to 1 atoms per unit formula, Table 6), which is more Mg- and K-rich than other end members suggesting that these sheet silicates are not major iron sources. Similarly, the epidote from the Maricao Formation is a clinozoisite, which is more Al-rich than Fe-rich. The pyroxenes are diopsidic to augitic in composition (Fig. 15; Table 6) indicating that none of these minerals are likely the major sources of iron.

Other mineral sources of iron are the iron sulfides; pyrite and chalcopyrite. As mentioned previously, pyrite was a common minor phase and chalcopyrite was only found as inclusions and microscopic veinlets in thin sections, but is more abundant within the porphyry copper deposits. Although these minerals locally constitute up to 5 to 10% of the observed minerals, their rapid weathering rates in oxidizing environments will make them important potential contributors of iron in the watersheds.

Río Pellejas had lower concentration of iron in water than Río Viví (Fig. 28). The range in Río Pellejas was from below detection limit to 0.14 mg/L (PRRP-3, May). The range in Río Viví was from 0.09 (PRRV-3, January) to 15.9 mg/L (PRRV-4sp, January) (Tables, 7, 8, and 9).

Concentrations of iron in the stream sediments in both watersheds are variable (Fig. 29a). In Río Pellejas, the iron concentration increases as it approaches the deposits, and the rise continues as it passes the deposits. The

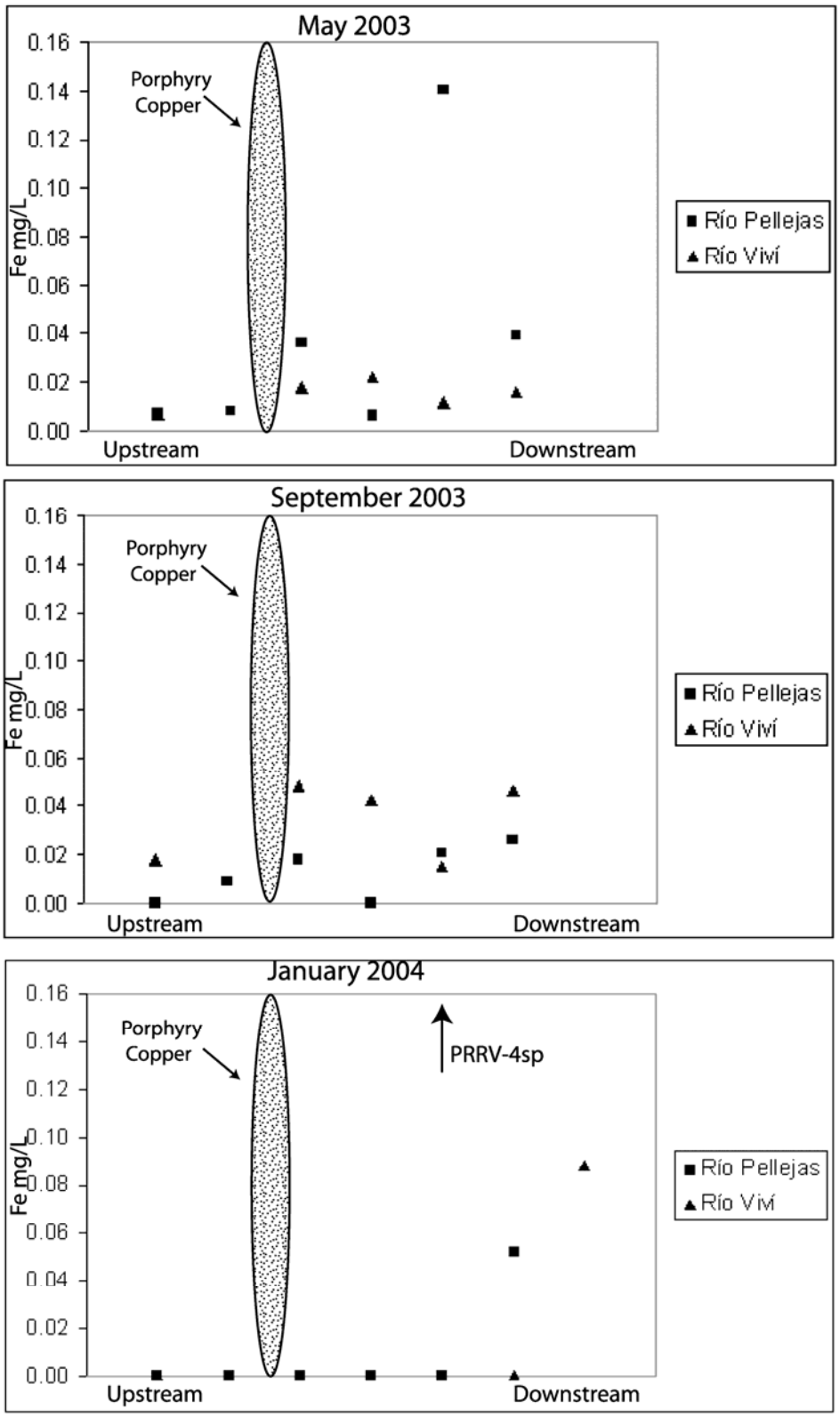

Figure 28. Concentration of dissolved iron in the two studied watersheds and its relation to the porphyry copper deposits. Sample site PRRV-4sp had a value of 15.9 mg/L that was not displayed for scale purposes.

Río Viví pattern sediments is different, because the highest iron concentration in the sediments is for the upstream site, (PRRV-1) with 9.83 wt% Fe; instead of increasing, the downstream samples decrease in iron (Fig. 29 a). Some of this variability may be due to differences in the zonation of primary hydrothermal minerals around the porphyry intrusions. Bedrock geology could possibly influence the iron concentration because most samples in Río Viví are volcanic-sedimentary rocks, whereas all the samples in Río Viví are plutonic rocks.

The saturation indices of the waters in both watersheds with respect to ferrihydrite ($Fe(OH)_3$) and goethite are very informative with respect to the iron budget of the study area. Figure 30 presents graphs of saturation indices for goethite and $Fe(OH)_3$ versus pH. For May, the saturation indices of goethite for Río Pellejas and Río Viví ranged from 3.2 (PRRV-3) to 7.8 (PRRP-3). During September, the values ranged from 2.7 (PRRV 3) to 7.5 (PRRV-5). In January, only a few samples had iron present above the detection limit, and the saturation indices ranged from 0.1 (PRRV-3) to 7.3 (PRRP-6).

The significant supersaturation of goethite suggests that some other phase, most likely poorly crystalline ferrihydrite, is controlling iron concentrations. Saturation indices of $Fe(OH)_3$ for both rivers during May ranged from -2.6 (PRRV-3) to 2.1 (PRRP-3); during September, the indices ranged from -3.2 (PRRV-3) to 1.5 (PRRV-5); and for January, they ranged between -5 (PRRV-3) and 1.9 (PRRP-6). Saturation indices of $Fe(OH)_3$ for most of the samples suggest also supersaturation, but some values especially those for PRRV-3, had negative values indicating undersaturation. The positive saturation index values

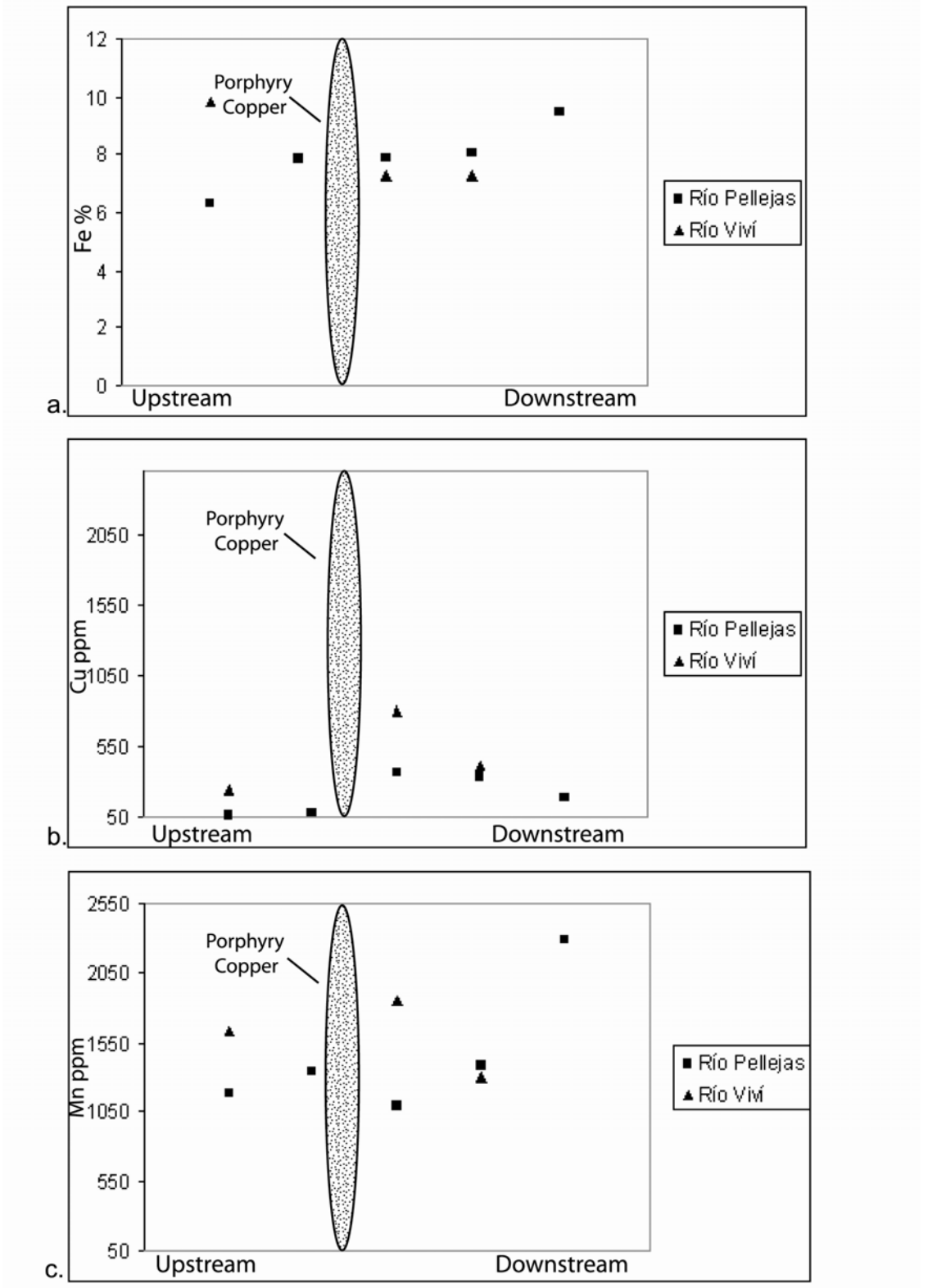

Figure 29. Concentration of iron (a), copper (b), and manganese (c) on the stream sediments of Río Pellejas and Río Viví from upstream to downstream of the porphyry copper deposits, plotted against relative position in the watershed.

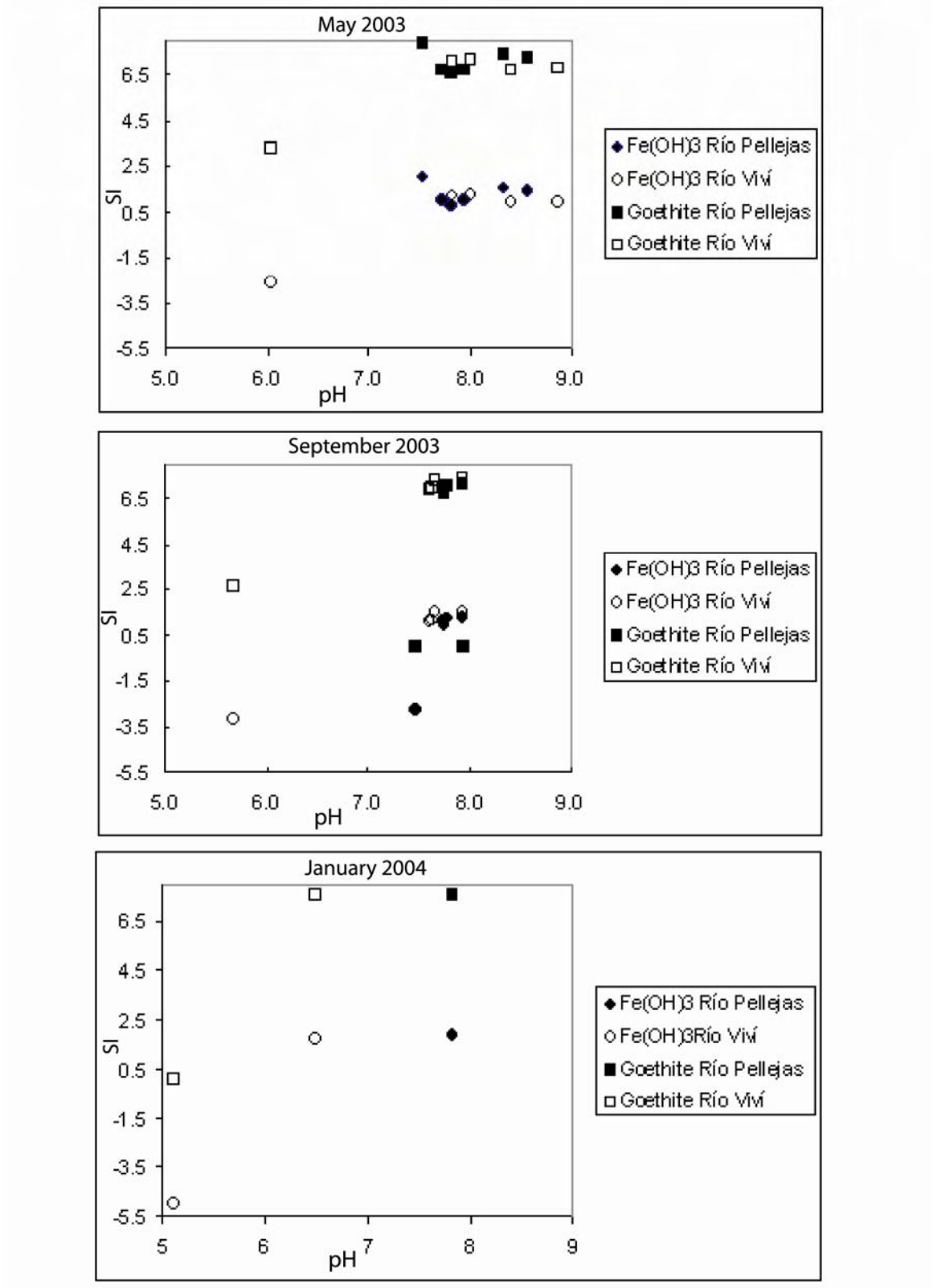

Figure 30. Graphs showing the SI index of goethite and Fe $(OH)_3$ versus pH. During January, many samples were below detection limits for Fe.

for $Fe(OH)_3$ may reflect the inclusion of colloidal iron that passed through the 0.45 μm filters, and was included in the nominal "dissolved" fraction. PRRV-3 was the site with lowest pH during the three sampling periods. Thus, the undersaturation of these waters reflects the greater solubility of iron and other metals at lower pH. On the basis of the saturation indices for $Fe(OH)_3$, ferrihydrite, both in the streams and the soils, is likely the dominant control on iron chemistry in both watersheds. Because of its near ubiquitous distribution throughout the study area, the presence of ferric hydroxides is likely to exert an important control on the distribution of metals such as Cu, Zn, and Cd through sorption reactions discussed below.

In general, water-chemistry data show an increase in iron concentration for both rivers as they passed the deposits, suggesting that the deposits are responsible for these increases.

Aluminum

Aluminum is the third most abundant element in the Earth's crust and constitutes 7.3 % by mass. Like many other metals, it can be toxic if it is consumed in excess. The EPA considered aluminum among the secondary water contaminants with a maximum level between 0.05 and 0.2 mg/L for drinking water. The metal exists as a variety of species, among them Al^{3+} and $AlOH^{2+}$, and its mobility increases at lower pH levels in soils and surface waters (Arent and Lewis, 1987).

Possible mineral sources of Al in the waters of Río Pellejas and Río Viví watersheds are plagioclase, hornblende, chlorite, biotite and epidote. Most of the plagioclases observed range from andesine to anorthite, which have a higher Al content than more sodic plagioclases such as albite and oligoclase. From the observed hornblendes, tschermakite had higher Al contents than magnesio-hornblende (Fig 16). The pycnochlorite and biotite have higher aluminum contents than epidote. In general from the observed minerals, their composition and abundance in the area, the main sources of Al are plagioclase, chlorite, and epidote. Feldspars were shown to be important sources for Ca, Na, and K. Biotite and hornblende are other possible sources; however, they constitute a relatively small percentage (about 10 %) compared to more than 35 % for plagioclases, and chlorites.

Secondary phases play important roles in the geochemical budget of aluminum. Figure 31 shows four Al phases: amorphous $Al(OH)_3$, boehmite, gibbsite, and kaolinite and their respective saturation indices, plotted as a function of pH. The saturation indices for $Al(OH)_3$ are below zero. Saturation indices for boehmite varied more and range from -1.48 to 1.35. Most of the values in May and September were negative, whereas in January most of them were positive. Similarly saturation indices of gibbsite range from -1.01 to 1.62, most of the values within both watersheds were positive, especially those from January. Finally, saturation indices for kaolinite were mostly positive ranging from -0.71 (PRRV-5) to 5.5 (PRRV-3). The significantly high saturation indices for kaolinite suggest that it is not exerting a control on the water

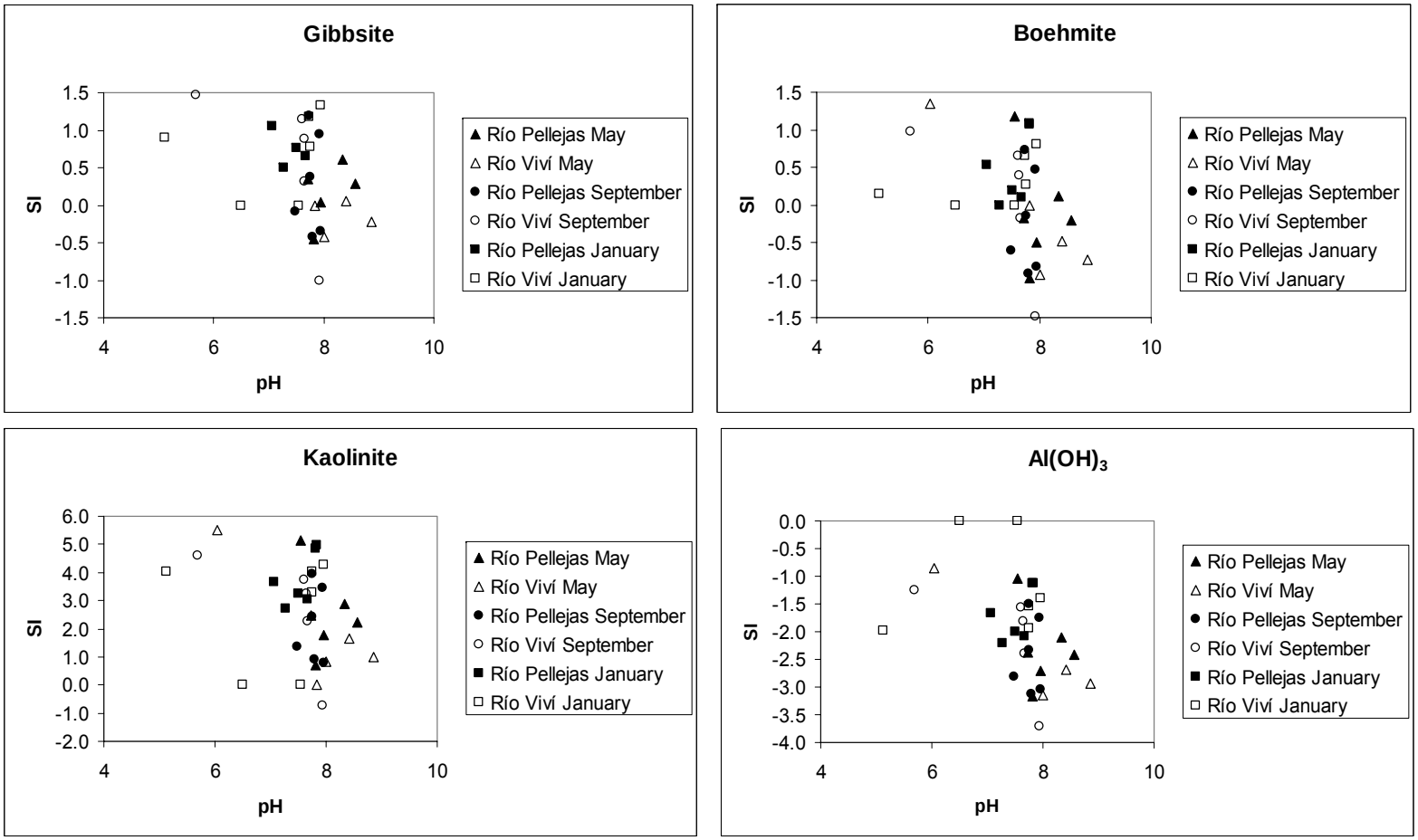

Figure 31. Saturation indices of different aluminum phases versus pH, during the three sampling periods.

chemistry, presumably because its precipitation is kinetically inhibited. Instead, other, less complex aluminum phases, such as amorphous $Al(OH)_3$, boehmite, or gibbsite play important roles. Aluminum hydroxides, such as gibbsite, $Al(OH)_3$, and boehmite, are very insoluble under neutral pH conditions and their solubility increases as the pH decreases (Smith and Huyck, 1999). Thus, because most of the water samples have neutral pH values, aluminum will be near saturation and therefore have a non-conservative behavior. Due to the fact that all the aluminum is behaving in a non-conservative manner, it is not a reliable geochemical indicator of the presence of the porphyry copper deposits in these watersheds.

Copper

The estimated crustal abundance of copper is 0.6 mg/kg. Archaeological evidence suggests that people have been using copper for at least 11,000 years (Thomas Jefferson N.A.F., 2004.). Because of its properties: high ductility, malleability, thermal and electrical conductivity, and its resistance to corrosion, copper has become a major industrial metal, ranking third after iron and aluminum in terms of quantities consumed (Edelstein, 2004).

Copper is considered an essential metal for human health and it must be ingested from 1.5 to 3.0 mg daily (Smith and Huyck, 1999). Despite of the relatively low toxicity to humans, copper and zinc are considered to be pollutants in water because of their high toxicity to aquatic life. The dominant aqueous copper species is Cu^{2+}. Similar to other metals, like Zn, Cd, Pb, it tends to be

more soluble under acidic conditions (Drever, 1997). According to Smith and Huyck (1999), copper is very mobile under acidic conditions (pH < 3) and has limited mobility in circumneutral pH's (pH > 5).

Copper is not a major cation in the waters of either watershed. Its concentration does not exceed the water-quality criteria, but there is a definite difference between the water sites that are upstream and downstream of the deposits. This is observed, for example, during January, in Río Pellejas upstream values are below detection limits, whereas downstream sites have copper values of 0.024 mg/L (PRRP-1). The copper value of the upstream site in Río Viví is 0.014 mg/L, whereas the highest copper concentration was for sample site PRRV-3 (0.204 mg/L). The sediments in the area also exhibit the same pattern, low copper concentrations in the upstream sites and high concentrations in the downstream sites (Appendix ID). Figure 29b shows that the concentration of copper in the sediments upstream of the deposits in the Río Pellejas watershed ranged from 64 to 79 mg/kg and in the Río Viví watershed the concentration was 235 mg/kg. Downstream concentrations in Río Pellejas ranged from 190 to 364 mg/kg, and from 410 to 804 mg/kg in Río Viví. All of the downstream concentrations that are close to the deposits have the higher copper contents, but decrease with increasing distance from the deposits.

Stream-sediment data show that the copper concentration increases as it reaches the porphyry copper deposits, as the distance between the sites and the deposits increase the copper concentration diminishes. Learned (1972) conducted a soil geochemical study in the area of Río Viví and found that the

highest concentration of copper was mostly over the Piedra Hueca deposit and the north western part of the Calá Abajo deposit. The lowest copper concentration occurred in the south-eastern area of Calá Abajo. This pattern is similar to the concentration of copper in the stream-sediment samples.

The only copper mineral found in the area was chalcopyrite (Fig. 5). As was mentioned in Chapter 2, several chalcopyrite veinlets were observed in pyrite from the batholitic and the epiclastic rocks of the Monserrate Formation. Plumlee (1999) noted that some trace elements are present in low, but significant quantities in basalts, andesites and volcanic tuffs; all these rock types are present in the study area and described in detail in Chapter 2.

The saturation indices calculated from the water geochemical data showed that no phases of copper are near saturation. Malachite, for example, has values in Río Pellejas that ranged from -3.98 to -1.96. Values in Río Viví are even lower, and ranged from -4.45 to -2.26. Copper has likely been sorbed from solution by secondary Fe hydroxides, which remove trace metals, such as copper, with increasing pH; therefore, the low aqueous copper concentration is probably a result of sorption either in the streams or closer to the deposits in the soils.

Manganese

Manganese constitutes about 0.10 percent of the Earth's crust (Hem, 1963). It is considered an essential element for human health, as well as a potentially toxic element. The EPA has established a secondary maximum

contaminant limit for manganese of 0.05 mg/L in water; this level is mostly to minimize taste or color problems in drinking water. Manganese is a metal that stays in solution at low pH's. Under alkaline conditions manganese oxides can sorb trace metals.

Manganese in igneous rocks commonly occurs as a minor constituent in pyroxenes, olivines and amphiboles. Electron probe microanalysis of pyroxenes and amphiboles from thin sections from the study area reveal low manganese concentrations (Table 6).

The concentration of manganese in the stream waters of Río Pellejas ranged from 0.0003 mg/L (PRRP-4) to 0.05 mg/L in PRRP-3 both in May 2003, whereas the concentrations in Río Viví ranged from between detection limits in the groundwater site PRRV-5 to 5.73 mg/L in sample site PRRV-4sp (January 2004); this is the highest concentration of manganese found between the two watersheds and it exceeds the water-quality guideline for drinking water (Tables 7,8, and 9). Manganese concentrations exceeded the water-quality guidelines for other sites: during the three sampling periods, sample site PRRV-3 surpassed the standard with values that ranged from 0.11 to 0.14 mg/L and PRRV-4 during January had a value 0.553 mg/L. In Río Pellejas, a sample site with concentrations close to the established guideline is PRRP-3 (May) with a value of 0.05 mg/L (Table 9).

Sediment samples in Río Pellejas show that manganese concentrations increase with increasing distance from the deposits. In Río Viví, the concentration in the first sample down stream from the deposit increases, but

samples farther downstream decrease. This pattern coincides with the results of Learned (1972) in which the highest concentrations of manganese in soils increase in the areas that surround the deposits, not in the deposits itself (Fig 29c).

None of the manganese phases were near saturation, except for rhodochrosite in one site (PRRV-4sp). Figure 32 shows that the saturation indices for rhodochrosite are far below saturation, indicating that manganese is behaving conservatively in solution. Based on the above information, manganese can be considered an indicator element for the Río Viví porphyry copper deposits, because its distribution is related to that of the deposits.

Zinc

The zinc concentration of the Earth's crust averages 65 to 70 ppm in the Earth crust (Shuman, 1980). It ranks fourth among metals in annual world consumption, being only surpassed by iron, aluminum, and copper (Cammarota, 1980). It is considered an essential element for plants and humans, although it is also considered as a potentially toxic metal. EPA has established a secondary maximum contaminant level of 5 mg/L for this element.

Mineralogical sources of zinc are mostly sphalerite, mafic silicates, and other sulfides. Sphalerite is commonly associated with sulfides like pyrite, marcasite, galena, and chalcopyrite. Zinc minerals were not found in the rock samples but based on the geology of the area it is assumed that the sphalerite is

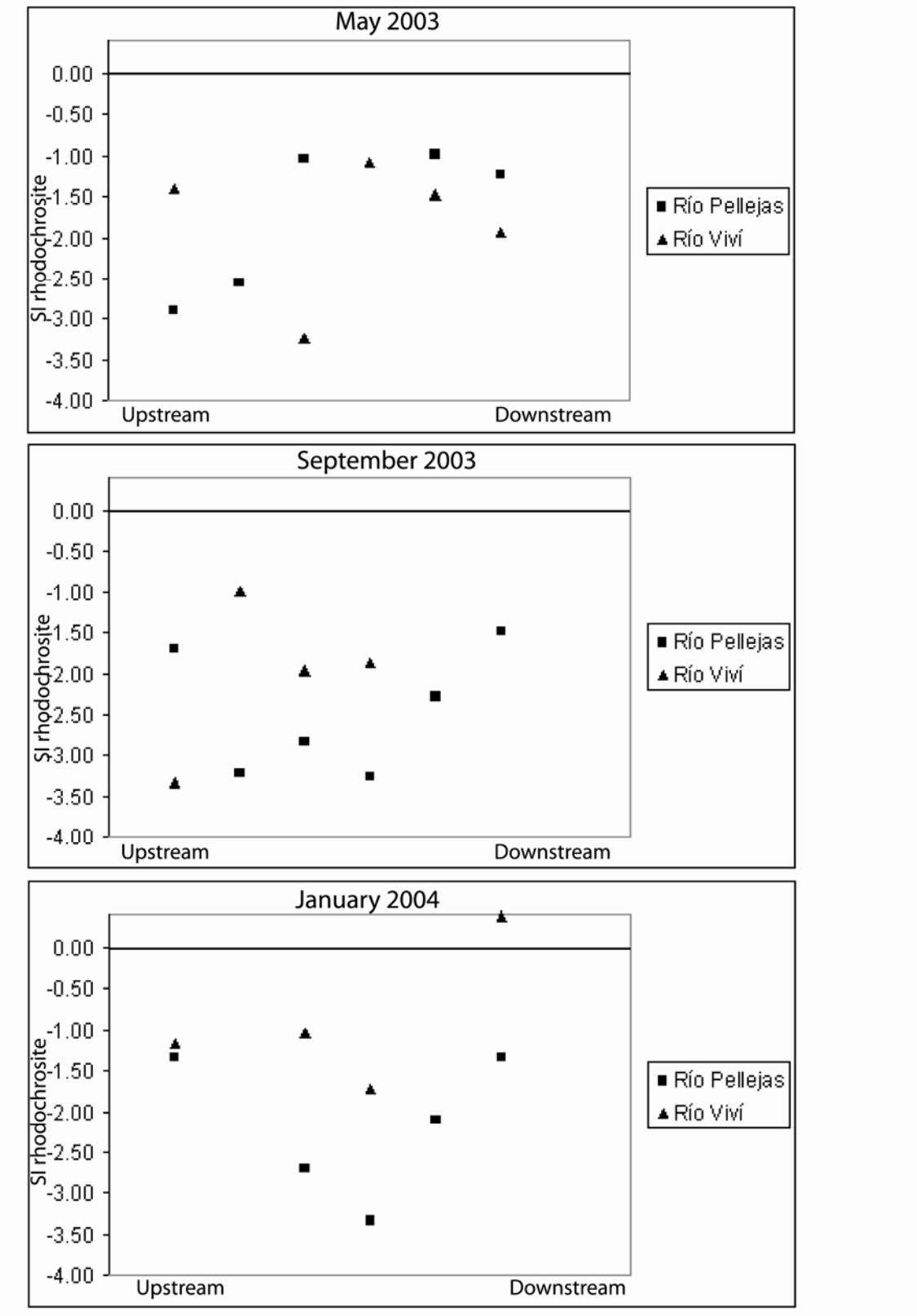

Figure 32 . Saturation indices of rhodochrosite for Río Pellejas and Río Viví during the three sampling periods.

part of the ore mineral assemblage associated with the porphyry copper deposits, and that the concentration of zinc in volcanic-sedimentary rocks, such as basalt, andesite and volcanic tuffs, will be higher than the concentration in plutonic rocks like granite (Martin et al., 1980).

Water samples showed a slight increase in zinc concentration as they passed the deposits. The highest zinc concentration in Río Pellejas was during January with values ranging from below detection limits (<0.005 mg/L) to 0.017 mg/L (PRRP-3; Fig. 12). Río Viví had, in general, higher values than Río Pellejas especially during September 2003; values ranged from 0.0014 mg/L for three sites, including one upstream (PRRV-1), one groundwater (PRRV-5), and the first downstream site in Río Viví (PRRV-4), to 0.04 mg/L (PRRV-3).

All zinc phases such as smithsonite, had negative saturation indices for all sites in both watersheds. Zinc sorbs strongly on ferric hydroxides at pH values above 7 (Martin et al., 1980). Low saturation indices could be an indication that zinc is being sorbed, because of the high pH values in most of the sites.

Stream sediments in Figure 13 demonstrate that higher concentrations of zinc are distributed away from the deposits; the sites closest to the deposits have the lowest concentrations. These results could indicate that these areas are part of the primary geochemical zonation of the hydrothermal system responsible for the porphyry copper deposits. Based on the above information zinc can be considered an indicator element for the copper deposits because its distribution is spatially related to the location of the porphyry copper deposits.

Cadmium

The cadmium concentration in the lithosphere ranges from 0.1 to 0.2 µg/kg, making it the sixty-seventh most abundant element (Nriagu 1980). Cadmium, like zinc and mercury, is mostly found in association with sulfide minerals. It is considered highly toxic to humans and aquatic ecosystems. Its maximum contaminant level in drinking water is 0.005 mg/L (Smith and Huyck, 1999). The most common source of cadmium in mineralized environments is sphalerite, where it occurs in solid solution.

Cadmium concentrations in the stream waters of Río Pellejas and Río Viví were mostly below detection limits for both upstream and downstream samples. The highest cadmium concentration from either river was for sample site PRRV-3 during September 2003. Sorption of cadmium increases at high pH; thus, its solubility decreases as the pH increases. Modeling results indicated that no cadmium phases were found to be near saturation. Stream-sediment samples had values of <2 mg/kg for all sample sites. This information suggests that the endowment of cadmium in this system is sufficiently low to make it an unreliable indicator element for the the porphyry copper deposits.

Cobalt

The concentration of cobalt in the Earth's crust is about 25 mg/kg (Smith and Huyck, 1999). It is considered an essential nutrient for human, but it can become potentially toxic element for humans and aquatic ecosystems. Major sources of cobalt are mafic and ultramafic igneous rocks. In the stream water

samples, the concentration of cobalt was low and mostly below detection limits. The highest concentration occurred in Río Viví in January with values that ranged from below detection limits to 0.006 mg/L for sample site PRRV-3, which was the site with the highest concentration during all three sampling periods. The stream-sediment samples showed that the concentration of cobalt increases as one approaches the porphyry copper deposits, but samples immediately downstream of the deposits decrease in concentration. Only in Río Pellejas do the concentrations increase downstream, whereas in Río Viví the concentrations remain lower. This pattern is similar to other metal concentrations and is possibly reflecting primary hydrothermal zonation around the deposits.

Cobalt is not a significant trace element in the water and stream samples. However, its distribution appears to correlate with the location of the copper deposits and is most reflected in the stream-sediment geochemistry.

Geochemical comparison with unmined and mined porphyry copper deposits elsewhere

Porphyry copper deposits as a group share many common geological and geochemical features. Thus, they represent a common starting point for weathering reactions, which can diverge considerably depending upon factors such as hydrologic setting, climatic setting, whether the deposit is unmined or has been disturbed by mining activities, and the mining and ore beneficiation techniques that have been used, among others. Plumlee et al., (1999) presented information on pH, temperature, and concentrations of various metals in waters associated with porphyry copper deposits mined in different climates in North

America. The first porphyry copper area described was Mount Washington, British Columbia, specifically ponds and lakes in open pits, and ground-water affected by open-pit mining, both in the quartz-sericite-pyrite-alteration zone. They also described groundwater affected by open-pit mining in the propylitic alteration zone of this area. Another porphyry copper deposit described was from the Alamosa River basin in Colorado in which three natural seeps were characterized from the quartz-sericite-pyrite-alteration zone. Finally, there is information for Globe, Arizona for one ground-water site affected by open-pit mining in a quartz-sericite-pyrite-alteration area.

The pH for the ponds and lakes in open pits in British Columbia ranged between 3.5 and 3.6; pH for the ground-water sites ranged from 3.7 to 5.7; that from propylitic alteration areas ranged 6.5 to 6.9 and for the site in Arizona, it was 3.6. The pH in the natural seeps in Colorado ranged from 2.3 to 2.8. Thus, the pH values closest to those of Puerto Rico, which ranged from 5.1 to 8.1, are the values from the areas of propylitic alteration in the Mount Washington area.

Sulfate concentrations of waters associated with the porphyry copper deposits of Puerto Rico ranged from 0.8 to 120 mg/L; the sulfate concentration in Mount Washington for the ponds and lakes ranged from 226 to 696 mg/L and from 50.9 to 608 mg/L in ground-water sites; in the propylitic alteration areas, they ranged from 15.9 to 192 mg/L. Natural seeps in Colorado had concentrations ranging from 407 to 13,400 mg/L. In Arizona, the sulfate concentration was 8,800 mg/L. Figure 33 a shows the sulfate concentrations of all these sites. Sulfate concentration in Puerto Rico is similar to the

concentrations at the propylitic alteration zones in Mount Washington and lower than the rest of the mined areas specially the Arizona and Colorado sites. The data used for Puerto Rico corresponds to the three sampling periods (May 2003, September 2003, and January 2004).

The iron concentration in the ponds and lakes in British Columbia ranged between 5.6 and 9.6 mg/L, from 1.29 to 56.2 mg/L for the ground-water sites, and between 0.017 to 0.03 mg/L in the propylitic alteration zone. In Arizona, the concentration was 2,800 mg/L and in Colorado, the iron concentration ranged from 130 to 1,900 mg/L. Iron concentrations in Puerto Rico ranged between below detection limit to 15.9 mg/L. Figure 33 b illustrates the iron concentrations of all these sites. Iron concentration in Puerto Rico is higher than the concentration in the propylitic areas in Mount Washington.

The aluminum concentration in the ponds and lakes of Mount Washington, British Columbia ranged between 7.2 and 22 mg/L, and between 0.07 and 10.7 mg/L in the ground-water sites; for the propylitic alteration area, the concentration was 0.05 mg/L. In Arizona, the concentration was 250 mg/L. In Colorado, the range was between 66 to 390 mg/L. In Puerto Rico, the aluminum concentration ranged from below detection limits to 0.89 mg/L (Fig. 33 c) and it is mostly higher than the aluminum concentration in the propylitic zone of Mount Washington.

Manganese in the ponds and lakes of Mount Washington, British Columbia ranged between 0.95 to 4.07 mg/L, and from 0.368 to 8.41 mg/L in the ground-water areas. In the propylitic zone, the range was between 0.0008 and 0.189 mg/L. In Arizona, the manganese concentration was 75 mg/L,

a.

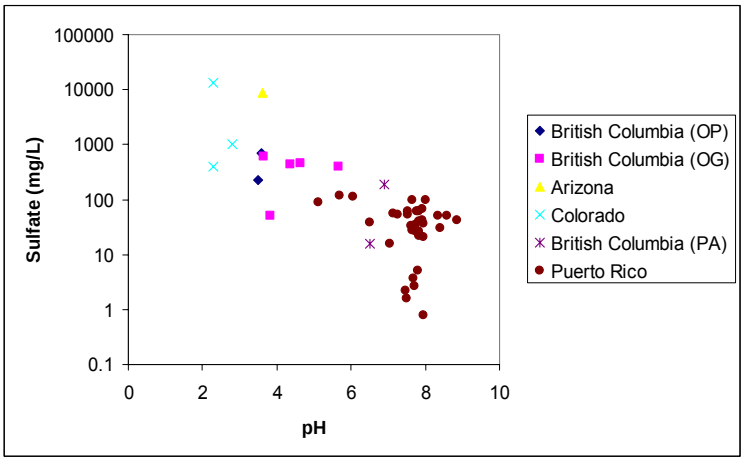

b.

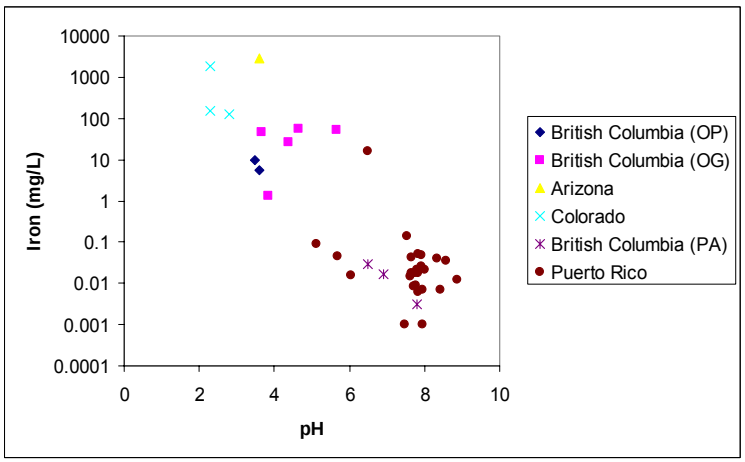

c.

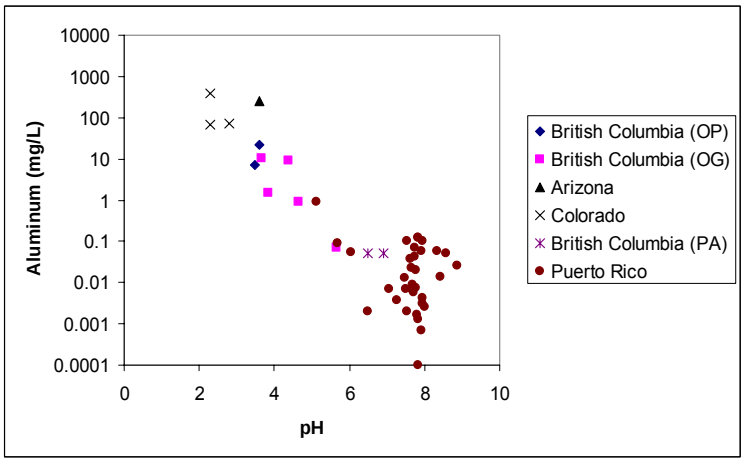

Figure 33. Sulfate, iron, and aluminum concentrations of different porphyry copper deposits, relative to pH. Data from Puerto Rico is from the three sampling periods (Appendix IA-IC).

and in Colorado the range was between 0.130 to 45 mg/L. Manganese concentrations in Río Viví porphyry copper deposits ranged from below detection limit to 5.73 mg/L. Figure 34 a shows these concentrations, it is observed that the manganese concentration in Puerto Rico is mostly higher than the concentration in the propylitic alteration areas of Mount Washington.

Copper concentrations in British Columbia ranged between 15 and 16.8 mg/L for the ponds and lakes, whereas for the groundwater sites the range was between 0.018 to 9.05 mg/L; and from below detection limits to 0.091 mg/L in the propylitic area. In Arizona, the copper concentration was 150 mg/L. The concentration of copper in the natural seeps of the Alamosa River basin area in Colorado ranged between 0.065 and 2.0 mg/L. In the Río Viví area, the range was from below detection limit to 0.20 mg/L. This concentration in Río Viví is similar to some of the groundwater sites in Mount Washington and the natural seeps in Colorado, and higher than the propylitic alteration sites of Mount Washington (Fig. 34 b).

Finally, zinc in the ponds and lakes of the British Columbia area ranged from 0.346 to 0.738 mg/L, the concentration in the ground-water sites ranged from 0.106 to 1.650 mg/L. The concentration in Arizona was 22 mg/L, and in the propylitic zone, in the ponds and lakes of Mount Washington, the range was from below detection limit to 0.022 mg/L; the range in the natural seeps of the Alamosa River basin in Colorado was between 0.420 to 2.7 mg/L. In Puerto Rico, the zinc ranged from below detection limit to 0.04 mg/L. In Figure 34 c, the

a.

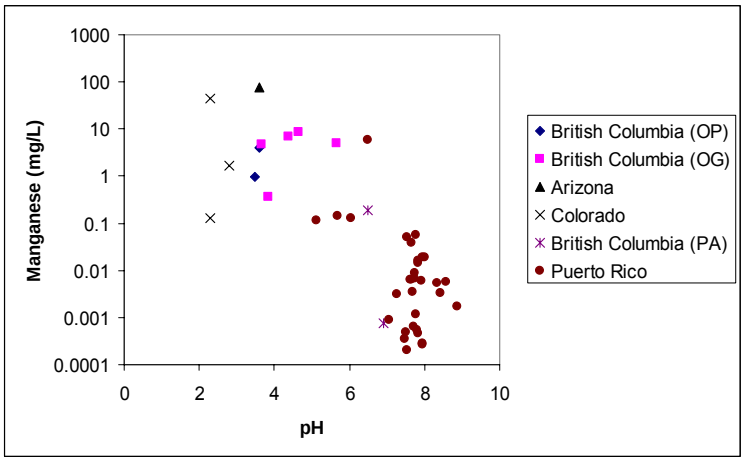

b.

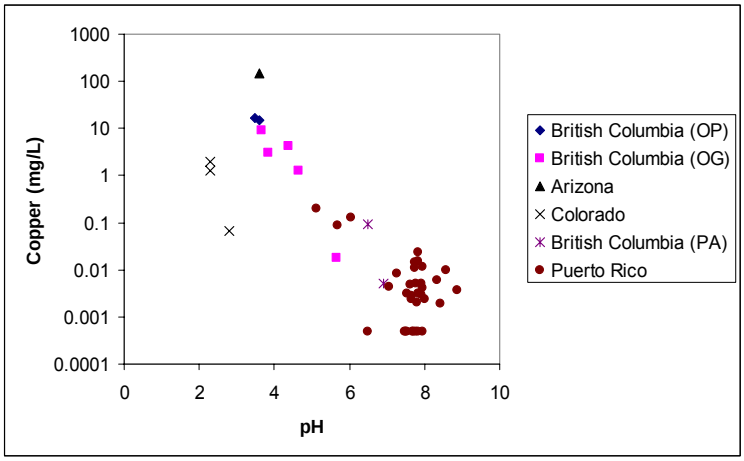

c.

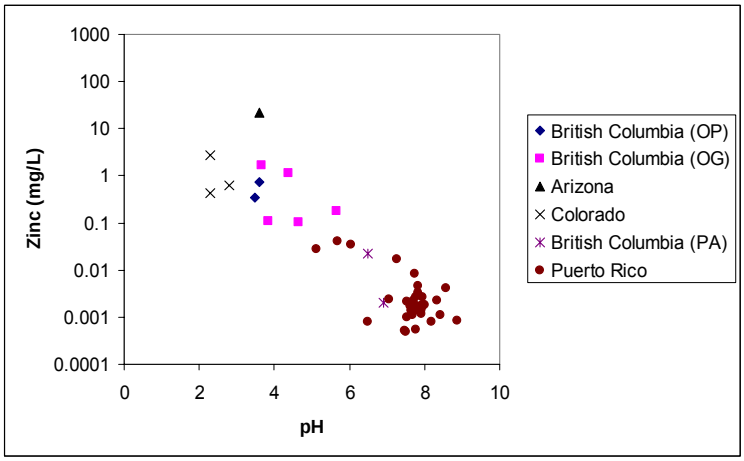

Figure 34. Manganese, copper and zinc concentrations of different porphyry copper deposits, relative to pH. Data from Puerto Rico is from the three sampling periods (Appendix IA-IC).

concentrations mentioned above are presented. The zinc concentration in Puerto Rico is similar but higher than the concentration in the propylitic zone in Mount Washington.

The different concentrations of metals presented above were from mined sites except for those from Puerto Rico. Mining procedures at the different sites included a variety of methods of extraction, crushing, and grinding. All of these ore processing methods will influence the behavior of their wastes, such as exposing the wastes to atmospheric oxygen, and increasing their surface area and thus, their reactivity. Another important factor that will strongly influence the different sites is the climate. For example in Colorado, where the natural seep data from the Alamosa River was obtained, the climate is colder and there is less precipitation than in Puerto Rico. Precipitation in Colorado occurs mostly during winter and when the snow melts; this span of time is less than in Puerto Rico where precipitation is higher and more evenly distributed throughout the year which will probably dilute any acid drainage that could form, even though the warm temperatures would tend to increase oxidation.

For most of the metal concentrations discussed above, the values most similar to those from Puerto Rico are from the propylitic alteration areas in the ground-water sites of Mount Washington, British Columbia. This information is important because it reveals similarities between the geochemistry of mined streams, like the groundwater sites affected by open pit mining in a colder climate and an unmined tropical porphyry copper deposit.

Geochemical exploration

Geochemical exploration together with developments in analytical and interpretive methods, have produced a new body of data and insights about different types of mineral deposits and prospects. Water-chemistry analyses have served in this study as a useful tool to characterize the streams in the areas in terms of how they are affected by the deposits and the geology and thus the effect in the quality of water. The stream sediments have also been very important tools; they give a long-term, time integrated characterization of the area. Elements that are recognized as pathfinder to target porphyry copper deposits in the study area are Cu, Zn, Mn and Fe.

Learned et al. (1972), indicated that the elements Cu, Zn, Mn, Mo and Pb are useful for identifying porphyry copper deposits. In the streams, Zn extends 5.2 km downstream of the deposits, in the stream-sediments, the halo extends for 3.2 km. Copper extends downstream of the deposits around 3.2 km in water and 5.2 km in the sediments. Manganese in the streams extends downstream about 2 km in water and 3.6 km in the sediments. Iron concentration extends downstream about 3.2 km in water, and in the stream sediments, the anomalous concentration extends 3.2 km downstream. Both molybdenum and lead had very low concentrations in most of the sites. Most of the metals in the stream sediments show the greatest dispersion of anomalous values relative to other media. The highest metal concentrations, that extend farther downstream of the deposits are mostly from stream sediments. Highest concentration of metals in the stream sediments are mostly in the farther sites whereas the highest

concentrations of metals in the water are closer to the deposits. The alteration of aqueous contents could be explained as a dilution process.

Remote Sensing

Remote sensing techniques in these heavily vegetated areas are very useful but the normalized difference vegetation index (NDVI) may not be the tool to characterize porphyry copper deposits in an area like Puerto Rico. This is because no definite signature for the porphyry copper deposits was revealed using the NDVI. The heavily vegetated area where the porphyries are located did not show any particular difference compared to the non-mineralized areas close to the deposits. A possible explanation is because the biodiversity of the area. For instance Diaz et al., (unpublished, 2003) showed that not all tree species take up metals at the same rate because the metal content in the leaves varies greatly depending on the species. As a result the NDVI will vary over short distances. Another possibility that could be affecting the NDVI is that at high pH, copper and other metals are sorbed and will not allowed the vegetation to uptake them, thus affecting the reflectance of the canopy.

More research in remote sensing needs to be performed in this area, especially field work to determine what the images are recording, and also soil geochemical analysis to determine the extent of the alteration areas of the porphyry copper deposits. Knowledge of the limits of the alteration areas of the deposits will help when looking for the specific vegetation index. For example, during the selection of the sampling points, instead of choosing points randomly

throughout the deposits, the points could be selected on the basis of the alteration zones, which will probably yield a different result.

Chapter 6

Conclusions

The porphyry copper deposits in Puerto Rico offer a unique opportunity to evaluate the geochemistry of metals in a tropical climate in a mineralized area where no mining has occurred. Knowledge of the original state of an undisturbed mineralized area is very important because it can be used as proxies to better understand the behavior of similar deposits elsewhere; it also provides guidelines for realistic remediation goals in areas of similar climate where historic mining has been conducted but for which no baseline data are available. In Puerto Rico, mineral exploration was conducted during the 1950s, but mining was never started.

Mineralized areas, both prior to and after mining, can contribute various chemical constituents to surface and ground water that reflect the complexity and the geologic and hydrologic setting. Acid-rock drainage associated with hydrothermal sulfide minerals can occur in both mined and unmined areas.

The objective of this research was to characterize the Puerto Rican porphyry copper deposits in order to document their specific geochemical signatures in the stream waters and stream sediments in different sites in the Río Viví and Río Pellejas watersheds, and to understand those factors that determine these signatures. This study included three samplings between 2003 and 2004 in these two watersheds and an assessment using a remote sensing technique known as normalized difference vegetation index (NDVI). Water was analyzed using inductively-coupled plasma mass spectrometry (ICP-MS), inductively-

coupled plasma atomic emission spectroscopy (ICP-AES) and ion chromatography. Solids (sediments and rocks) were analyzed using X-ray diffraction (XRD), optical microscopy, scanning electron microscopy (SEM), electron microprobe analysis, and bulk ICP-AES. Remote sensing images were analyzed using the program ENVI 3.6 (Environment for Visualizing Images) using the (NDVI) for images of the area taken in 2001.

Geochemical analysis shows that concentration of certain metals in water such as Fe, Al, Mn, Cu, had higher concentrations in Río Viví, particularly at sites that are downstream of the porphyry copper deposits. In Río Viví, the river cuts the porphyry copper deposits, whereas in Río Pellejas, the deposits are upslope from the river. Anions such as sulfate were also higher in Río Viví than in Río Pellejas. Metals in the stream sediments such as copper and manganese increased downstream from the deposits. Therefore, the deposits clearly exert an important influence on the water chemistry in these watersheds.

Aluminum, Fe and Mn exceeded the drinking water-quality guidelines established by U.S. EPA. Aluminum concentration surpassed the water-quality parameters for both rivers, whereas only Fe and Mn exceeded guidelines in Río Viví. For all three of these elements, the guidelines are secondary criteria, meaning that they pertain to the aesthetic properties of the water (i.e., color, taste), and not human-health concerns. Geochemical modeling of the surface - and ground-water compositions suggests that the combination of near neutral to slightly alkaline pH value and the prevalence of secondary ferric hydroxides in the soils and streams throughout the study plays a dominant role in the

environmental signature of the deposits in all media including surface water, stream sediments, and soils. The main process by which this influence occurs is through the sorption of metals on secondary ferric hydroxides, which is strongly dependent upon pH (Smith, 1999). Above pH 7, most metals (i.e. Cu, Pb, Zn, Cd) should be bound to the surface of ferric hydroxides, whether they occur in the soils or stream beds. Thus, geochemical anomalies in these elements should be restricted to the immediate vicinity of the deposits. Therefore, any zonation in elements such as copper and zinc probably reflect primary hydrothermal zonation of the mineral deposit rather than differential dispersion associated with weathering. Because of the strong removal of these base metals through sorption, an elevated dissolved concentration of these elements in surface water is not expected and was not observed. In contrast, sulfate is not significantly sorbed at high pH, thus explaining why it is the most distinct indicator in surface waters of the presence of the deposits.

An important feature that was observed in the Río Viví watershed is that two sites had unusual concentrations. These sites, PRRV-3 and PRRV-4sp, are tributaries of Río Viví (Fig. 3) and they had the lowest pH values, and the highest concentrations of SO_4, Fe, Mn, Cu, and Zn. These two sites are located in two different tributaries close to the downstream extent of the study area; however, neither of these tributaries flows over known deposits. This may suggest that there is other source that is influencing these concentrations, possibly additional, as yet undiscovered deposits.

Compared to other porphyry copper deposits in the United States, surface water in Río Viví had metal concentrations similar to those from several sites in a mined deposit at Mount Washington, British Columbia. This comparison suggest that even without mining activity, the porphyry copper deposits in Puerto Rico can produce metal concentrations in surface waters comparable to those from mined areas. However, the waters from Mount Washington are far from the extremes that can be achieved around mined porphyry copper deposits (Plumlee et al., 1999)

The remote sensing NDVI showed a series of mixed values for the mineralized and non-mineralized areas. In other words, no definite signature was identified for the mineralized areas that correspond to the porphyry copper deposits. Although there were areas within the deposits with low NDVI values that could be classified as alteration zones where little or no vegetation grows, the signature cannot be extended through the mineralized area because of an inadequate understanding of the true extent of altered facies in the study area. Other factors that are possibly affecting the reflectance of the area are the biodiversity and sorption of metals like copper and zinc.

Recommendations

More research needs to be done at the north side of the Río Viví watershed where the two sites with anomalous metal concentrations were found to help understand why these elevated concentrations are occurring there. The elevated concentrations may reflect the presence of undiscovered porphyry

copper deposits, or alternatively, the lower pH conditions and the lower sorptive capacity of ferric hydroxides at these pH values.

The IKONOS satellite images used were useful in terms of physically visualizing the porphyry copper mineralized area due to its high resolution. The NDVI did reveal differences among the terranes, but it was not useful in revealing specific diagnostic differences between the mineralized and un-mineralized areas that can be unambiguously related to the presence of hydrothermal mineralization or alteration. It is suggested that if the NDVI tool is going to be used again in this area, first, a field survey that includes research on the particular botany and soils associated with the deposits needs to be done. This will help in the selection of regions of interest that result in the NDVI.

In general, background geochemical surveys in areas such as those around the unmined porphyry copper deposits in Puerto Rico are essential and necessary to determine accurately how natural and anthropogenic geochemical variations affect the surrounding environment, the ecosystem and especially human health.

References

Abrams, M.J., Brown D., Lepley, L., and Sadowski, R., 1983, Remote sensing for porphyry copper deposits in southern Arizona: Economic Geology, v. 78, p. 591-604.

Alpers, C.N., and Nordstrom, D.K., 2000, Estimation of premining conditions for trace metal mobility in mineralized areas: an overview: Proceedings from the Fifth International Conference on Acid Rock Drainage, v. II, p 473-484.

Alpers, C.N., and Nordstrom, D.K., 1999, Geochemical modeling of water rock interactions in mining environments: Reviews in Economic Geology, v. 6a, p. 289-323.

Arent, L.J., and Lewis, T.E., 1987, The stability of aluminum species in a natural audit sample: Possible application as a quality control solution: Environmental chemistry and toxicology of aluminum, Proceedings of the 194th Annual meeting of the American Chemical Society, p. 41-57.

Barabas, A., 1982, Potassium-Argon Dating of Magmatic Events and Hydrothermal Activity Associated with Porphyry Copper Mineralization in West Central Puerto Rico: Economic Geology, v.77, p.109-126.

Blum, A.E., and Stillings, L.L., 1995, Feldspars dissolution kinetics: Reviews in mineralogy, v. 31, p. 291-351.

Bradley, R.A., 1971, The geology of the Río Viví porphyry copper deposits, Puerto Rico: Geol. Soc. Am. (abstr.), v. 3, p. 511

Brantley, S.L., and Chen, Y., 1995, Chemical weathering rates of pyroxenes and amphiboles: Reviews in Mineralogy, v. 31, p. 119-172.

Briggs, P.H., and Meier, A.L., 2002, The determination of forty-two elements in geological materials by inductively coupled plasma-mass spectrometry, *in* Taggart, J.E., Jr. (ed.): Analytical methods for chemical analysis of geologic and other materials: U.S. Geological Survey Open-File Report 02-0223, Chapter I. http://pubs.usgs.gov/of/2002/ofr-02-0223/I20NAWQAPlus_M.pdf.

Briggs, R.P., 1968, Geologic Map of the Arecibo Quadrangle: U.S. Geological Survey, Miscellaneous Geologic Investigations Map I-551.

Cammarota, A.V. Jr, 1980, Production and uses of Zinc: Zinc in the environment, Part 1. Ecological cycling, Nriagu, J.O (ed.): John Wiley & Sons, Inc.

Campbell J.B., 2002, Introduction to Remote Sensing, Third Edition: Guilford Press, p. 189-190.

Carranza, E.J.M., 2002, Geologically – Constrained Mineral Potential Mapping, Examples from the Philippines: ITC Publication no. 86, p. 9-44.

Cox, D.P., 1985, Geology of the Tanamá and Helecho porphyry copper deposits and vicinity, Puerto Rico: U.S. Geological Survey Professional Paper 1327.

Cox, D.P., Larsen, R.R., and Tripp, R.B., 1973, Hydrothermal alteration in Puerto Rican porphyry copper deposits: Economic Geology, v. 68, no. 8, p. 1329-1334.

Cox, D.P. and Learned, R.E., 1977, Geochemical expression of porphyry copper deposits in Puerto Rico: Mining Engineer (abstr.), v. 29, no.1 , p. 80.

Cox, D.P., González, I.P., and Nash., J.T., 1975, Geology, geochemistry and fluid inclusion petrography of the Sapo Alegre porphyry copper prospect and its metavolcanic wallrocks, west-central Puerto Rico: USGS Journal Research, v. 5, p. 689-703.

Crock, J.G. Arbogast B. F. and Lamothe P.J., 1999 Laboratory methods for the analysis of environmental samples: Reviews in Economic Geology, v.6A, p. 265-287.

Diaz, E., Rodríguez,N., and Massol, A., 2003, Parcela de monitoría de biodiversidad del Bosque del Pueblo: unpublished.

Diaz, P.L., Aquino, Z., Figueroa-Alamo, C., Vachier, R.J., Sánchez, A. V., 2000, Water Resources Data Puerto Rico and the U.S. Virgin Islands Water Year 2000: USGS Water-Data Report PR-00-1.

Drever, J.I., 1997, The Geochemistry of Natural Waters, Surface and Groundwater Environments: Third Edition; Prentice Hall, p. 436.

Edelstein, D.L., 2002, Copper: U.S. Geological Survey Minerals Yearbook.

Edelstein, D.L., 2004, Copper Statistics and Information: http://minerals.er.usgs.gov/minerals/pubs/commodity/copper/.

Filipek, L.H., Nordstrom, D.K., and Ficklin, W.H., 1987, Interaction of acid mine drainage with waters and sediments of West Squaw Creek in the West Shasta Mining District, California: Environ. Sci. Technol, v. 21, no.4, p. 388-396.

Ficklin, W.H., and Mosier, E.L., 1999, Laboratory methods for the analysis of environmental samples: Reviews in Economic Geology, v. 6a, p. 249-264.

Florida LAKEWATCH Department of Fisheries and Aquatic Sciences University of Florida Gainesville, 1999, A Beginner's Guide to Water Management- The ABCs: http://lakewatch.ifas.ufl.edu/LWcirc.html.

Ginés Sánchez, C., Ramos Pérez, C.R., and McDowell, W.R., 1986, Chemistry of a tropical rainforest stream: Changes along an altitudinal gradient: Third Caribbean Islands Water Resources Congress. Proceedings of a Symposium held in St. Thomas, U.S. Virgin Islands July 22-25 1986, p. 29-32.

Gorham, E., 1961, Factors influencing supply of major ions to inland waters, with special reference to the atmosphere: Geological Society of America Bulletin, v 72, p. 795-840.

Hammarstrom, J. M, Piatak, N.M., Seal R.R., II, Briggs, P.H., Meier, A. L., and Muzik, T.L., 2003, Geochemical characteristics of TP3 mine wastes at the Elizabeth copper mine Superfund Site, Orange Co., Vermont: U.S. Geological Survey Open File Report 03-431, p. 40.

Hammarstrom, J. M, Seal R.R., II, Ouimette, A.P., 2000, Sources of metals and Acidity at the Elizabeth and Ely mines: Geochemistry and mineralogy of solid mine waste and the role of secondary minerals in metal recycling: Society of Economic Geologist guidebook series, v. 35, p. 213-248.

Hem, J.D., 1963, Chemical equilibria and rates of manganese oxidation: US Geological Survey Water-Supply Paper 1667-A.

Hey, M.H., 1954, A new review of the chlorites: Mineralogical Magazine, v. 30 p. 277-292.

Kesler, S. E., 1994, Mineral Resources, Economics and the Environment: Macmillan College Publishing Co., p. 207-214.

Kretz, R., 1983, Symbols for rock forming minerals: American Mineralogist, v. 68, p 277-279.

Krushensky, R.D., and Curet, A.F., 1984, Geological map of the Monte Guilarte Quadrangle, Puerto Rico: Miscellaneous Geologic Investigations Map I-1556.

Labovitz, M. L. Masuoka, E. J., Bell, R., Siegrist, A.W., and Nelson R.F., 1983, The application of remote sensing to geobotanical exploration for metal sulfides-results from the 1980 field season at Mineral, Virginia: Economic Geology v. 78, p. 750-760.

Lamothe, P.J., Meier, A.L., and Wilson, S., 2002, The determination of forty-four elements in aqueous samples in inductively coupled plasma-mass spectrometry, *in* Taggart, J.E., Jr. ed., Analytical methods for chemical analysis of geologic and other materials: U.S. Geological Survey Open-File Report 02-0223, Chapter H. http://pubs.usgs.gov/of/2002/ofr-02-0223/H21&23OFR99-151_M.pdf.

Learned, R.E., 1972, Gold, a useful pathfinder element in the search for porphyry copper deposits in Puerto Rico: Proceedings of the Fourth International Geochemical Exploration Symposium, London, 17 to 20 April 1972.

Lide, D.R., 2004, CRC Handbook Chemistry and Physics, 85th Edition: CRC Press I Llc.

Lutjen, G.P., 1971, The curious case of the Puerto Rican copper mines: Engineering and Mining Journal, v. 172, p. 74-84.

MacDonald, D.D., Ingersoll, C.G., and Berger, T.A., 2000, Development and evaluation of consensus-based sediment quality guidelines for freshwater ecosystems: Arch. Environ. Contam. Toxicol. 39, p. 20-31.

Martin J.H., Knauer G.A. and Flegal A.R., 1980, Distribution of zinc in natural waters: Zinc in the environment Part 1 Ecological cycling, Nriagu, J.O ed., John Wiley & Sons, Inc.

Mattson, P.H., 1968 a., Geologic Map of the Adjuntas Quadrangle: U.S. Geological Survey, Miscellaneous Geologic Investigations Map I-519.

Mattson, P.H., 1968 b., Geologic Map of the Jayuya Quadrangle: U.S. Geological Survey, Miscellaneous Geologic Investigations Map I-520.

McDowell, W.H., 1990, Influence of sea salt aerosols and long range transport on precipitation chemistry at El Verde, Puerto Rico: Atmospheric Environment, v. 24a, p. 2813-2821.

McDowell, W.H, and Asbury, C.E., 1994, Export of carbon, nitrogen, and major ions from three tropical montane watersheds: Limnology and Oceanography. v. 39, p. 111-125.

Nelson, A.E., 1967, Geologic Map of the Utuado Quadrangle, Puerto Rico: U.S. Geological Survey, Miscellaneous Geologic Investigations Map I-480.

Nriagu, J.O., 1989, A global assessment of natural sources of atmospheric trace metals: Nature, v. 338, p 47-49.

Nriagu, J.O. 1980, Cadmiun in the environment, Part 1: Ecological Cycling: John Wiley & Sons, Inc, p. 682.

Oliva, P., Viers, J., and Dupré, B., 2003, Chemical weathering in granitic environments: Chemical Geology, 202, p 225-256.

Parkhurst, D.L., and Appelo, C.A.J. 1999, Users guide to PHREEQC (Version 2) A computer program for speciation, batch-reaction, one dimensional transport, and inverse geochemical calculations: USGS WRIR 99-4259 http://wwwbrr.cr.usgs.gov/projects/GWC_coupled/phreeqc/html/final.html

Plumlee, G.S., 1999, The environmental geology of mineral deposits: Reviews in Economic Geology, v. 6a, p. 71-116

Plumlee, G.S., Smith, K.S., Montour, M.R., Ficklin, W.H., and Mosier, E.L., 1999, Geologic controls on the composition of natural waters and mine waters draining Diverse Mineral Deposit Types: Reviews in Economic Geology, v. 6b, p. 373-407.

Research Systems Inc., 2004, ENVI, From Images to Information: http://www.RSInc.com/envi.

Runnels, D.D., Dupon, D.P., Jones, R.L., and Cline, D.J., 1998, Determination of natural background concentrations of dissolved components in water at mining, milling and smelting sites: Mining Engineering, 50 (2), p. 65-71.

Seal R.R., II,., Hammarstrom, J.M., Southworth, S.C., Meier, A.L., Haffner, D.P., Schultz, A.P., Plumlee, G.S., Flohr, M.J.K., Jackson, J.C., Smith, S.M., and Hageman, P.L., 1998, Preliminary report on water quality associated with the abandoned Fontana and Hazel Creek mines, Great Smoky mountains National Park, North Carolina and Tennessee: Open-File Report 98-476.

Seal R.R., II,. Kornfeld, J.M, Meier A. L., and Hammarstrom, J. M., 2001, Geochemical settings of mine drainage in the Vermont copper belt: Society of Economic Geologist, Guidebook Series, v. 34, p.255-276.

Shuman, L.M., 1980, Zinc in soils: Zinc in the environment Part 1 Ecological cycling, Nriagu, J.O, ed., John Wiley & Sons, Inc.

Sillitoe, R.H., 1993, Gold rich porphyry copper deposits: geological model and exploration implications: Geological Association of Canada Special Paper 40, p 465-478.

Smith, K. S., and Huyck, H.L.O., 1999, An overview of the abundance, relative mobility, bioavailability, and human toxicity of metals: Reviews in Economic Geology, v. 6A, p. 29 -70.

Space Imaging, 2001, IKONOS Relative Spectral Response and Radiometric Calibration Coefficients: http://www.spaceimaging.com/products/ikonos/spectral.htm

Sposito, G., 1989, The environmental chemistry of Aluminum: CRC Press Inc. 317 p.

Thomas Jefferson National Accelerator Facility - Office of Science Education, 2004: http://education.jlab.org/itselemental/ele029.html

Tiltley, S.R., and Beane, R.E., 1981, Porphyry copper deposits: Economic Geology 75th Anniversary Volume, p. 214-269.

Tipping, E., Backes, C.A., and Hurley, M.A., 1987, Modeling the interactions of Al species, protons and Ca^{2+} with humic substances in acid waters and soils: Environmental chemistry and toxicology of aluminum, Proceedings of the 194th Annual meeting of the American Chemical Society, p. 59-82.

White, A.F., and Blum, A.E., 1995, Effects of climate on chemical weathering in watersheds: Geochimica et Cosmochimica Acta, v. 59, p. 1729-1747.

White, A.F., Bullen, T.D., Vivit, D.V., Schulz, M.S., and Clow, D.W., 1999, The role of disseminated calcite in the chemical weathering of granitoid rocks: Geochimica et Cosmochimica Acta, v. 63. p. 1939-1953.

Appendix IA
Geochemistry of filtered water samples
May-03

Sample	pH	S.C. µS/cm	T water C	Dissolved Oxygen mg/L	Flow L/s	Hardness of water mg/L	Cl mg/L	F mg/L	SO_4 mg/L	Alkalinity $CaCO_3$ mg/L
PRRP-1-1	8.57	298	24	9	/	124.35	9.1	<0.1	51	68.22
PRRP-2-1	7.82	120.5	21.8	8	/	33.94	6.3	<0.1	22	0
PRRP-3-1	7.54	272	22.3	3	/	98.48	6.3	0.1	62	48.13
PRRP-4-1	7.95	144.2	19.5	7	0.5	57.49	2.3	<0.1	0.8	40.28
PRRP-5-1	7.72	218	20.4	7	24.78	86.13	4.5	<0.1	2.7	75.08
PRRP-6-1	8.34	298	23	7	539.6	126.97	8.4	<0.1	50	63.37
PRRV-1-1	8.41	236	20.6	8	193.5	92.52	8	<0.1	31	64.41
PRRV-2-1	8.86	246	22.3	10	/	95.82	8.1	<0.1	42	64.08
PRRV-3-1	6.04	296	22.8	8	56.46	102.86	7.7	0.1	110	64.41
PRRV-4-1	8.01	377	23.1	7	/	147.44	12	0.1	96	39.42
PRRV-5-1	7.83	412	22.8	8	0.016	179.21	8.9	0.1	60	122.99
FB051403	7.14	1.3	/	/	/	0.66	23	1.2	57	14.84

Appendix IA
(cont.)
May-03

Sample	ICPMS Ag mg/L	ICPMS Al mg/L	ICPMS Au mg/L	ICPMS As mg/L	ICPMS Ba mg/L	ICPMS Be mg/L	ICPMS Bi mg/L	ICPMS Ca mg/L	ICPMS Cd mg/L	ICPMS Ce mg/L	ICPMS Co mg/L
PRRP-1-1	<0.00001	0.052	<0.00001	<0.002	0.014	<.00005	<0.00002	37	<.00002	0.00002	<0.00002
PRRP-2-1	0.000035	0.0013	<0.00001	<0.002	0.0074	<.00005	<0.00002	7.8	<.00002	<0.00001	<0.00002
PRRP-3-1	<0.00001	0.1	<0.00001	<0.002	0.015	<.00005	<0.00002	30	<.00002	0.00015	0.000081
PRRP-4-1	0.000019	0.0042	<0.00001	<0.002	0.018	<.00005	<0.00002	16	<.00002	<0.00001	<.00002
PRRP-5-1	<0.00001	0.0057	<0.00001	<0.002	0.008	<.00005	<0.00002	24	<.00002	<0.00001	<.00002
PRRP-6-1	<0.00001	0.058	<0.00001	<0.002	0.015	<.00005	<0.00002	36	<.00002	0.000021	<.00002
PRRV-1-1	<0.00001	0.014	<0.00001	<0.002	0.015	<.00005	<0.00002	25	<.00002	<0.00001	<.00002
PRRV-2-1	<0.00001	0.026	<0.00001	<0.002	0.014	<.00005	<0.00002	26	<.00002	<0.00001	<.00002
PRRV-3-1	<0.00001	0.056	<0.00001	<0.002	0.047	0.00012	<0.00002	31	0.00024	0.0013	0.0058
PRRV-4-1	<0.00001	0.0025	<0.00001	<0.002	0.028	<.00005	<0.00002	42	<.00002	<0.00001	<.00002
PRRV-5-1	<0.00001	<0.0001	<0.00001	<0.002	0.023	<.00005	<0.00002	51	<.00002	<0.00001	<.00002
FB051403	0.000089	<0.0001	<0.00001	<0.002	<.00002	<.00005	<0.00002	<0.05	<.00002	<0.00001	<.00002

Appendix IA (cont.)
May-03

Sample	ICPMS Cr	ICPMS Cs	ICPMS Cu	ICPMS Dy	ICPMS Er	ICPMS Eu	ICPMS Fe	ICPMS Mn	ICPMS Mo	ICPMS Ni	ICPMS Pb
	mg/L	mg/L	mg/L	mg/L	mg/L	mg/L	mg/L	mg/L	mg/L	mg/L	mg/L
PRRP-1-1	<0.001	<0.00001	0.01	0.00001	<0.000005	<0.000005	0.036	0.0058	0.00044	<0.0001	<.00005
PRRP-2-1	<0.001	<0.00001	0.0032	<0.000005	<0.000005	<0.000005	0.006	0.00047	0.00052	<0.0001	<.00005
PRRP-3-1	<0.001	<0.00001	0.0032	0.000024	0.000012	6.7E-06	0.14	0.05	0.00031	<0.0001	0.000058
PRRP-4-1	0.001	<0.00001	<0.0005	6.6E-06	<0.000005	<0.000005	0.0069	0.00029	0.00023	<0.0001	<.00005
PRRP-5-1	<0.001	<0.00001	<0.0005	<0.000005	<0.000005	<0.000005	0.0084	0.00063	0.00024	<0.0001	<.00005
PRRP-6-1	<0.001	<0.00001	0.0059	8.2E-06	<0.000005	<0.000005	0.039	0.0053	0.00038	<0.0001	<.00005
PRRV-1-1	0.001	<0.00001	0.0019	<0.000005	<0.000005	<0.000005	0.0072	0.0033	0.00032	<0.0001	<.00005
PRRV-2-1	<0.001	<0.00001	0.0037	<0.000005	<0.000005	<0.000005	0.012	0.0017	0.00061	<0.0001	<.00005
PRRV-3-1	<0.001	<0.00001	0.13	0.00025	0.00016	0.000068	0.016	0.13	0.0018	0.0021	0.00023
PRRV-4-1	<0.001	<0.00001	0.0024	<0.000005	5.8E-06	<0.000005	0.022	0.019	0.002	<0.0001	<.00005
PRRV-5-1	0.0013	0.00037	<.0005	0.000005	<0.000005	<0.000005	0.018	0.000078	0.0019	<0.0001	<.00005
FB051403	<0.001	<0.00001	<.0005	<0.000005	<0.000005	<0.000005	0.0014	0.000015	0.00046	<0.0001	<.00005

Appendix IA (cont.)

May-03

Sample	ICPMS Rb	ICPMS Se	ICPMS Sr	ICPMS Tl	ICPMS U	ICPMS W	ICPMS Zn	ICPAES Ca	ICPAES K	ICPAES Mg	ICPAES Na
	mg/L	mg/L	mg/L	mg/L	mg/L	mg/L	mg/L	mg/L	mg/L	mg/L	mg/L
PRRP-1-1	0.0012	<.0002	0.16	<0.00005	0.00002	<.00003	0.004	35.8	1.6	8.5	12
PRRP-2-1	0.0016	0.00024	0.059	0.000088	<.000005	0.0001	0.0014	8	1.1	3.4	7.3
PRRP-3-1	0.0012	<.0002	0.14	<0.00005	0.000021	0.00003	0.0021	26.6	2.9	7.8	9.3
PRRP-4-1	0.00099	<.0002	0.09	<0.00005	8.3E-06	0.00007	0.0016	16.6	1.3	3.9	7.6
PRRP-5-1	0.00075	<.0002	0.13	<0.00005	0.000011	0.00006	0.0023	23.3	0.89	6.8	9.1
PRRP-6-1	0.0014	<.0002	0.16	<0.00005	0.00002	<0.00003	0.0023	35.7	1.8	9.2	12.2
PRRV-1-1	0.00095	0.00027	0.12	<0.00005	0.000017	0.00004	0.0011	25.2	1.5	7.2	10.8
PRRV-2-1	0.0012	<.0002	0.13	<0.00005	0.000015	0.00006	0.00083	25.7	1.7	7.7	10.7
PRRV-3-1	0.0027	0.00025	0.21	<0.00005	0.000035	0.00003	0.034	29.5	2	7.1	11.8
PRRV-4-1	0.0014	0.00051	0.23	<0.00005	0.000014	<0.00003	0.0018	41.1	2.6	10.9	15.8
PRRV-5-1	0.00057	0.00031	0.42	<0.00005	0.000014	<0.00003	0.0016	50.2	0.58	13.1	16
FB051403	<.00001	<.0002	<.00002	0.000058	<.000005	0.000095	0.0021	<0.1	<0.1	<0.1	<0.1

Appendix IA (cont.)

May-03

Sample	ICPAES Si mg/L	Log Activity Al^{+3}	Log Activity Ba^{+2}	Log Activity CO_3^{-2}	Log Activity Ca^{+2}	Log Activity Fe^{+2}	Log Activity Fe^{+3}	Log Activity SO_4^{-2}	SI Andularia	SI Al $(OH)_3$	SI Albite
PRRP-1-1	17	-17.257	-7.175	-4.711	-3.206	-10.373	-19.417	-3.452	-0.23	-2.41	-1.71
PRRP-2-1	14.2	-15.617	-7.373	/	-3.783	-8.663	-17.76	-3.732	-1.98	-3.17	-3.54
PRRP-3-1	17.6	-12.679	-7.148	-5.873	-3.323	-6.596	-15.68	-3.35	0.55	-1.04	-1.32
PRRP-4-1	14.7	-15.382	-6.967	-5.555	-3.467	-8.784	-17.938	-5.191	-1.18	-2.7	-2.82
PRRP-5-1	16.4	-14.433	-7.342	-5.508	-3.342	-8.131	-17.262	-4.693	-1.15	-2.38	-2.53
PRRP-6-1	16.1	-16.184	-7.142	-4.966	-3.201	-9.518	-18.586	-3.461	-0.1	-2.1	-1.63
PRRV-1-1	13.4	-16.823	-7.112	-4.903	-3.333	-10.257	-19.383	-3.642	-0.84	-2.68	-2.38
PRRV-2-1	12.8	-18.535	-7.16	-4.482	-3.343	-11.653	-20.737	-3.514	-0.8	-2.93	-2.37
PRRV-3-1	18	-8.035	-6.708	-7.235	-3.311	-6.75	-15.823	-3.113	-0.92	-0.86	-2.52
PRRV-4-1	16.8	-16.245	-6.919	-5.491	-3.163	-8.768	17.833	-3.194	-1.24	-3.14	-2.82
PRRV-5-1	11.9	/	-6.982	-5.177	-3.076	-8.304	-17.377	-3.416	/	/	/
FB051403	<0.1										

Appendix IA (cont.)

May-03

Sample	SI Annite	SI Anorthite	SI Barite	SI Boehmite	SI Calcite	SI Chalcedony	SI Chlorite 14	SI Chlorite 7A	SI Dolomite	SI $Fe(OH)_3$	SI Gibbsite
PRRP-1-1	1.02	-2.1	-0.64	-0.2	0.56	-0.01	5.08	1.7	0.83	1.4	0.29
PRRP-2-1	-0.36	-5.91	-1.08	-0.97	/	-0.04	-6.28	-9.68	/	0.81	-0.45
PRRP-3-1	6.75	-1.54	-0.48	1.17	-0.73	0.05	-2.92	-6.32	-1.68	2.05	1.68
PRRP-4-1	0.56	-4.49	-2.1	-0.5	-0.57	0	-4.27	-7.69	-1.49	1.02	0.04
PRRP-5-1	1.29	-4.04	-1.99	-0.18	-0.39	0.04	-4.46	-7.87	-1.03	1.01	0.35
PRRP-6-1	2.22	-2	-0.6	0.11	0.3	-0.01	3.32	-0.07	0.34	1.54	0.61
PRRV-1-1	-0.62	-3.45	-0.71	-0.49	0.22	-0.06	1.58	-1.83	0.19	0.96	0.05
PRRV-2-1	-1.85	-3.07	-0.66	-0.73	0.64	-0.13	5.93	2.53	1.08	0.95	-0.22
PRRV-3-1	2.71	-4.12	0.18	1.35	/	0.05	-17.79	-21.18	-5.02	-2.59	1.85
PRRV-4-1	1.36	-4.65	-0.11	-0.93	-0.19	0.01	-1.73	-5.12	-0.63	1.31	-0.43
PRRV-5-1	/	/	-0.39	/	0.21	-0.13	/	/	0.17	1.22	/
FB051403											

Appendix IA (cont.)

May-03

Sample	SI Goethite	SI Illite	SI Kaolinite	SI Quartz	SI SiO_2	PHREEQC % Error
PRRP-1-1	7.26	0.85	2.24	0.42	-0.85	7.01
PRRP-2-1	6.58	-1.99	0.71	0.49	-0.85	23.84
PRRP-3-1	7.84	3.23	5.14	0.49	-0.8	0.62
PRRP-4-1	6.71	-0.56	1.78	0.45	-0.86	26.36
PRRP-5-1	6.73	0.01	2.48	0.48	-0.82	12.14
PRRP-6-1	7.36	1.36	2.89	0.42	-0.86	10.89
PRRV-1-1	6.69	-0.16	1.66	0.38	-0.92	4.67
PRRV-2-1	6.75	-0.44	0.99	0.31	-0.98	1
PRRV-3-1	3.22	1.89	5.5	0.49	-0.79	-19.44
PRRV-4-1	7.13	-1.21	0.85	0.45	-0.83	9.13
PRRV-5-1	7.03	/	/	0.31	-0.98	4.29
FB051403						

Appendix IB
Geochemistry of filtered water samples

Sample	pH	S.C. µS/cm	T water C	Dissolved Oxygen mg/L	Flow Flow	Sep-03 Hardness of water mg/L	Cl mg/l	F mg/L	SO_4 mg/L	Alkalinity $CaCO_3$ mg/L
PRRP-1-2	7.74	233	24.9	7	413.9	90.81	7.5	<0.1	35	39.36
PRRP-2-2	7.95	109.8	24.8	7	0.1	33.62	6.2	<0.1	21	15.4
PRRP-3-2	7.79	255	24.1	7	0.16	98.8	6	0.1	61	31.93
PRRP-4-2	7.48	119.4	21.3	9	2.95	47.37	4.9	<0.1	2.2	34.58
PRRP-5-2	7.76	216	21.7	7	35.1	81.24	7.3	<0.1	5	59.94
PRRP-6-2	7.93	272	25	8	306.4	104.98	8.2	<0.1	42	52.72
PRRV-1-2	7.64	197.1	23.7	7	262.2	72.94	7	<0.1	28	33.41
PRRV-2-2	7.61	198.2	22.9	7	166.82	76.58	7.1	<0.1	34	27.99
PRRV-3-2	5.68	303	23	7	46.25	98.38	7.8	0.1	120	-2.37
PRRV-4-2	7.66	390	24.1	7	5.25	151.42	11	0.1	99	47.89
PRRV-5-2	7.93	432	25.3	6	0.02	192.56	10	0.2	66	103.65
FB091703	8.19	10.8	25.3	/	/	0.66	<0.1	<0.1	<0.2	0.29
PRRP-6-2l	7.93	272	25	8	306.4	103.14	8.3	<0.1	42	46.6

Appendix IB (cont.)

Sep-03

Sample	ICPMS Ag mg/L	ICPMS Al mg/L	ICPMS Au mg/L	ICPMS As mg/L	ICPMS Ba mg/L	ICPMS Be mg/L	ICPMS Bi mg/L	ICPMS Ca mg/L	ICPMS Cd mg/L	ICPMS Ce mg/L	ICPMS Co mg/L
PRRP-1-2	<0.00001	0.07	<0.00001	<0.0002	0.012	<0.00005	<0.00001	19	<.00002	0.000043	0.000033
PRRP-2-2	<0.00001	0.0031	<0.00001	<0.0002	0.0073	<0.00005	<0.00001	6.1	<.00002	<0.00001	<.00002
PRRP-3-2	<0.00001	0.0017	<0.00001	0.00044	0.0065	<0.00005	<0.00001	21	<.00002	<0.00001	<.00002
PRRP-4-2	<0.00001	0.013	<0.00001	<0.0002	0.014	<0.00005	<0.00001	9.7	<.00002	0.000019	<.00002
PRRP-5-2	<0.00001	0.0076	<0.00001	<0.0002	0.0064	<0.00005	<0.00001	17	<.00002	<0.00001	<.00002
PRRP-6-2	<0.00001	0.06	<0.00001	<0.0002	0.012	<0.00005	<0.00001	23	<.00002	0.000029	0.000034
PRRV-1-2	<0.00001	0.023	<0.00001	<0.0002	0.015	<0.00005	<0.00001	16	<.00002	0.000033	0.000024
PRRV-2-2	<0.00001	0.037	<0.00001	<0.0002	0.014	<0.00005	<0.00001	16	0.000022	0.000034	0.000038
PRRV-3-2	<0.00001	0.089	<0.00001	<0.0002	0.041	0.00012	<0.00001	27	0.00029	0.0012	0.0067
PRRV-4-2	<0.00001	0.007	<0.00001	<0.0002	0.027	<0.00005	<0.00001	38	0.000022	<0.00001	<.00002
PRRV-5-2	<0.00001	0.0007	<0.00001	0.0034	0.018	<0.00005	<0.00001	47	0.000026	<0.00001	<.00002
FB091703	0.000057	0.0012	<0.0001	<0.0002	<0.00002	<0.00005	<0.0001	<0.05	<.00002	<0.0001	<.00002
PRRP-6-2DupFA	<0.00001	0.058	<0.0001	<0.0002	0.012	<0.00005	<0.0001	23	0.000024	<0.0001	0.000034

Appendix IB (cont.)

Sep-03

Sample	ICPMS Cr mg/L	ICPMS Cs mg/L	ICPMS Cu mg/L	ICPMS Dy mg/L	ICPMS Er mg/L	ICPMS Eu mg/L	ICPMS Fe mg/L	ICPMS Mn mg/L	ICPMS Mo mg/L	ICPMS Ni mg/L	ICPMS Pb mg/L
PRRP-1-2	<0.001	<0.00001	0.011	0.000012	6.2E-06	<0.000005	0.018	0.0068	0.00014	<.0001	<.00005
PRRP-2-2	<0.001	<0.00001	0.004	<0.000005	<0.000005	<0.000005	<.001	0.00027	0.00019	<.0001	<.00005
PRRP-3-2	<0.001	0.000014	0.002	<0.000005	<0.000005	<0.000005	0.021	0.00055	0.012	<.0001	<.00005
PRRP-4-2	<0.001	<0.00001	<.0005	0.000013	0.000056	<0.000005	<.001	0.00036	0.000075	<.0001	<.00005
PRRP-5-2	<0.001	<0.00001	<.0005	<0.000005	<0.000005	<0.000005	0.0088	0.0012	0.00015	<.0001	<.00005
PRRP-6-2	<0.001	<0.00001	0.0052	6.6E-06	<0.000005	<0.000005	0.026	0.0059	0.00019	<.0001	<.00005
PRRV-1-2	<0.001	<0.00001	0.0024	0.000012	6.6E-06	<0.000005	0.018	0.0065	0.00019	0.00017	<.00005
PRRV-2-2	<0.001	<0.00001	0.0048	0.00001	9.5E-06	<0.000005	0.015	0.0065	0.00036	0.00015	0.000065
PRRV-3-2	<0.001	<0.00001	0.088	0.0002	0.00011	0.000049	0.046	0.14	0.00045	0.0024	<.00005
PRRV-4-2	<0.001	<0.00001	0.0028	6.3E-06	5.8E-06	<0.000005	0.042	0.038	0.002	<.0001	<.00005
PRRV-5-2	<0.001	0.000032	0.003	<0.000005	<0.000005	<0.000005	0.048	0.000057	0.0018	<.0001	<.00005
FB091703	<0.001	<0.0001	<.0005	<0.00005	<0.00005	<0.00005	<.001	<.00001	0.000081	<.0001	<.00005
PRRP-6-2[	<0.001	<0.0001	0.0049	7.1E-06	5.2E-06	<0.00005	0.024	0.006	0.0002	0.00013	<.00005

Appendix IB (cont.)

Sep-03

Sample	ICPMS Rb mg/L	ICPMS Se mg/L	ICPMS Sr mg/L	ICPMS Tl mg/L	ICPMS U mg/L	ICPMS W mg/L	ICPMS Zn mg/L	ICPAES Ca mg/L	ICPAES K mg/L	ICPAES Mg mg/L	ICPAES Na mg/L
PRRP-1-2	0.0009	<.0002	0.09	<0.00005	0.000012	<.00002	0.0014	25.5	2	6.6	9.4
PRRP-2-2	0.0018	<.0002	0.046	<0.00005	<.000005	0.000055	0.0018	8.2	1.5	3.2	6.6
PRRP-3-2	0.0026	<.0002	0.054	<0.00005	6.3E-06	0.000024	0.0017	26.4	2.6	8	9.3
PRRP-4-2	0.00086	<.0002	0.058	<0.00005	5.4E-06	0.000033	0.00052	13.7	1.4	3.2	6.4
PRRP-5-2	0.00069	<.0002	0.092	<0.00005	0.000008	<.00002	0.00055	22	1.1	6.4	8.4
PRRP-6-2	0.00096	<.0002	0.096	<0.00005	0.000015	<.00002	0.0016	29.2	2.1	7.8	10.4
PRRV-1-2	0.00094	<.0002	0.088	<0.00005	6.4E-06	0.000023	0.0014	19.5	1.8	5.9	7.9
PRRV-2-2	0.001	<.0002	0.088	<0.00005	7.1E-06	<.00002	0.0017	20.3	1.9	6.3	8
PRRV-3-2	0.0022	<.0002	0.16	<0.00005	0.000023	<.00002	0.04	28.2	1.9	6.8	11.1
PRRV-4-2	0.0013	<.0002	0.2	<0.00005	0.000015	<.00002	0.0014	42.2	3.1	11.2	15.1
PRRV-5-2	0.00043	<.0002	0.36	<0.00005	0.000011	0.00002	0.0014	53.9	0.6	14.1	16.2
FB091703	<.00001	<.0002	<.00002	<0.00005	<.000005	0.000042	0.00078	<0.1	<0.1	<0.1	<0.1
PRRP-6-2[	0.00097	<.0002	0.096	<0.00005	0.000014	<.00002	0.0012	28.3	2	7.9	10.2

Appendix IB (cont.)

Sep-03

Sample	ICP-AES Si mg/L	Log Activity Al^{+3}	Log Activity Ba^{+2}	Log Activity CO_3^{-2}	Log Activity Ca^{+2}	Log Activity Fe^{+2}	Log Activity Fe^{+3}	Log Activity SO_4^{-2}	SI Andularia	SI $Al(OH)^3$	SI Albite
PRRP-1-2	14.6	-13.901	-7.209	-5.736	-3.321	-8.216	-17.238	-3.589	-0.21	-1.49	-1.88
PRRP-2-2	13.5	-16.075	-7.381	-5.924	-3.777	/	/	-3.755	-1.77	-3.04	-3.47
PRRP-3-2	18.3	-15.634	-7.508	-5.782	-3.324	-8.227	-17.268	-3.356	-1.36	-3.12	-3.16
PRRP-4-2	12.9	-14.211	-7.073	-6.067	-3.546	/	/	-4.743	-1.96	-2.81	-3.69
PRRP-5-2	15.6	-14.06	-7.438	-5.553	-3.364	-8.323	-17.422	-4.422	-1.09	-2.34	-2.59
PRRP-6-2	15.4	-14.739	-7.223	-5.422	-3.275	-8.617	-17.637	-3.523	-0.2	-1.75	-1.85
PRRV-1-2	13	-13.858	-7.096	-5.909	-3.425	-7.842	-16.893	-3.67	-0.79	-1.82	-2.5
PRRV-2-2	12.2	-13.449	-7.134	-6.026	-3.412	-7.78	-16.85	-3.588	-0.58	-1.56	-2.32
PRRV-3-2	15.2	-7.345	-6.77	/	-3.325	-6.253	-15.321	-3.068	-1.91	-1.24	-3.51
PRRV-4-2	15.7	-14.506	-6.939	-5.741	-3.155	-7.565	-16.606	-3.184	-0.88	-2.39	2.54
PRRV-5-2	11.3	-16.711	-7.094	-5.133	-3.049	-8.377	-17.39	-3.383	-3.12	-3.7	-4.02
FB091703	<0.1										
PRRP-6-2D	15.8										

Appendix IB (cont.)

Sep-03

Sample	SI Annite	SI Anorthite	SI Barite	SI Boehmite	SI Calcite	SI Chalcedony	SI Chlorite 14	SI Chlorite 7A	SI Dolomite	SI $Fe(OH)^3$	SI Gibbsite
PRRP-1-2	2.65	-2.07	-0.83	0.73	-0.58	-0.07	-1.69	-5.07	-1.4	1.09	1.2
PRRP-2-2	/	-5.27	-1.16	-0.82	-1.22	-0.1	-4.22	-7.59	2.51	/	-0.35
PRRP-3-2	1.67	-5.09	-0.88	-0.91	-0.63	0.04	-4.04	-7.42	-1.45	1.21	-0.42
PRRP-4-2	/	-5.76	-1.79	-0.61	-1.15	-0.07	-9.32	-12.73	-2.64	-2.81	-0.09
PRRP-5-2	1.17	-3.89	-1.84	-0.14	-0.46	0	-3.85	-7.25	-1.14	0.97	0.38
PRRP-6-2	2.6	-2.12	-0.78	0.47	-0.22	-0.05	0.07	-3.3	-0.66	1.26	0.94
PRRV-1-2	2.44	-3.21	-0.77	0.39	-0.86	-0.1	-3.99	-7.37	-1.91	1.14	0.88
PRRV-2-2	2.56	-2.81	-0.72	0.65	-0.97	-0.12	-3.91	-7.3	-2.13	1.09	1.15
PRRV-3-2	-5.76	-5.75	0.16	0.97		-0.02	-22.31	-25.78	/	-3.17	1.47
PRRV-4-2	3.36	-3.84	-0.14	-0.17	-0.42	-0.02	-3.51	-6.89	-1.09	1.48	0.31
PRRV-5-2	0.44	-6.05	-0.51	-1.48	0.3	-0.18	-3.08	-6.45	0.37	1.51	-1.01
FB091703											
PRRP-6-2DupFA											

Appendix IB (cont.)

Sep-03

Sample	SI Goethite	SI Illite	SI Kaolinite	SI Quartz	SI SiO_2	PHREEQC % Error
PRRP-1-2	6.98	1.9	3.96	0.36	-0.91	14.58
PRRP-2-2	/	-1.7	0.79	0.33	-0.94	4.21
PRRP-3-2	7.07	-1.35	0.92	0.47	-0.8	8.59
PRRP-4-2	/	-1.61	1.36	0.37	-0.93	18.22
PRRP-5-2	6.74	0.05	2.45	0.44	-0.85	14.71
PRRP-6-2	7.15	1.6	3.47	0.38	-0.88	10.02
PRRV-1-2	6.98	0.86	3.24	0.33	-0.94	12.69
PRRV-2-2	6.9	1.4	3.75	0.32	-0.97	14.3
PRRV-3-2	2.65	0.34	4.59	0.41	-0.87	-4.27
PRRV-4-2	7.34	0.05	2.26	0.41	-0.87	6.65
PRRV-5-2	7.41	-3.65	-0.71	0.25	-1.02	10.77
FB091703						
PRRP-6-2DupFA						

Appendix IC
Geochemistry of filtered water samples

Jan-04

Sample	pH	S.C. µS/cm	T water C	Dissolved Oxygen mg/L	Flow L/s	Hardness of water mg/L	Cl mg/l	F mg/L	SO_4 mg/L	Alkalinity $CaCO_3$ mg/L
PRRP-1-3	7.82	221	20	10	479	27.39	8.6	<0.1	26	39.87
PRRP-2-3	7.06	101.6	20.9	7	/	51.6	6.3	<0.1	16	5.86
PRRP-3-3	7.27	239	22.8	8	/	91.02	6	0.1	54	23.57
PRRP-4-3	7.5	139	18.4	10	1.33	74.33	5.1	<0.1	1.6	37.21
PRRP-5-3	7.67	208	19.6	8	35.1	76.03	7.5	<0.1	3.7	39.33
PRRP-6-3	7.83	260	19.7	8	483	76.44	8.6	<0.1	40	36.51
PRRV-1-3	7.74	207	20.9	7	233.64	76.54	7.7	<0.1	26	28.81
PRRV-2-3	7.95	222	21.4	8	451	83.06	7.9	<0.1	37	33.5
PRRV-3-3	5.12	244	21.2	8	136.22	71.14	7.7	0.1	90	-0.71
PRRV-4-3	7.76	200	22	8	87.27	89.52	9.9	0.1	60	22.31
PRRV-4-3[illegible]	6.5	475	22.2	2	/	174.25	11	0.1	38	121.99
PRRV-5-3	7.54	411	22.4	7	0.02	226.7	8.8	0.1	54	82.19

Appendix IC (Cont.)

Jan-04

Sample	ICPMS Ag mg/L	ICPMS Al mg/L	ICPMS As mg/L	ICPMS Ba mg/L	ICPMS Be mg/L	ICPMS Bi mg/L	ICPMS Ca mg/L	ICPMS Ce mg/L	ICPMS Cd mg/L	ICPMS Co mg/L	ICPMS Cr mg/L
PRRP-1-3	<0.003	0.126	<.001	0.0135	<0.00005	<0.0002	23.2	0.00011	<.00002	0.00017	<0.001
PRRP-2-3	<0.003	0.007	<.001	0.00858	<0.00005	<0.0002	6.44	<0.00001	<.00002	<.00002	<0.001
PRRP-3-3	<0.003	0.0038	<.001	0.00551	<0.00005	<0.0002	24	<0.00001	0.00005	<.00002	<0.001
PRRP-4-3	<0.003	0.007	<.001	0.0192	<0.00005	<0.0002	15.7	<0.00001	<.00002	<.00002	<0.001
PRRP-5-3	<0.003	0.009	<.001	0.00831	<0.00005	<0.0002	23.1	<0.00001	<.00002	<.00002	0.0012
PRRP-6-3	<0.003	0.123	<.001	0.0144	<0.00005	<0.0002	26.4	0.00005	0.00005	0.00036	<0.001
PRRV-1-3	<0.003	0.0419	<.001	0.0164	<0.00005	<0.0002	20.7	0.00005	<.00002	0.00017	<0.001
PRRV-2-3	<0.003	0.103	<.001	0.0118	<0.00005	<0.0002	21.1	0.00006	0.00003	0.00022	<0.001
PRRV-3-3	<0.003	0.895	<.001	0.0423	0.0001	<0.0002	21.2	0.00174	0.00015	0.00646	<0.001
PRRV-4-3	<0.003	0.0202	<.001	0.027	<0.00005	<0.0002	27.9	0.00001	0.00003	0.0001	<0.001
PRRV-4-3S	<0.003	<.002	<.001	0.188	<0.00005	<0.0002	62.9	0.00001	<.00002	0.00209	<0.001
PRRV-5-3	<0.003	<.002	0.0038	0.0223	<0.00005	<0.0002	52.2	<0.00001	<.00002	<.00002	<0.001

Appendix IC (Cont.)

Jan-04

Sample	ICPMS Cs mg/L	ICPMS Cu mg/L	ICPMS Dy mg/L	ICPMS Er mg/L	ICPMS Eu mg/L	ICPMS Fe mg/L	ICPMS Ga mg/L	ICPMS Gd mg/L	ICPMS Ge mg/L	ICPMS Ho mg/L	ICPMS K mg/L
PRRP-1-3	<0.00002	0.024	0.00004	0.00002	0.00001	<.05	<0.00005	0.00004	<0.00005	0.000006	2.01
PRRP-2-3	<0.00002	0.0043	<0.00005	<0.000005	<0.000005	<.05	<0.00005	<0.000005	<0.00005	<0.000005	1.55
PRRP-3-3	0.00002	0.0083	<0.00005	<0.000005	<0.000005	<.05	<0.00005	<0.000005	<0.00005	<0.000005	2.49
PRRP-4-3	<0.00002	<.0005	0.000008	0.000006	<0.000005	<.05	<0.00005	0.00001	<0.00005	<0.000005	1.25
PRRP-5-3	<0.00002	<.0005	<0.00005	<0.000005	<0.000005	<.05	<0.00005	<0.000005	<0.00005	<0.000005	1.14
PRRP-6-3	<0.00002	0.015	0.00002	0.00001	0.000005	0.052	<0.00005	0.00002	<0.00005	<0.000005	1.56
PRRV-1-3	<0.00002	0.0143	0.00002	0.00001	0.000009	<.05	<0.00005	0.00002	<0.00005	<0.000005	1.49
PRRV-2-3	<0.00002	0.0118	0.00002	0.00001	0.000005	<.05	<0.00005	0.00002	<0.00005	<0.000005	1.81
PRRV-3-3	<0.00002	0.204	0.00037	0.00023	0.0001	0.088	<0.00005	0.00037	<0.00005	0.000074	2.03
PRRV-4-3	<0.00002	0.0052	0.000005	0.000007	<0.000005	<.05	<0.00005	0.000007	<0.00005	<0.000005	2.93
PRRV-4-3S	<0.00002	<.0005	0.000006	0.00001	0.00002	15.9	0.00007	<0.000005	0.00006	<0.000005	6.55
PRRV-5-3	0.00004	<.0005	0.000007	<0.000005	<0.000005	<.05	<0.00005	<0.000005	0.0002	<0.000005	0.53

Appendix IC (Cont.)

Jan-04

Sample	ICPMS La mg/L	ICPMS Li mg/L	ICPMS Mg mg/L	ICPMS Mn mg/L	ICPMS Mo mg/L	ICPMS Na mg/L	ICPMS Nd mg/L	ICPMS Ni mg/L	ICPMS P mg/L	ICPMS Pb mg/L	ICPMS Pr mg/L
PRRP-1-3	0.00009	0.0006	6.22	0.0143	<.002	9.06	0.00014	<.0004	0.09	<.000005	0.00004
PRRP-2-3	<0.00001	0.0006	3.02	0.0009	<.002	6.2	<0.00001	<.0004	< 0.01	<.000005	<0.00001
PRRP-3-3	<0.00001	0.0006	7.03	0.0031	0.0172	8.49	<0.00001	0.0004	0.03	<.000005	<0.00001
PRRP-4-3	0.00002	0.0004	3.64	0.0005	<.002	7.18	0.00004	<.0004	0.05	<.000005	<0.00001
PRRP-5-3	<0.00001	0.0006	6.19	0.0034	<.002	8.42	0.00001	<.0004	0.05	<.000005	<0.00001
PRRP-6-3	0.00004	0.0002	7.49	0.0158	<.002	9.89	0.00007	<.0004	0.05	<.000005	0.00001
PRRV-1-3	0.00006	0.0006	6.34	0.009	<.002	8.92	0.00008	0.0004	0.05	<.000005	0.00002
PRRV-2-3	0.00004	0.0007	7.06	0.0187	<.002	9.03	0.00007	0.0005	0.03	<.000005	0.00001
PRRV-3-3	0.00098	0.0016	5.55	0.113	<.002	10.4	0.00133	0.0026	< 0.01	0.0001	0.0003
PRRV-4-3	0.00002	0.0011	7.33	0.0553	<.002	12.5	0.00003	<.0004	0.02	<.000005	<0.00001
PRRV-4-3[illegible]	<0.00001	0.0008	18.2	5.73	0.0021	16.5	0.00001	<.0004	< 0.01	<.000005	<0.00001
PRRV-5-3	<0.00001	0.0036	12.5	<.0002	0.0025	14.7	<0.00001	<.0004	< 0.01	<.000005	<0.00001

Appendix IC (Cont.)

Jan-04

Sample	ICPMS Rb mg/L	ICPMS Sc mg/L	ICPMS Sb mg/L	ICPMS Se mg/L	ICPMS Si mg/L	ICPMS Sm mg/L	ICPMS SO4 mg/L	ICPMS Sr mg/L	ICPMS Tb mg/L	ICPMS Th mg/L	ICPMS Tl mg/L
PRRP-1-3	0.00134	0.0044	0.00048	<.001	15.7	0.00003	29	0.125	0.000005	<0.0002	<0.0001
PRRP-2-3	0.00279	0.0039	<0.0003	<.001	14.2	<0.00001	17	0.0536	<0.000005	<0.0002	<0.0001
PRRP-3-3	0.00366	0.0054	<0.0003	0.002	17.4	<0.00001	53	0.0697	<0.000005	<0.0002	<0.0001
PRRP-4-3	0.00096	0.0042	<0.0003	<.001	15.7	<0.00001	< 2	0.0961	<0.000005	<0.0002	<0.0001
PRRP-5-3	0.00093	0.0047	<0.0003	<.001	17.6	0.00001	5	0.129	<0.000005	<0.0002	<0.0001
PRRP-6-3	0.00118	0.0051	<0.0003	<.001	16.4	0.00002	38	0.132	<0.000005	<0.0002	<0.0001
PRRV-1-3	0.00116	0.0044	<0.0003	<.001	16.3	0.00002	28	0.112	<0.000005	<0.0002	<0.0001
PRRV-2-3	0.00159	0.0043	<0.0003	<.001	15.9	0.00002	40	0.113	<0.000005	<0.0002	<0.0001
PRRV-3-3	0.00272	0.0056	<0.0003	<.001	18.9	0.00027	87	0.161	0.000058	<0.0002	<0.0001
PRRV-4-3	0.00189	0.0053	<0.0003	<.001	19.3	<0.00001	65	0.164	<0.000005	<0.0002	<0.0001
PRRV-4-3[illegible]	0.00184	0.0062	<0.0003	<.001	16.8	<0.00001	38	0.288	<0.000005	0.00024	<0.0001
PRRV-5-3	0.00055	0.0041	<0.0003	<.001	12.3	<0.00001	55	0.424	<0.000005	<0.0002	<0.0001

Appendix IC (Cont.)

Jan-04

Sample	ICPMS Tm mg/L	ICPMS U mg/L	ICPMS W mg/L	ICPMS Y mg/L	ICPMS Yb mg/L	ICPMS Zn mg/L	ICPMS Zr mg/L	ICPAES Ca mg/L	ICPAES K mg/L	ICPAES Mg mg/L	ICPAES Na mg/L
PRRP-1-3	<0.000005	<.0001	<.0005	0.00018	0.00001	0.0033	<0.0002	20.9	1.8	5.9	9.1
PRRP-2-3	<0.000005	<.0001	<.0005	0.00002	<0.000005	0.0024	<0.0002	6.2	1.4	2.9	6.1
PRRP-3-3	<0.000005	<.0001	<.0005	<0.00001	<0.000005	0.0171	<0.0002	22.4	2.4	6.6	8.3
PRRP-4-3	<0.000005	<.0001	<.0005	0.00008	<0.000005	<0.0005	<0.0002	14.9	1.1	3.5	7.2
PRRP-5-3	<0.000005	<.0001	<.0005	0.00004	<0.000005	0.0011	<0.0002	20.9	0.96	5.8	8.3
PRRP-6-3	<0.000005	<.0001	<.0005	0.00012	0.000007	0.0046	<0.0002	24	1.5	7.2	9.9
PRRV-1-3	<0.000005	<.0001	<.0005	0.00014	0.00001	0.0082	<0.0002	19.4	1.4	6.3	9.2
PRRV-2-3	<0.000005	<.0001	<.0005	0.00014	0.000009	0.0026	<0.0002	19.3	1.6	6.9	9.3
PRRV-3-3	0.00003	<.0001	<.0005	0.0024	0.00018	0.028	<0.0002	19.6	1.8	5.4	10.6
PRRV-4-3	<0.000005	<.0001	<.0005	0.00008	0.000006	0.0026	<0.0002	24.6	2.6	7.2	12.8
PRRV-4-3[illegible]	<0.000005	<.0001	<.0005	0.00009	0.000009	0.0008	<0.0002	62.8	5.8	17	14.4
PRRV-5-3	<0.000005	<.0001	<.0005	0.00008	<0.000005	0.001	<0.0002	49.2	0.47	12.5	15.4

Appendix IC (Cont.)

Jan-04

Sample	ICPAES Si mg/L	Log Activity Al^{+3}	Log Activity Ba^{+2}	Log Activity CO_3^{-2}	Log Activity Ca^{+2}	Log Activity Fe^{+2}	Log Activity Fe^{+3}	Log Activity SO_4^{-2}	SI Andularia	SI $Al(OH)_3$	SI Albite
PRRP-1-3	13.8	-13.444	-7.141	-5.698	-3.396	/	/	-3.703	0.31	-1.12	-1.39
PRRP-2-3	13	-11.78	-7.295	-7.262	-3.886	/	/	-3.861	-1.21	-1.67	-2.96
PRRP-3-3	16.4	-13.079	-7.567	-6.438	-3.384	/	/	-3.395	-1.09	-2.21	-2.92
PRRP-4-3	14.5	-13.247	-6.937	-6.045	-3.511	/	/	-4.885	-0.96	-1.99	-2.56
PRRP-5-3	15.4	-13.926	-7.316	-5.846	-3.377	/	/	-4.544	-0.91	-2.09	-2.39
PRRP-6-3	15.6	-13.464	-7.135	-5.733	-3.349	-7.583	-16.731	-3.528	0.4	-1.13	-1.19
PRRV-1-3	14.9	-13.699	-5.904	-5.904	-3.425	/	/	-3.701	-0.25	-1.55	-1.82
PRRV-2-3	14.2	-14.201	-7.214	-5.633	-3.438	/	/	-3.552	0.09	-1.39	-1.52
PRRV-3-3	17.1	-5.154	-5.722		-3.453	-5.938	-15.465	-3.169	-2.38	-1.98	-4.21
PRRV-4-3	16.7	-14.217	-6.887	-5.988	-3.351	/	/	-3.358	-0.24	-1.93	-1.92
PRRV-4-3S	15.3	/	-6.058	-6.524	-2.978	-3.784	-12.871	-3.651	/	/	/
PRRV-5-3	11.7	/	-6.983	-5.641	-3.072	/	/	-3.456	/	/	/

Appendix IC (Cont.)

Jan-04

Sample	SI Annite	SI Anorthite	SI Barite	SI Boehmite	SI Calcite	SI Chalcedony	SI Chlorite 14	SI Chlorite 7A	SI Dolomite	SI $Fe(OH)_3$	SI Gibbsite
PRRP-1-3	/	-1.54	-0.79	1.08	-0.64	-0.03	-1.61	5.03	-1.55	/	1.62
PRRP-2-3	/	-4.66	-1.12	0.53	-2.69	-0.07	-11.52	-14.93	-5.41	/	1.06
PRRP-3-3	/	-4.53	-0.96	-0.01	-1.35	0.01	-8.24	-11.63	-2.92	/	0.5
PRRP-4-3	/	-4.07	-1.74	0.2	-1.11	0.01	-7.86	-11.29	-2.59	/	0.76
PRRP-5-3	/	-3.7	-1.8	0.1	-0.77	0.02	-5	-8.42	-1.83	/	0.65
PRRP-6-3	5.05	-1.4	-0.6	1.07	-0.63	0.02	-1.08	-4.5	-1.5	1.87	1.61
PRRV-1-3	/	-2.48	-0.72	0.65	-0.87	-0.01	-2.79	-6.21	-1.94	/	1.18
PRRV-2-3	/	-1.77	-0.74	0.81	-0.61	-0.04	-0.17	-3.58	-1.37	/	1.33
PRRV-3-3	-11.11	-9.36	1.46	0.15	/	0.25	-34.28	-37.85	/	-5	0.9
PRRV-4-3	/	-2.98	-0.23	0.27	-0.88	0.03	-2.81	-6.21	-1.98	/	0.78
PRRV-4-3S	/	/	0.31	/	-1.04	-0.01	/	/	-2.33	1.74	/
PRRV-5-3	/	/	0.43	/	-0.25	-0.13	/		-0.77	/	/

Appendix IC(Cont.)

Jan-04

Sample	SI Goethite	SI Illite	SI Kaolinite	SI Quartz	SI SiO_2	PHREEQC % Error
PRRP-1-3	/	2.94	4.87	0.41	-0.89	11.82
PRRP-2-3	/	0.58	3.67	0.38	-0.92	15.33
PRRP-3-3	/	0.05	2.71	0.45	-0.83	8.64
PRRP-4-3	/	0.57	3.25	0.46	-0.85	19.88
PRRP-5-3	/	0.58	3.05	0.47	-0.83	28.22
PRRP-6-3	7.57	3.1	4.97	0.47	-0.83	10
PRRV-1-3	/	1.88	4.03	0.43	-0.86	18.87
PRRV-2-3	/	2.42	4.28	0.4	-0.89	9.38
PRRV-3-3	0.14	-1	4.04	0.75	-0.66	-1.09
PRRV-4-3	/	1.3	3.31	0.47	-0.82	11.22
PRRV-4-3[illegible]	7.53 /	/		0.43	-0.86	27.87
PRRV-5-3	/ /	/		0.31	-0.98	16.9

Appendix ID
Geochemistry of sediment samples

Sample	ICP- AES Al %	ICP- AES Ca %	ICP- AES Fe %	ICP- AES K %	ICP- AES Mg %	ICP- AES Na %	ICP- AES P %	ICP- AES Ti %	ICP- AES Ag mg/kg
PRRP-1-1-ss	8.145	0.924	7.89	0.88	0.996	0.751	0.052	0.485	<2
PRRP-4-1-ss	6.71	0.404	6.3	0.64	0.56	0.162	0.03	0.536	<2
PRRP-5-1-ss	10.11	0.956	7.84	0.46	1.171	0.499	0.047	0.586	<2
PRRP-6-1-ss	8.223	1.122	8.05	1.03	1.122	0.804	0.061	0.466	<2
PRRP-7-1-ss	9.064	1.877	9.46	0.89	1.604	0.914	0.07	0.598	<2
PRRP-7-1dup ss	8.52	1.887	10.64	0.84	1.506	0.932	0.06	0.681	<2
PRRV-1-1-ss	7.734	1.792	9.83	0.77	1.085	0.967	0.055	0.547	<2
PRRV-2-1-ss	8.462	1.732	7.28	1.09	1.123	1.327	0.054	0.362	<2
PRRV-4-1-ss	8.221	0.796	7.29	1.26	1.063	0.824	0.045	0.396	<2

Appendix ID (cont.)
Geochemistry of sediment samples

Sample	ICP- AES As mg/kg	ICP- AES Au mg/kg	ICP- AES Ba mg/kg	ICP- AES Be mg/kg	ICP- AES Bi mg/kg	ICP- AES Cd mg/kg	ICP- AES Ce mg/kg	ICP- AES Co mg/kg	ICP- AES Cr mg/kg	ICP- AES Cu mg/kg	ICP- AES Eu mg/kg
PRRP-1-1-SS	<10	<8	257	1	<50	<2	24	20	45	364	2
PRRP-4-1-SS	<10	<8	277	1	<50	<2	26	18	17	64	<2
PRRP-5-1-SS	<10	<8	216	1	<50	<2	24	26	45	79	2
PRRP-6-1-SS	<10	<8	309	1	<50	<2	24	23	50	331	2
PRRP-7-1-SS	<10	<8	302	1	<50	<2	26	26	75	190	3
PRRP-7-1dup	<10	<8	272	1	<50	<2	24	26	82	155	3
PRRV-1-1-SS	<10	<8	337	1	<50	<2	27	24	29	235	3
PRRV-2-1-SS	<10	<8	418	1	<50	<2	21	20	26	410	2
PRRV-4-1-SS	<10	<8	406	<1	<50	<2	17	23	26	804	2

Appendix ID (cont.)
Geochemistry of sediment samples

Sample	ICP- AES Ga mg/kg	ICP- AES Ho mg/kg	ICP- AES La mg/kg	ICP- AES Li mg/kg	ICP- AES Mn mg/kg	ICP- AES Mo mg/kg	ICP- AES Nb mg/kg	ICP- AES Nd mg/kg	ICP- AES Ni mg/kg	ICP- AES Pb mg/kg	ICP- AES Sc mg/kg
PRRP-1-1-SS	18	<4	11	8	1100	2	7	13	21	6	15
PRRP-4-1-SS	16	<4	10	9	1180	<2	8	14	10	9	18
PRRP-5-1-SS	21	<4	10	12	1340	<2	10	13	28	<4	24
PRRP-6-1-SS	18	<4	11	8	1390	3	6	14	32	14	16
PRRP-7-1-SS	19	<4	12	11	2290	<2	5	17	41	6	21
PRRP-7-1dup	19	<4	11	11	2470	<2	4	16	35	5	20
PRRV-1-1-SS	18	<4	12	7	1630	<2	5	16	20	8	14
PRRV-2-1-SS	18	<4	10	8	1300	4	7	12	23	<4	14
PRRV-4-1-SS	17	<4	8	12	1850	10	7	11	22	<4	18

Appendix ID (cont.)
Geochemistry of sediment samples

Sample	ICP- AES Sn mg/kg	ICP- AES Sr mg/kg	ICP- AES Ta mg/kg	ICP- AES Th mg/kg	ICP- AES U mg/kg	ICP- AES V mg/kg	ICP- AES Y mg/kg	ICP- AES Yb mg/kg	ICP- AES Zn mg/kg
PRRP-1-1-ss	<50	120	<40	<6	<100	240	13	2	132
PRRP-4-1-ss	<50	61	<40	<6	<100	183	25	3	109
PRRP-5-1-ss	<50	113	<40	<6	<100	270	14	2	104
PRRP-6-1-ss	<50	127	<40	<6	<100	234	14	2	217
PRRP-7-1-ss	<50	156	<40	<6	<100	314	18	3	152
PRRP-7-1dup	<50	158	<40	<6	<100	370	18	3	146
PRRV-1-1-ss	<50	177	<40	<6	<100	275	16	3	291
PRRV-2-1-ss	<50	185	<40	<6	<100	202	14	2	166
PRRV-4-1-ss	<50	102	<40	<6	<100	216	15	2	150